AD_____

Award Number: W81XWH-12-1-0391

TITLE: Meta-Analytical Online Repository of Gene Expression Profiles of MDS Stem Cells

PRINCIPAL INVESTIGATOR: Dr. Amit Verma, M.D.

CONTRACTING ORGANIZATION: Albert Einstein College of Medicine
Bronx, NY 10461-1602

REPORT DATE: December 2015

TYPE OF REPORT: Final

PREPARED FOR: U.S. Army Medical Research and Material Command
Fort Detrick, Maryland 21702-5012

DISTRIBUTION STATEMENT: Approved for Public Release;
Distribution Unlimited

The views, opinions and/or findings contained in this report are those of the author(s) and should not be construed as and official Department of the Army position, policy or decision unless so designated by other documentation.

REPORT DOCUMENTATION PAGE

Form Approved
OMB No. 0704-0188

1. REPORT DATE	2. REPORT TYPE	3. DATES COVERED
December 2015	Final	30 Sep 2012 - 29 Sep 2015

4. TITLE AND SUBTITLE
Meta-Analytical Online Repository of Gene Expression Profiles of MD Of MDS Stem Cells

5a. CONTRACT NUMBER

5b. GRANT NUMBER
W81XWH-12-1-0391

5c. PROGRAM ELEMENT NUMBER

6. AUTHOR(S)
Dr. Amit Verma

E-Mail: amit.verma@einstein.yu.edu

5d. PROJECT NUMBER

5e. TASK NUMBER

5f. WORK UNIT NUMBER

7. PERFORMING ORGANIZATION NAME(S) AND ADDRESS(ES)

Albert Einstein College of Medicine
Cancer Center
1300 Morris Park Avenue
Bronx, NY 10461-1602

8. PERFORMING ORGANIZATION REPORT NUMBER

9. SPONSORING / MONITORING AGENCY NAME(S) AND ADDRESS(ES)
U.S. Army Medical Research and Materiel Command
Fort Detrick, Maryland 21702-5012

10. SPONSOR/MONITOR'S ACRONYM(S)

11. SPONSOR/MONITOR'S REPORT NUMBER(S)

12. DISTRIBUTION / AVAILABILITY STATEMENT
Approved for Public Release; Distribution Unlimited

14. ABSTRACT

We proposed to create an repository of gene expression profiles of CD34+ stem cells from patients with myelodysplastic syndromes (MDS) and healthy controls. We have devised a novel meta-analytical approach to integrate and normalize gene expression studies generated in different labs on different platforms and have shown it to be feasible and biologically valid in numerous publications. We have now successfully integrated data from 183 MDS samples in the database. This dataset has been used to screen for expression of all TGF-β related genes and has led to the discovery that negative regulator, SMAD7, was significantly underexpressed in MDS stem cells. This discovery elucidated the mechanism of activation of TGF-β signaling in MDS. A recent study again utilized this dataset and revealed that Interleukin 8 and its receptor CXCR2 are elevated in MDS stem cells. This study is leading to a clinical trial with IL8 inhibitors in MDS. We have now added information about MDS subtypes, blood counts, IPSS scores, patient demographics and mutations in these samples. Investigators will be allowed to access this database online. This resource will continually be updated with newer data on an ongoing basis.

15
SUBJECT TERMS
MDS, Stem Cells, Gene Expression

16. SECURITY CLASSIFICATION OF:			17. LIMITATION OF ABSTRACT	18. NUMBER OF PAGES	19a. NAME OF RESPONSIBLE PERSON
a. REPORT	b. ABSTRACT	c. THIS PAGE			USAMRMC
U	U	U	UU		19b. TELEPHONE NUMBER *(include area code)*

Table of Contents

Introduction:

MDS is a heterogeneous group of diseases characterized by bone marrow failure that leads to cytopenias. Newer therapeutic developments are impeded by limited insights into disease pathophysiology. Lack of cell lines and valid mouse models underscore the importance of research based on primary patient samples. These samples are hard to obtain in sufficient numbers. Our proposal will create a gene expression database that will include large numbers of all MDS subtypes. Moreover, this database will be generated by compiling gene expression profiles from CD34+ purified stem cells, thus ensuring that these profiles are not diluted due to heterogeneity of whole bone marrow samples. In addition to allowing researchers to study the expression patterns of selected genes, this database will also allow researchers to identify subtypes of MDS patients that will potentially benefit from novel therapies that target specific genes or genetic pathways.

Body:

We had previously shown that meta-analysis of microarray studies demonstrates feasibility of inter-platform data integration and reveals novel hematopoietic stem cell signatures. We tested the feasibility of conducting a meta-analysis of GE studies by using publically available data from studies that used normal bone marrow-derived hematopoietic progenitors. Data was integrated using both RefSeq and UniGene identifiers and normalized. We observed that in spite of variability introduced by experimental conditions and different microarray platforms, our meta-analytical approach can distinguish biologically distinct normal tissues by clustering them based on their cell of origin(1).

After demonstrating the feasibility of our meta-analytical approach, we wanted to construct a database of MDS stem cells and normal controls. We have now integrated data from 183 MDS CD34+ samples and 17 healthy controls. The data was integrated using unigene IDs, normalized and shown to be valid for further analysis (2). We have subsequently used this database in 4 studies that have led to important insights into the pathophysiology of MDS (2-5). In the first study, we showed that the SMAD2 protein is overexpressed in MDS. This protein is an effector of the TGF-β signaling pathway and is activated by the TGF-β receptor I kinase. In the next two studies, we wanted to determine the reasons for activation of TGF- β signaling pathway in MDS stem cells. Therefore, we used the MDS gene expression database to screen for expression of all TGF- β related genes and discovered that the negative regulator, SMAD7, was significantly underexpressed in MDS stem cells (3, 5). SMAD7 protein is an endogenous inhibitor of the TGF-β receptor I kinase. Functional studies revealed that reduction in SMAD7 (observed in the meta-analysis) leads to overactivation of the TGF-β receptor kinase even in the absence of high extracellular levels of the cytokine. These studies thus established SMAD7 reduction as a key intracellular event that leads to myelosuppressive TGF-β signaling and ineffective hematopoiesis in MDS (3, 5).

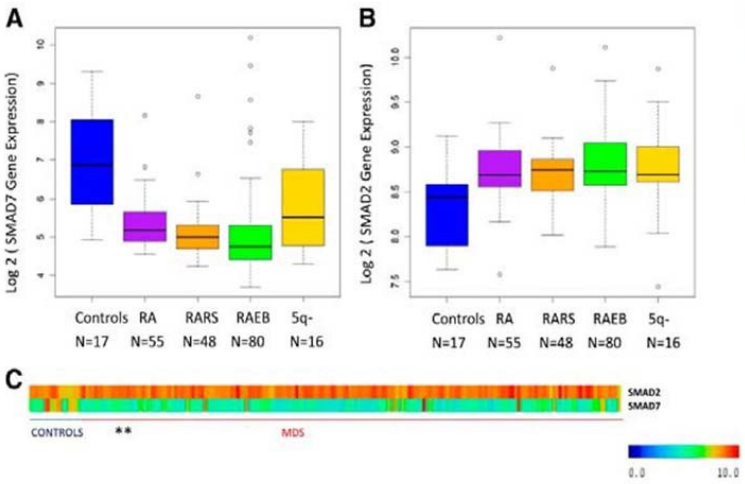

Figure 1. *SMAD7* expression is significantly decreased in MDS CD34+ cells. (A) SMAD7 expression in 183 samples of MDS CD34+ cells and 17 healthy controls reveals reduction in all subsets of MDS. (false discovery rate < 0.1, Benjamin Hochberg correction multiple testing). (B) *SMAD2*, the effector SMAD protein for TGF-β signaling, was found to be increased in the same samples. (C) Heatmaps showing expression values for both genes. (The 5q- patients were a subset of the RA patient cohort.)

In another study, we determined that DOCK4, a GTPase exchange factor is underexpressed in MDS (Fig 2). This study also utilized the database we created to show DOCK4 underexpression in a large number of MDS samples (Fig 2)(Shown at Fig5 from ref 4).

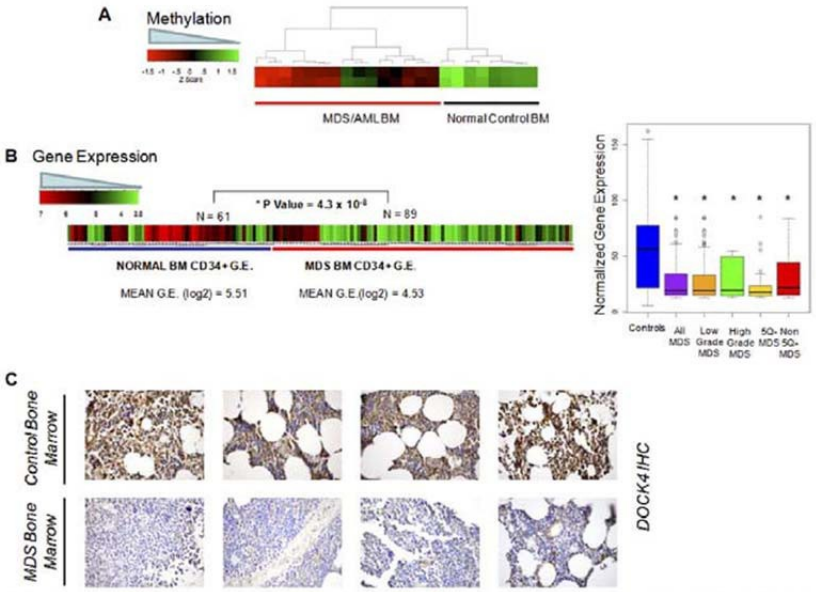

FIGURE 5. **Validation in independent cohorts demonstrate reduction in DOCK4 in marrow samples from MDS/AML.** Methylation values obtained from the HELP assay performed on marrow (*BM*) samples in an independent cohort of patients (38) show hypermethylation of the promoter in MDS/AML samples (*A*). Gene expression values from various studies on MDS and normal bone marrow-derived CD34$^+$ cells were obtained and normalized. Mean expression of *DOCK4* was significantly reduced in 89 MDS cases when compared with 61 controls (two-tailed *t* test) (*B, left panel*); box plots of MDS subtypes show significantly reduced levels of DOCK4 in all subtypes of MDS (*B, right panel*). Bone marrow biopsy samples were stained with DOCK4 antibody and show decreased expression in four representative cases of MDS when compared with controls (*C*).

After demonstrating the utility of this database in this study, we now propose to add information about MDS subtypes, blood counts, IPSS scores, patient demographics to this database. Investigators will be allowed to access this database online. This resource will continually be updated with newer data on an ongoing basis.

IL8 and its receptor CXCR2 is expressed in primary MDS samples and is associated with worse clinical outcome (6)

IL8 and other CXCL ligands bind to the CXCR1 and CXCR2 receptors to trigger many different biological processes. We evaluated the expression of these ligands and receptors in a large cohort of

AML samples analyzed by RNA-seq (TCGA, n=200). We observed that among the CXCR1 and 2 ligands, IL8 was most significantly expressed in AML (mean RPKM=36(IL8) vs 12(CXCL2), 3(CXCL3), 2(CXCL1) and 0.2 (CXCL5); P value < 0.001), and CXCR2 expression was significantly higher than CXCR1 expression (mean RPKM=4(CXCR2) vs 2(CXCR1), P < 0.001) in leukemic cells (Fig 2A,B). We evaluated CXCR2 overexpression for prognostic impact in this cohort and observed that samples with higher expression of the receptor had a significantly worse prognosis compared to CXCR2 lower expressing patients (median overall survival of 245 days in high CXCR2 cases vs 854 in low CXCR2 cases, Log rank P Value =0.003)(Fig 2C). Next, we evaluated the expression of CXCR2 in MDS stem and progenitor cells (HSPC) in another large cohort of 183 samples generated from the DOD grant. CXCR2 expression was found to be higher in MDS samples when compared to healthy controls (P Value =0.001, FDR<10%) (Fig 2D). Cases with high CXCR2 were found to present with worse disease phenotype manifesting with lower hemoglobin levels and a higher percentage of transfusion dependence (53% for CXCR high vs 35% for CXCR2 low, P value <0.001) (Fig 2E,F). Correlation with mutations obtained from targeted sequencing of a subset of MDS cases revealed significant enrichment of TET2 mutations in CXCR2 low expressers, with no other significant correlations with other mutations (Supp Table 2). Taken together, these data demonstrate that high CXCR2 expression in HSPCs is an adverse prognostic factor in both AML and MDS.

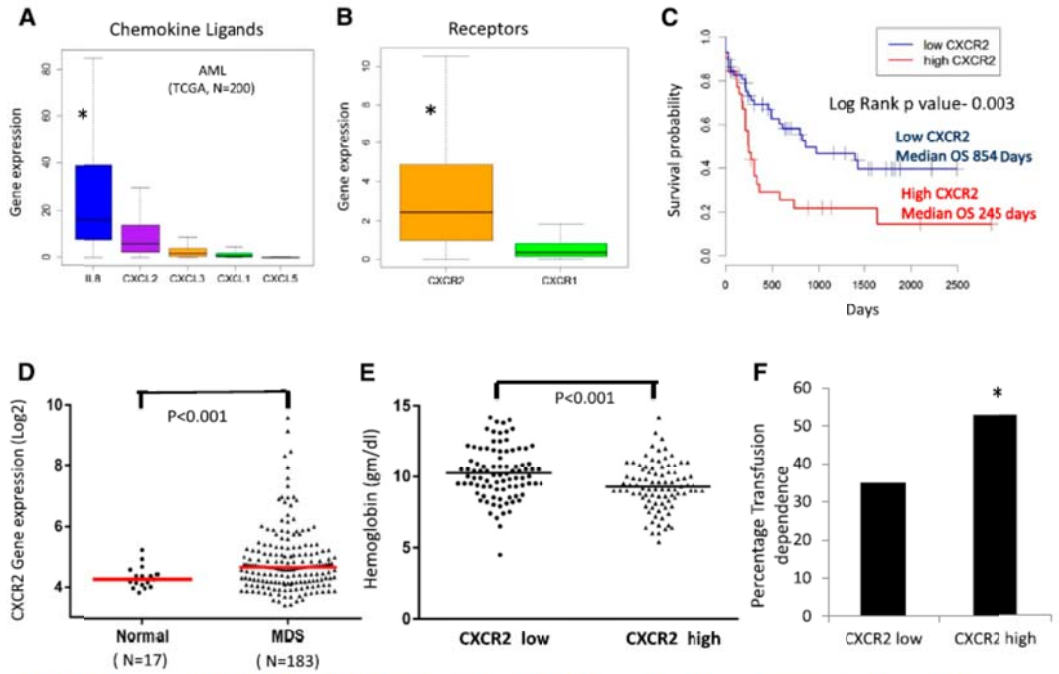

Figure 2. CXCR2 is expressed in primary AML and MDS samples and is associated with worse clinical outcomes. Expression of (A) chemokine ligands and (B) receptors was evaluated in the TCGA RNA-seq dataset from 200 AML samples (data shown as boxplots). (C) Median overall survival of AML patients with high CXCR2 was significantly worse than in patients with lower expression (log rank, $P = .003$). (D) Gene expression data of $CD34^+$ cells from 183 MDS patients and 17 healthy controls shows significantly higher expression of CXCR2 in MDS $CD34^+$ cells (*t* test, $P < .001$, FDR < 5%). MDS patients with (E) high CXCR2 expression (>median) have lower hemoglobin levels (*t* test, $P < .001$) and (F) higher RBC transfusion dependence (test of proportions, $P < .05$).

Gene expression signature of MDS HSPCs with high CXCR2 is similar to known preleukemic stem cell profiles and includes many important functional pathways

To determine the genetic pathways that were differentially expressed in MDS HSPCs with high expression of CXCR2, we identified differentially expressed transcripts between the CXCR2 high and low patient subsets (using median CXCR2 expression as cutoff in a cohort of 183 MDS CD34+ samples, FDR<0.1)(Fig 3A). Ingenuity pathway analysis revealed significant dysregulation of pathways involved in chemokine signaling, cytokine-cytokine receptor interaction, innate immunity signaling, hematopoietic cell lineage regulation, and others, in CXCR2 high patients, and also included many genes that play important roles in molecular leukemogenesis (Fig 3B, Supp Table 3). Next, we tested whether the high CXCR2 expression signature had any overlap with known preleukemic stem cell gene expression profiles. Gene set enrichment analysis with two recently published preleukemic stem cell signatures (GSE35008 and GSE30377), including one from our own group, revealed highly significant enrichment, demonstrating that HSPCs from CXCR2 high MDS patients have a similar transcriptomic profile than known pre-leukemic and leukemia-initiating cell populations (Fig 3C).

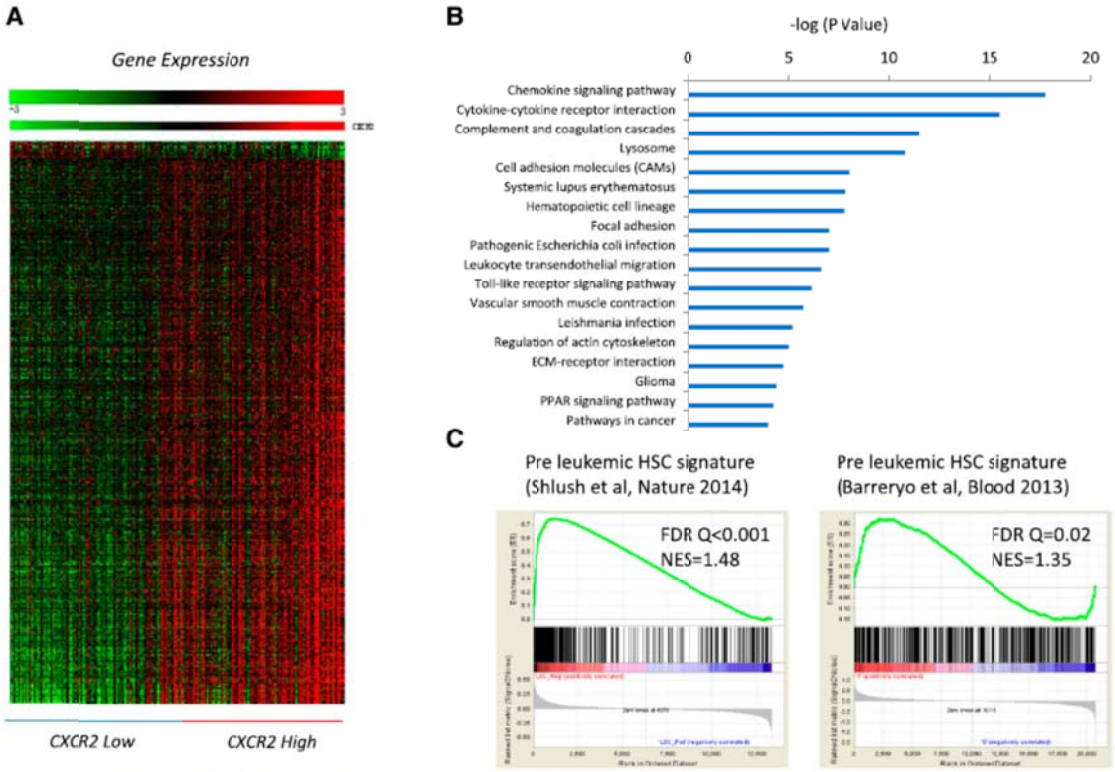

Figure 3. Important functional pathways are dysregulated in MDS cases with high expression of CXCR2. (A) Gene expression profiles from samples with low and high CXCR2 were compared, and differentially expressed transcripts were identified (FDR < 0.1). (B) Significantly dysregulated pathways are shown. The gene signature of high CXCR2 MDS cases is similar to previously published preleukemic stem cell signatures. (C) Gene Set Enrichment Analysis plots show significant enrichment of 2 recent preleukemic gene expression signatures.

Key Research Accomplishments:

We have shown the feasibility of constructing a meta-analytical database of MDS stem cell samples and controls, and have shown that this database can be used in basic as well as translation studies in MDS.

Reportable Outcomes:

Manuscripts:

Hosono N, Makishima H, Jerez A, Yoshida K, Przychodzen B, McMahon S, Shiraishi Y, Chiba K, Tanaka H, Miyano S, Sanada M, Gómez-Seguí I, **Verma AK**, McDevitt MA, Sekeres, Ogawa S, Maciejewski JP. Recurrent genetic defects on chromosome 7q in myeloid neoplasms. ***Leukemia***
2014 Jan 16. PMID: 24429498

Bhagat T, Zhou L, Sokol L, Caceres G, Gundabolu K, Gordon S, Mantzaris I, Gligich O, Yu Y, Bhattacharyya S, Jing X, Polineni R, Tamari R, Bhatia K, Pellagatti A , Boultwood J, Kambhampati S, Steidl U, Stein C, Ju W, Liu G, Kenny P, List A, Bitzer M, **Verma A.**
miR-21 mediates hematopoietic suppression in MDS by activating TGF- β signaling ***Blood*** 2013, Apr 11;121(15):2875-81. PMID: 23390194

Schinke C, Giricz O, Li W, Shastri A, Gordon S, Barreryo L, Bhagat T, Bhattacharyya S, Ramachandra N, Bartenstein M, Pellagatti A, Boultwood J, Wickrema A, Yu Y, Will W, Wei S, Steidl U*, Verma A*. * co-corresponding authors IL8-CXCR2 pathway inhibition as a novel therapeutic strategy against MDS and AML stem cells. ***Blood.*** 2015, Mar 25. PMID: 25810490

Conclusion:

We have shown the feasibility of constructing a meta-analytical database of MDS stem cell samples and controls, and have shown that this database can be used in basic as well as translation studies in MDS. We will now incorporate mutational and clinical information to this database in the new phase of the funding period.

References:

1. Sohal, D., Yeatts, A., Ye, K., Pellagatti, A., Zhou, L., Pahanish, P., Mo, Y., Bhagat, T., Mariadason, J., Boultwood, J., et al. 2008. Meta-analysis of microarray studies reveals a novel hematopoietic progenitor cell signature and demonstrates feasibility of inter- platform data integration. *PLoS ONE* 3:e2965.
2. Zhou, L., Nguyen, A.N., Sohal, D., Ying Ma, J., Pahanish, P., Gundabolu, K., Hayman, J., Chubak, A., Mo, Y., Bhagat, T.D., et al. 2008. Inhibition of the TGF-beta receptor I kinase promotes hematopoiesis in MDS. *Blood* 112:3434-3443.
3. Bhagat, T.D., Zhou, L., Sokol, L., Kessel, R., Caceres, G., Gundabolu, K., Tamari, R., Gordon, S., Mantzaris, I., Jodlowski, T., et al. 2013. miR-21 mediates hematopoietic suppression in MDS by activating TGF-beta signaling. *Blood*.
4. Zhou, L., Opalinska, J., Sohal, D., Yu, Y., Mo, Y., Bhagat, T., Abdel-Wahab, O., Fazzari, M., Figueroa, M., Alencar, C., et al. 2011. Aberrant epigenetic and genetic marks are
seen in myelodysplastic leukocytes and reveal Dock4 as a candidate

pathogenic gene on chromosome 7q. *J Biol Chem* 286:25211-25223.

5. Zhou, L., McMahon, C., Bhagat, T., Alencar, C., Yu, Y., Fazzari, M., Sohal, D., Heuck, C., Gundabolu, K., Ng, C., et al. 2011. Reduced SMAD7 leads to overactivation of TGF-
beta signaling in MDS that can be reversed by a specific inhibitor of TGF-beta receptor I kinase. *Cancer Res* 71:955-963.

6. Schinke, C., Giricz, O., Li, W., Shastri, A., Gordon, S., Barreyro, L., Bhagat, T., Bhattacharyya, S., Ramachandra, N., Bartenstein, M., et al. 2015. IL8-CXCR2 pathway inhibition as a therapeutic strategy against MDS and AML stem cells. *Blood* 125:3144-3152.

Appendices:
None

OPEN ACCESS Freely available online

PLoS one

Meta-Analysis of Microarray Studies Reveals a Novel Hematopoietic Progenitor Cell Signature and Demonstrates Feasibility of Inter-Platform Data Integration

Davendra Sohal[1], Andrew Yeatts[1], Kenny Ye[1], Andrea Pellagatti[2], Li Zhou[1], Perry Pahanish[1], Yongkai Mo[1], Tushar Bhagat[1], John Mariadason[1], Jacqueline Boultwood[2], Ari Melnick[1], John Greally[1], Amit Verma[1]*

1 Albert Einstein College of Medicine, Bronx, New York, United States of America, **2** John Radcliffe Hospital, Oxford, United Kingdom

Abstract

Microarray-based studies of global gene expression (GE) have resulted in a large amount of data that can be mined for further insights into disease and physiology. Meta-analysis of these data is hampered by technical limitations due to many different platforms, gene annotations and probes used in different studies. We tested the feasibility of conducting a meta-analysis of GE studies to determine a transcriptional signature of hematopoietic progenitor and stem cells. Data from studies that used normal bone marrow-derived hematopoietic progenitors was integrated using both RefSeq and UniGene identifiers. We observed that in spite of variability introduced by experimental conditions and different microarray platforms, our meta-analytical approach can distinguish biologically distinct normal tissues by clustering them based on their cell of origin. When studied in terms of disease states, GE studies of leukemias and myelodysplasia progenitors tend to cluster with normal progenitors and remain distinct from other normal tissues, further validating the discriminatory power of this meta-analysis. Furthermore, analysis of 57 normal hematopoietic stem and progenitor cell GE samples was used to determine a gene expression signature characteristic of these cells. Genes that were most uniformly expressed in progenitors and at the same time differentially expressed when compared to other normal tissues were found to be involved in important biological processes such as cell cycle regulation and hematopoiesis. Validation studies using a different microarray platform demonstrated the enrichment of several genes such as SMARCE, Septin 6 and others not previously implicated in hematopoiesis. Most interestingly, alpha-integrin, the only common stemness gene discovered in a recent comparative murine analysis (Science 302(5644):393) was also enriched in our dataset, demonstrating the usefulness of this analytical approach.

Citation: Sohal D, Yeatts A, Ye K, Pellagatti A, Zhou L, et al. (2008) Meta-Analysis of Microarray Studies Reveals a Novel Hematopoietic Progenitor Cell Signature and Demonstrates Feasibility of Inter-Platform Data Integration. PLoS ONE 3(8): e2965. doi:10.1371/journal.pone.0002965

Editor: Magnus Rattray, University of Manchester, United Kingdom

Received October 24, 2007; **Accepted** July 18, 2008; **Published** August 13, 2008

Funding: NIH 1R01HL082946, NIH RO1AG02913801, Community foundation for Southwestern Michigan JP McCarthy grant, Immunooncology Training Program T32 CA009173 and a gift from Janet and Arthur N. Hershaft.

Competing Interests: The authors have declared that no competing interests exist.

* E-mail: averma@aecom.yu.edu

Introduction

Microarray-based studies of global gene expression have led to dramatic advances in our understanding of various biological processes. This technology has become one of the most rapidly growing investigational methods in medical research and numerous studies have been completed using this method. There are many available platforms [1] for microarray analysis, and newer technologies and better gene annotations have led to constant refinement of these platforms. This has resulted in a large amount of data in public repositories, like the Gene Expression Omnibus [2]. Meta-analysis of these data has the potential to yield important biological information, but is hampered by technical issues. Cross-platform comparability has been a major hindrance to this approach. This problem arises because matching probe-sets across platforms is a difficult task. Different platforms use different probe lengths and sequences, and mapping them to one common gene or set of genes is beset with problems. Another limitation is different gene annotations used by different platforms. The nucleic acid sequences for various species are submitted to and maintained in the GenBank® database by the National Center of Biotechnology Information (NCBI) [3]. There are different annotation methods in use to parse these sequences into genes or gene clusters. UniGene is one method for partitioning GenBank nucleic acid sequences into unique gene-oriented clusters, each of which represents a unique gene. These UniGene identifiers (IDs) are created by finding transcript sequences that match distinct transcription areas or genes. UniGene IDs have been used as the matching criterion to merge data across various platforms, but this has led to a substantial portion of the data remaining unmatched in previous studies [4,5,6,7,8]. Recent approaches have tried using Reference Sequence (RefSeq) IDs as the matching criterion [9]. RefSeq is a public access database, also maintained by NCBI. This database is built by using sequence data from

GenBank, EMBL Data Library (UK) and DNA Data Bank (Japan) [10]. This set is also constantly updated, and input from various investigators is also used to maintain this set. Since both UniGene and RefSeq are billed as non-redundant sets of transcript IDs, and have been used in prior studies with mixed results, it is still unclear as to which approach is better.

We attempted to conduct a meta-analysis of all gene expression studies using hematopoietic progenitor cells to determine a gene expression signature characteristic of these cells. Our aim was to integrate data from all studies that used normal hematopoietic progenitors and stem cells into a unified normalized database. This was done using both UniGene as well as RefSeq gene IDs to assess which identifier provides the best yield. Our results show that experimental conditions, laboratory where the experiments were performed and different microarray platforms can result in significant variability in gene expression patterns from similar sources of cells. In spite of experimental variability, meta-analytical studies do have the power to discriminate biologically distinct tissues on the basis of their normalized gene expression patterns. Gene expression datasets from similar cells of origin cluster together despite diseased phenotypes and genetic alterations. The similarity seen among gene expression profiles of leukemias, myelodysplasia and normal hematopoietic progenitors, when compared to non-hematopoietic tissues, validates the functional discriminatory power of this meta-analysis. Finally, analysis of merged normal hematopoietic progenitor cell gene expression datasets led to the discovery of a common gene expression signature characteristic of these cells. Genes that are most uniformly expressed in normal hematopoietic tissues and at the same time being differentially expressed as compared to other normal tissues were found to be involved in important biological processes such as hematopoiesis and development. The expression patterns of these genes were validated in a different microarray platform using material from three different hematopoietic progenitor and stem cell experiments.

Methods

Data collection

Normal hematopoietic cell gene expression data were collected from the NCBI's Gene Expression Omnibus (GEO) database (Figure 1). Bone marrow, hematopoietic, CD34 and stem cells were used as search terms to locate datasets containing gene expression profiles of normal human hematopoietic cells. Normal bone marrow/peripheral blood CD34 profiles used as controls in studies of leukemia and other hematological diseases were also included. Most studies used the Affymetrix U95, the U133A/B and the U133 Plus 2.0 Array Platforms. A handful of studies using older Affymetrix platforms, like the HG-Focus Target Array and the Full Length HuG Array, were discarded because combining data from these yielded a lot of non-matching probe-sets.

Gene expression data for other normal tissues assayed on the same platforms were also obtained from GEO. In a study where multiple sets were available, we picked one set each for every tissue, again to minimize correlation within individual datasets. These were picked using computer-generated random numbers.

To obtain diseased stem cell data, we identified a few studies with multiple datasets on myelodysplasia, acute myeloid leukemia (AML) and acute lymphoblastic leukemia (ALL) samples. Where several datasets were available per study, we picked a subset, again using random numbers, to obtain about 10 samples per each study. Table 1 shows the details of these datasets [11,12,13,14,15,16,17,18,19].

Integration of datasets

Initially, we used the comparison spreadsheets provided by the chip manufacturer, Affymetrix [20]. These files link the probe-set IDs of various platforms. However, the yield therein was poor. For example, using the link file between the U133 and the U133 Plus platforms, 44635 U133 IDs matched to only 9908 U133 Plus IDs. Therefore, UniGene and RefSeq IDs were evaluated as variables

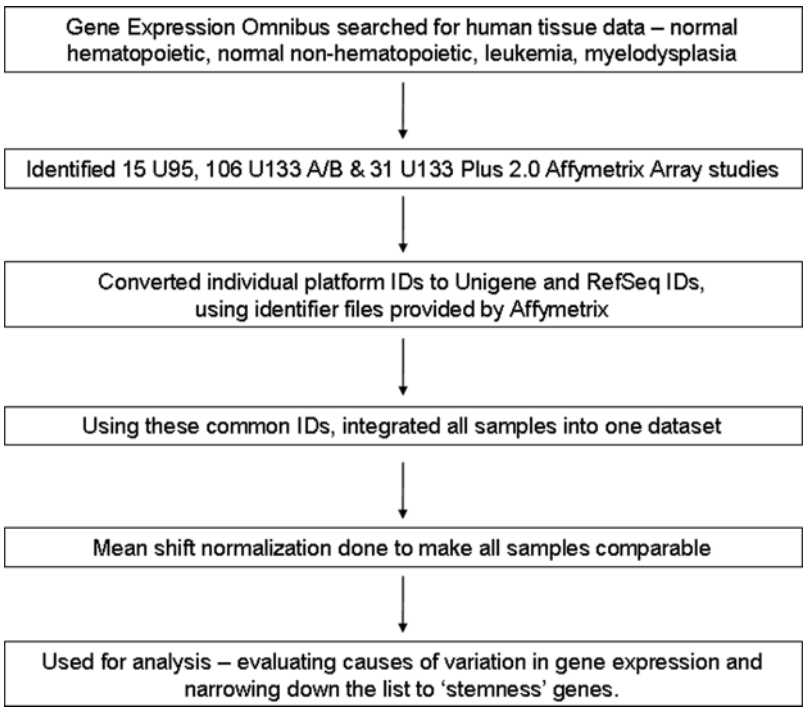

Figure 1. Schema of data collection and analysis.
doi:10.1371/journal.pone.0002965.g001

Table 1. Sources of data for the meta-analysis*

Author	Source of cells	No. of datasets	Platform
Sternberg A, et al [11]	CD34, MDS	22	U133 A/B
Oswald J, et al [12]	CD34	3	U133 A/B
Su AI, et al [13]	CD34, various normal NHTs	19	U133 A/B
Eckfeldt CE, et al [14]	CD34	18	U133 A/B
Bhatia M, et al (GEO)	CD34	15	U133 A/B
Pellagatti A, et al [15]	CD34, MDS	22	U133 Plus 2.0
Breit S, et al [16]	Bone marrow	9	U95
Ge X, et al [17]	Various normal NHTs	19	U133 A/B
Gutierrez NC, et al [18]	Bone marrow (AML)	9	U133 A/B
Roth RB, et al (GEO)	Various normal NHTs	7	U133 Plus 2.0
Cheok MH, et al [19]	Bone marrow (ALL)	6	U95

*NHTs: Non-hematopoietic tissues, GEO: Gene Expression Omnibus database set,
MDS: Myelodysplastic syndrome, AML: Acute myeloid leukemia, ALL: Acute lymphoblastic leukemia
Numbers in brackets are reference numbers.
doi:10.1371/journal.pone.0002965.t001

to cross link data from various platforms. Individual probe-set IDs for each platform were linked to the corresponding UniGene IDs using annotation files, again provided by Affymetrix [20]. These UniGene IDs were then used to combine data across the three platforms. Once probe-set IDs and their expression values were combined, the expression value for each UniGene ID was obtained. In many instances, more than one probe-set matched to the same UniGene ID, resulting in multiple expression values for each such ID. In such cases, the expression value was calculated as the mean of the various values for each UniGene ID.

Probe-set IDs which did not match to any UniGene ID were dropped. Also, if any UniGene ID had data for only one platform, it was dropped, as it was considered to not match across at least two of the three platforms. Moreover, in many cases, one probe-set ID matched to more than one UniGene ID. In such cases, each UniGene ID was considered to have the same gene expression value and the data were expanded accordingly.

An identical process was used to merge data across platforms using RefSeq ID as the match identifier, instead of UniGene ID. Of interest, RefSeq IDs can be either protein IDs or transcript IDs. Protein IDs provided slightly better results (as detailed further) than transcript IDs, and were therefore used in this study.

Data analysis

Once expression values for each UniGene or RefSeq ID were obtained, these were used to do the analysis. First, the datasets were normalized using quantile normalization to ensure that inherent large-scale expression differences in the datasets based on different sources and laboratories were minimized. Unsupervised hierarchical clustering using average linkage with (1 - Pearson correlation coefficient) as the distance measure was done for each of the three 'types' of tissue – normal hematopoietic cells, normal non-hematopoietic tissues and diseased hematopoietic cells. This allowed us to look at how the datasets cluster – whether by platform, laboratory, experiment or otherwise.

To determine a gene signature for hematopoietic progenitor and stem cells, we used the datasets derived from 57 CD34+ sets, as whole bone marrow sets may not be a true reflection of these progenitors, being as they are a mixture of various cell types. To find out which genes were most consistently expressed across these samples, we used the coefficient of variation – defined as the standard deviation divided by the mean – of the expression values for each ID, calculated across all stem cell samples. The coefficient of variation was used to incorporate consistency in gene expression as well as "enrichment" of genes in the hematopoietic progenitor cells. Prior studies have used similar reasoning [21].

We then used this set of consistently expressed genes and compared their expression in normal hematopoietic progenitors versus that in non-hematopoietic tissues, to identify which genes could differentiate these two tissue sources. This was done using significance analysis of microarrays (SAM) [22,23]. Similarly, normal hematopoietic progenitor gene expression was compared to diseased hematopoietic data, to identify a subset of genes that may be most relevant to hematological stem cell disorders. All IDs with missing values for any of the samples were deleted.

All data analyses were done using SAS (SAS Institute, Cary, NC), the R language and ArrayAssist Expression software package (Stratagene Corporation, La Jolla, CA).

Results

Integration of data using protein identifiers

A total of 66 individual normal hematopoietic cell expression profiles were identified in NCBI's GEO database (Table 1). Nine were derived from whole bone marrow samples and 57 were from selected CD34-positive cells. These studies were performed on 3 different microarray platforms (Table 2). Since the probe-set identifiers and complementary oligos were different on these platforms, we integrated the data using both UniGene and RefSeq protein IDs (Figure 1, showing schema).

The Affymetrix annotation files yielded 12,626 unique probe-sets in the U95 platform, 44,761 in the U133 A/B platform and 54,676 unique probe-sets in the U133 Plus 2.0 platform. Using UniGene IDs as the matching criterion, 11,635, 40,787 and 45,867 probe-sets matched to at least one other platform, respectively. After combining data from all the three platforms, we ended up with a total of 20,717 UniGene IDs. Since one probe-set can match to more than one UniGene ID and vice versa, a relatively small number of U95 probe-sets matched to 20,717 UniGene IDs. Using RefSeq protein IDs as the matching parameter, 11,722, 37,395 and 42,462 probe-sets matched to at least one other platform, respectively. As many of the probe-sets

Table 2. Platform and tissue type for various datasets.

	U95	U133 A/B	U133 Plus 2.0	Total
Normal hematopoietic stem cells	9	46	11	66
Normal tissues, non-hematopoietic	0	36	7	43
Diseased hematopoietic stem cells	6	23	11	40
Total	15	105	29	149

doi:10.1371/journal.pone.0002965.t002

Table 3. Pairwise absolute correlation coefficients for normal hematopoietic cell samples

	Mean (Range)	Median
Same study	0.87 (0.26–1.00)	0.95
Different study	0.35 (0.00–0.93)	0.04
Same platform	0.83 (0.26–1.00)	0.82
Different platform	0.02 (0.00–0.06)	0.01
Same cells (CD34 or BM)	0.58 (0.01–1.00)	0.79
Different cells	0.01 (0.00–0.01)	0.01

doi:10.1371/journal.pone.0002965.t003

from the two newer platforms were coding for the same protein, we ended up with a total of 28,497 unique RefSeq protein IDs that were common to all three platforms. After removing the probe-sets where expression values were missing for any dataset, a total of 8,598 unique UniGene IDs and 8,345 unique RefSeq IDs were obtained that were common to all platforms. These were quantile-normalized using ArrayAssist (Stratagene Corporation, California, USA) to adjust for hybridization intensities and used for the meta-analysis.

Experimental conditions, microarray platforms and source of cells can influence gene expression patterns

Sixty-six hematopoietic gene expression profiles from either whole bone marrow or selected CD34 cells were grouped using unsupervised clustering based on Pearson correlation coefficient. In spite of similar cell types, the studies grouped primarily based on the laboratory where the data was obtained from. The next level of clustering was defined by the microarray platform used for the studies. Barring two bone marrow samples from the Plus 2.0 platform that were similar to one bone marrow sample from the 133A/B platform, all the samples clustered depending on which platform they were from. The samples from the U95 platform stayed as a separate group (Figure 2). The last level of similarity was based on the exact source of the cells used for the RNA.

The correlation coefficients between various datasets validated the clustering order of laboratory, platform and source (Table 3). The correlation was strongest between samples obtained from the same laboratory/study, with a mean (median) absolute correlation coefficient of 0.87 (0.95). When the platform was the same, a slightly lesser though still strong correlation of 0.83 was obtained. These results illustrate that the cause of variability in gene expression studies can be due to experimental conditions/protocols used in individual laboratories, platforms used as well as sources of cells in that order.

Gene expression studies from biologically distinct tissue types can be compared despite varying platforms and experimental conditions

We next wanted to determine the degree of dissimilarity of hematopoietic datasets to gene expression (GE) datasets obtained from other biologically distinct tissues. GE profiles from human adrenal, appendix, brain, breast, colon, heart, kidney, liver, lung, ovary, pancreas, pituitary, prostate, salivary gland, skin, small intestine, smooth muscle, spleen, stomach, testis, thyroid, urinary bladder and uterus samples were obtained from the GEO database and used for this analysis. Unsupervised clustering showed that samples from the same tissue of origin clustered tightly together in spite of different platforms/laboratories used for the analysis

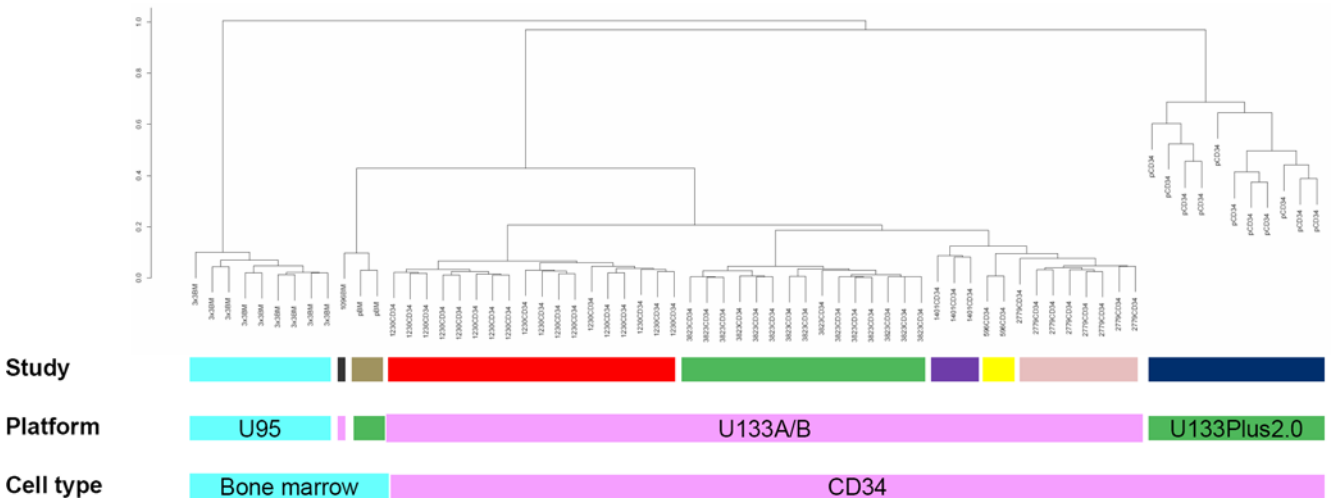

Figure 2. Normal bone marrow HSC clustering. Experimental conditions, microarray platforms and sources of cells influence gene expression patterns of normal bone marrow derived HSCs. Dendrogram of normal bone marrow derived hematopoietic cells based on unsupervised hierarchical clustering, using (1 - Pearson correlation coefficient) as the distance measure. Same color in each horizontal row indicates same group.
doi:10.1371/journal.pone.0002965.g002

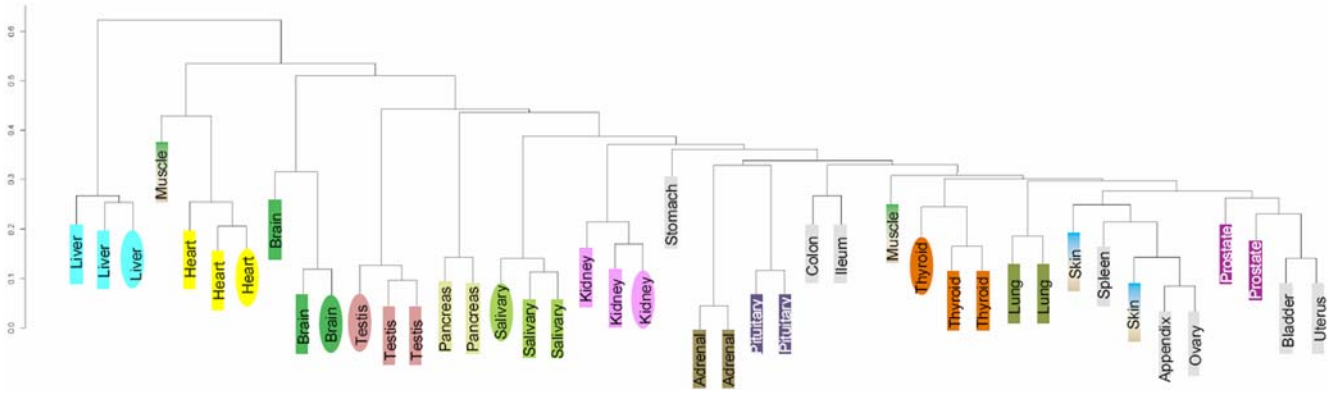

Figure 3. Distinguishing normal non-hematopoietic tissues. Despite differing platforms and experimental conditions, GE profiles can separate out normal tissues based on cell/tissue of origin. Dendrogram based on unsupervised hierarchical clustering, using (1 - Pearson correlation coefficient) as the distance measure. Rectangles indicate samples from the U133 A/B platform and ovals from the U133 Plus 2.0 platform. Triplicate sets of samples from human liver, heart, testis, kidney, etc. are from different studies, and their grouping together is a strong indicator of comparability across studies and platforms.
doi:10.1371/journal.pone.0002965.g003

(Figure 3). Clustering of triplicate sets of liver, heart, brain, salivary gland, testis, kidney and thyroid tissues from different laboratories and platforms clearly indicates that our analysis can detect the similarity of expression at the source tissue level. The mean (and median) correlation coefficients were also not very dependent on the laboratory/study or the platform (Table 4). The highest correlation was observed between similar tissues. These results demonstrate that despite inter-platform and inter-study variability, meta-analysis of gene expression profiles has the potential of revealing differences between tissues with a high degree of dissimilarity (Table 4).

Gene expression datasets from similar cells of origin can cluster together despite diseased phenotypes and genetic alterations

To further test the discriminatory ability of the meta-analysis, we next grouped datasets from hematologic malignancies with the normal hematopoietic and non-hematopoietic tissues analyzed within the same microarray platform (U133 A/B). We wanted to determine whether biological variability seen in hematopoietic stem cell disorders such as acute leukemias and myelodysplastic syndromes would be distinguishable in our analysis. Unsupervised clustering showed that even though diseased hematopoietic cells were separated from the normal cells, they were significantly more dissimilar to non-hematopoietic tissues (Figure 4A). In fact, some individual GE profiles from bone marrow CD34+ samples from myelodysplastic syndromes were very similar to normal CD34+ cells and clustered within their groups. We believe that this was a strong validation of our analytical approach as myelodysplasia is a preleukemic disorder with varying levels of pathology and can have cases that are genetically very similar to normal hematopoietic stem cells [24]. We did a similar analysis using RefSeq IDs as the matching criterion between different datasets. Interestingly, clustering using RefSeq IDs provided more heterogeneous results (Figure 4B) and grouped non-hematopoietic tissues along with hematopoietic tissues, thus demonstrating that UniGene IDs are better at discriminating biological subsets.

Table 4. Pairwise absolute correlation coefficients for normal non-hematopoietic cell samples.

	Mean (Range)	Median
Same study	0.58 (0.27–0.91)	0.59
Different study	0.55 (0.23–0.95)	0.55
Same platform	0.58 (0.24–0.95)	0.59
Different platform	0.51 (0.23–0.88)	0.49
Same tissue	0.77 (0.68–0.95)	0.80
Different tissue	0.57 (0.23–0.88)	0.59

doi:10.1371/journal.pone.0002965.t004

Hematopoietic progenitor and stem cell signature

After validating the strength of the meta-analysis, we wanted to determine a gene expression signature of hematopoietic progenitors. Using the lowest 20th percentile, to obtain the best possible initial yield, a total of 1,719 genes were obtained with a low coefficient of variation among the 57 CD34+ GE profiles (range 0.15–0.39). These were the genes deemed to be most characteristic of the stem and progenitor cells as their expression was most consistently enriched among all the samples.

Using this list of genes, we next determined the genes that were able to discriminate normal hematopoietic and non-hematopoietic cells by using significance analysis of microarrays (SAM). We used 100 permutations to compute the expected significance 'score', and a false discovery rate (FDR) of 0.29% was achieved by using the lower- and upper-most 10% of genes. A total of 349 genes were called as significant (Figure 5).

To better understand how differentially expressed genes were integrated into specific regulatory and signaling pathway networks, we used Ingenuity Pathway Analysis (Ingenuity Systems, Redwood City, USA). Functional analysis of overexpressed genes indicated that this list is highly enriched for proteins involved in hematopoiesis and cell cycle, further validating our approach (Figure 5, Table 5). Several of these genes have already been described to have important roles in development of the hematologic system. In addition, our analysis revealed a variety of novel functional genes like SWI/SNF family member 4, SMARCE1 and Septin 6. Many of the genes identified in our database were also found to be enriched in 3 independent HSC studies performed in our laboratory using a different Nimblegen platform (Supplementary Table S1). Cross validation suggests that

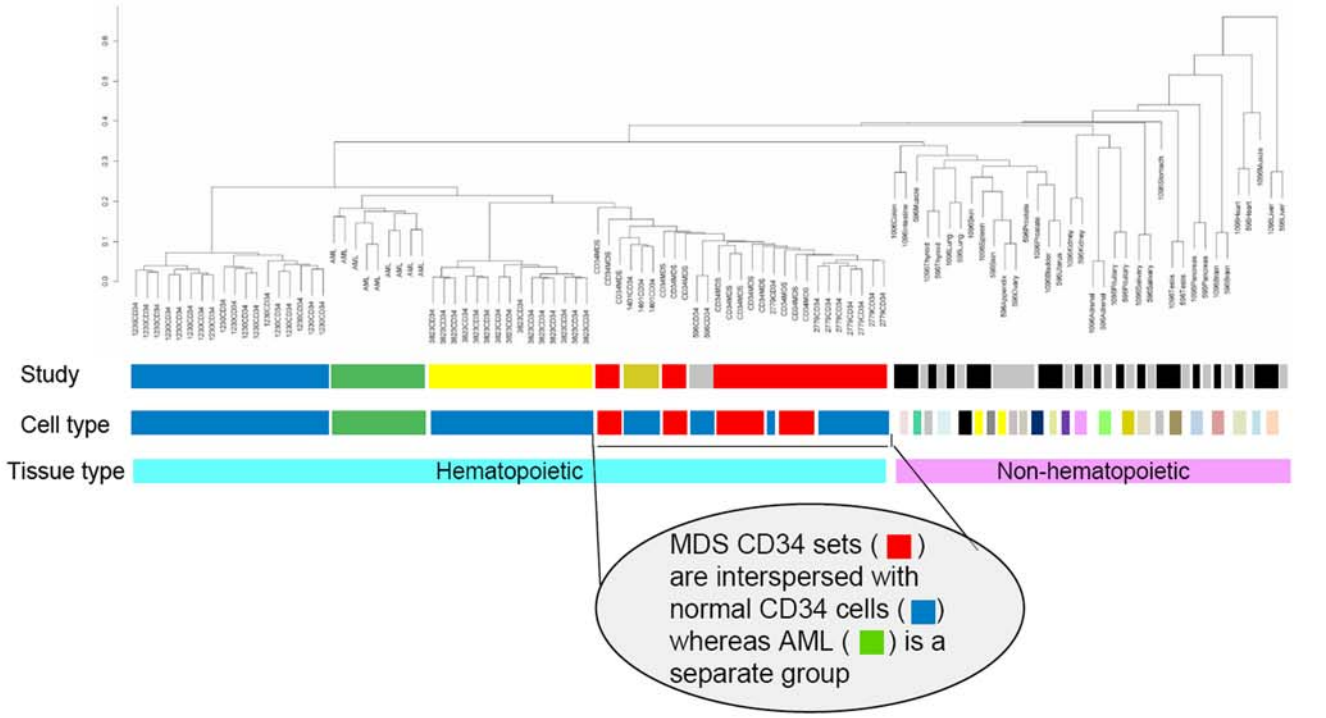

A: Cluster dendrogram of normal hematopoietic, diseased hematopoietic and non hematopoietic tissues derived microarray studies reveals biological relationships between them

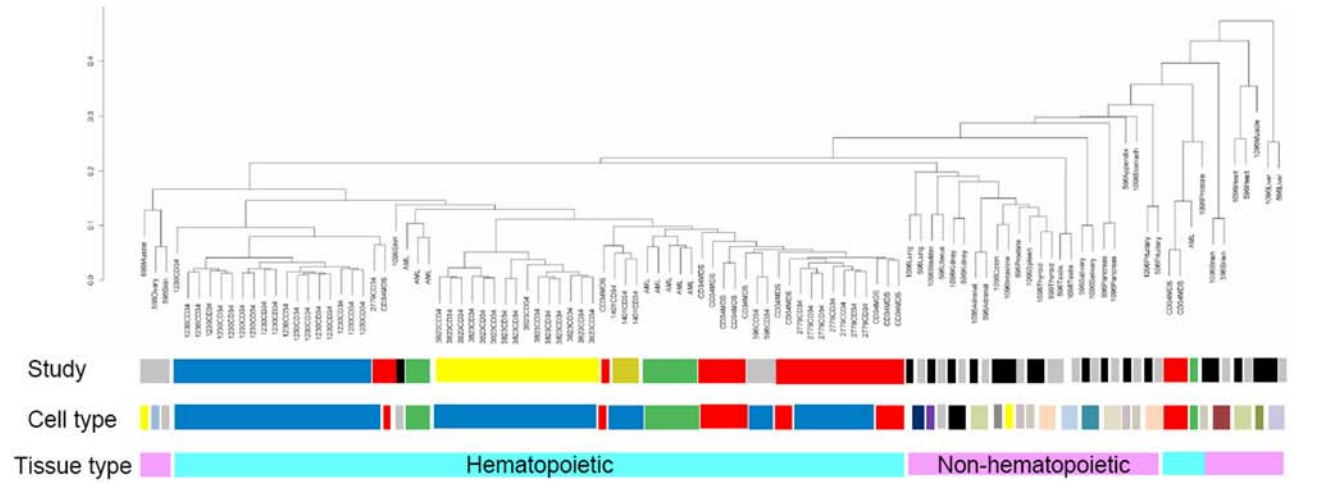

B: Clustering dendrogram of various samples from the U133 A/B platform integrated using Refseq IDs.

Figure 4. A: Biological relationships identified. Dendrogram of normal hematopoietic, diseased hematopoietic and non hematopoietic tissues GE profiles reveals biological relationships between them. MDS sets intersperse with normal hematopoietic tissues whereas AML samples are a separate group, exactly as their biological dissimilarity patterns. Dendrogram based on unsupervised hierarchical clustering, using (1 - Pearson correlation coefficient) as the distance measure. Same color in each horizontal row indicates same group. UniGene IDs were used for integrating data. **B: Clustering using RefSeq IDs.** Same clustering as in 4A, showing poorer performance of RefSeq IDs, compared to UniGene IDs, in uncovering biological relationships. Dendrogram based on unsupervised hierarchical clustering, using (1 - Pearson correlation coefficient) as the distance measure. Same color in each horizontal row indicates same group.
doi:10.1371/journal.pone.0002965.g004

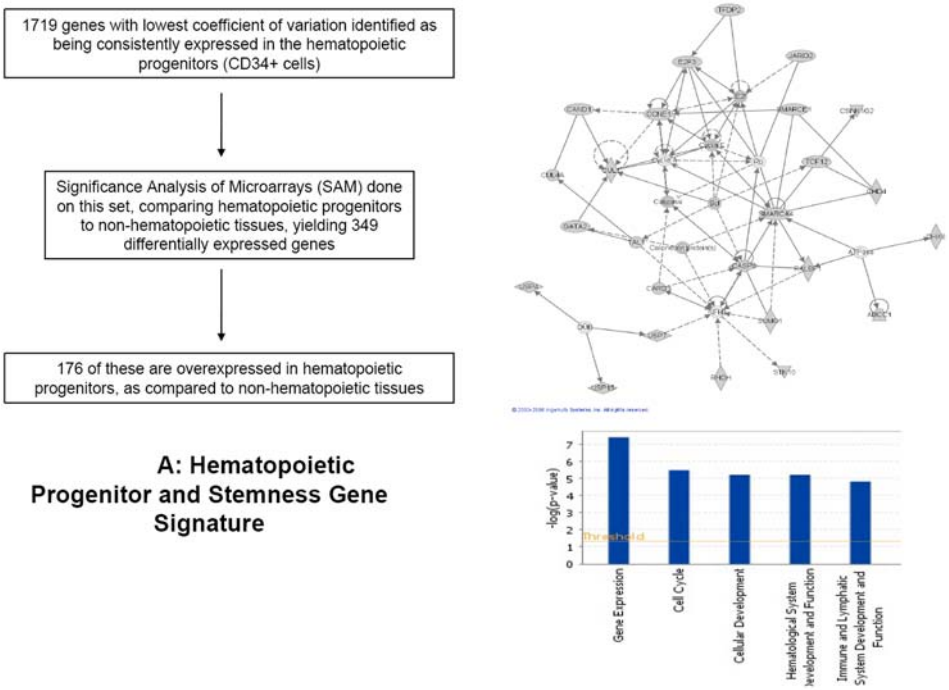

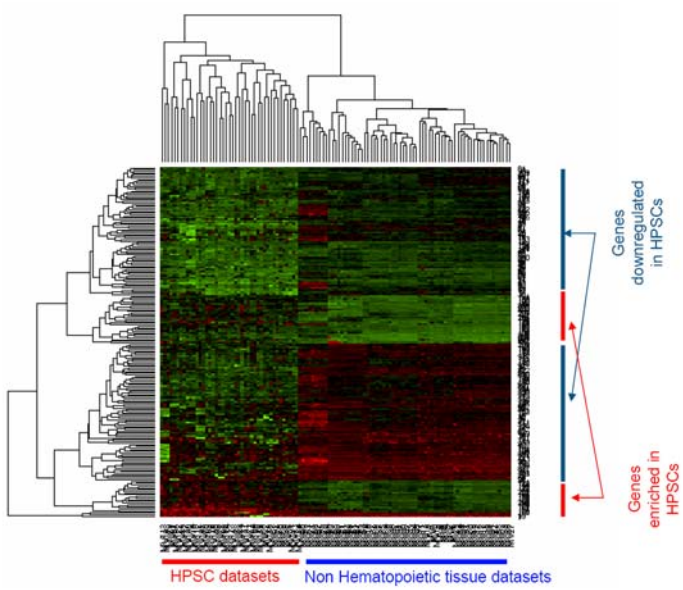

Figure 5. A: ''Stemness genes''. 349 UniGene IDs were identified as being consistently expressed amongst the normal hematopoietic cells and differentially expressed between hematopoietic and non-hematopoietic cells. Genes enriched in hematopoietic progenitor and stem cell datasets were involved in important functional pathways in the cell, including drug metabolism, hematological system development, cell signaling and cancer and cell death, as shown in the bar graph alongside. One such network is shown, which includes the GATA2, Cyclin E and SMARCE1 genes. **B: Heatmap of ''stemness'' genes.** 349 Unigene IDs were identified as being consistently expressed amongst the normal hematopoietic cells and differentially expressed between hematopoietic and non-hematopoietic cells. Out of these, 176 genes were enriched in HSC datasets when compared to other tissue types.
doi:10.1371/journal.pone.0002965.g005

these genes need to be tested as potential markers of HSCs and may have functionally important roles in hematopoiesis. We also found 171 genes to be differentially underexpressed in hematopoietic progenitors (Table 6). Our database and integration files will be online in a searchable format to aid other hematology and stem cell researchers (http://greallylab.aecom.yu.edu/).

Table 5. 'Stemness genes'*

Major functions	Well-annotated genes
Gene Expression, Cell Cycle, Cellular Development,	ABCC1, CASP8, CSNK1G2, E2F3, GATA2, JARID2, RALBP1, SMARCA4, SMARCE1, STK10, SUMO1, TAL1, TCF12, TFDP2, USP4, USP7
Cell Morphology, Cellular Assembly and Organization, Cell Signaling	C1ORF2, GLIPR1, HSPA9, ING2, LPIN1, MAP3K4, MAP4K1, NCK1, NFATC1, PAK2, PPM1F, PPP3CA, TP53, UBE3A, ZNF84, BRPF1, EWSR1, HSPA4, LYN, MAPKAPK5, PHF21A, PTEN, TIMM17A, TROVE2
Cancer, Cellular Growth and Proliferation, Tumor Morphology	ATP6V0A2, CD47, HNRPUL1, MLLT10, MPHOSPH9, MTR, PDS5A, SEC63, SH3BGRL
Others	TIPRL, TSR1, TXNDC9, SFRS17A, CENTB2, THOC2, KIAA0368, PAX3, TFIP11, TUFT, FMR1, NUFIP1

*Some important genes differentially **over-expressed** in hematopoietic progenitors, as compared to non-hematopoietic tissues
doi:10.1371/journal.pone.0002965.t005

Discussion

Microarray analysis of global gene expression has led to rapid advances in our understanding of various physiological and pathological processes. Although many hundreds of studies have been done, doubts have been raised about the reproducibility and applicability of this data [25,26,27,28]. Inter-study variability can be attributed to differing probes on the arrays, different protocols for RNA extraction, labeling and hybridization, and differences in the quality of cells. In spite of these factors, a number of studies have also demonstrated reproducibility of microarray studies performed at different platforms and laboratories, though most used the same source of RNA for these analyses [29,30,31]. The MicroArray Quality Control consortium (MAQC) was formed to address these questions and recently reported that reproducibility can be enhanced by better matching of microarray probes between platforms [32]. They concluded that matching probe-sets within the same exons and using similar experimental protocols can lead to more reproducible results when performed on major commercial microarray platforms. Our results take these findings a step further and demonstrate that GE studies done using different platforms and distinct sources of material have the power to discriminate between biologically distinct tissues and thus can also be used to analyze various scientific questions. Earlier attempts to address study specific biases have used statistical algorithms including ANOVA based correction models [33,34]. We did not use these algorithms as we found adequate discrimination between biologically distinct tissues, demonstrating that the degree of differential gene expression is so large that it is found even in presence of possible study-specific biases. It is possible that some of the more subtle results seen in our analysis, however, may prove artificial once these biases have been removed by appropriate methods.

Furthermore, this meta-analysis can be accomplished simply by using UniGene and RefSeq identifiers as common variables between array platforms, though UniGene is shown to be slightly better at achieving this discrimination in our dataset. This difference between UniGene and RefSeq results, albeit small, is likely due to the different methods of identifying and assigning transcripts used in the process, and has been observed in prior studies also [4,5,6,7,8,9,10]. Even though we did observe variability due to different laboratory protocols as seen by previous studies, a superior correlation between tissues with similar sources of cells was able to surpass this limitation and make the meta-analysis scientifically useful.

Our study demonstrated that results obtained through this approach can be reconciled with the biology of hematopoietic cells and malignancies thereof. For example, samples from acute myeloid leukemia and myelodysplasia were found to be transcriptionally closer to normal hematopoietic cells than non-hematopoietic cells, even though these studies are done in many different laboratories. MDS is a preleukemic disorder of varying grades of pathology and can have an indolent course in most patients [15,24]. The fact that MDS samples clustered with normal hematopoietic samples in some cases shows that our analysis can interpret biological relationships even between studies performed by different experimental protocols and laboratories.

After demonstrating that our approach can be used to biologically characterize sources of cells, we attempted to use this database to discover gene signatures characteristic of hematopoietic progenitor and stem cells. Due to the heterogeneity of our source dataset, we imposed very stringent criteria to discover genes characteristic of hematopoietic progenitors. Out of the 349 genes that were differentially expressed in normal progenitors, 124 are differentially expressed in diseased hematopoietic cells, demon-

Table 6. Genes quiescent in HSC progenitor cells*

Major functions	Well-annotated genes
Skeletal and Muscular System Development, Function and Disorders, Genetic Disorders	ADD1, APBB3, ARHGAP1, ATP2A2, BCL2L2, BGN, CALCOCO1, CALD1, CALM1, COL18A1, COL6A1, DDR1, ESRRA, FMOD, MYH9, NCOA1, PFN2, PXN, RHOC, SQSTM1, TPM1
Cellular Assembly and Organization, Cellular Function and Maintenance, Cell Signaling	APP, CADM1, CD59, CLSTN1, ERBB2, F8, FLOT1, GDI1, IKBKG, MAPK13, MYO1C, NDRG2, NFE2L1, PTRF, RAB5B, RAB5C, SFRP1, SHC1, SPTAN1, WFS1
Protein Degradation, Cellular Movement, Cell Morphology	ARF3, ARFIP2, CES2, COL1A1, CTNND1, EIF4G1, GSK3A, GSTA1, GSTM2, KIF5C, MFN2, MMP14, PAPSS2, PCDHGC3, PTPRF, SDC1, TIMP3, TSPAN3
Others	CDC42EP4, CHST10, DEFB1, FKBP1A, HDLBP, LPP, S100A13, TEGT, AKAP1, CLOCK, JAM3, PCTK1, TLE2, TMPRSS6, TNFAIP1, TRIP10, USP13, SPOCK2

*Some important genes differentially **under-expressed** in hematopoietic progenitors, as compared to non-hematopoietic tissues
doi:10.1371/journal.pone.0002965.t006

strating that hematologic malignancies result in disruption of important functional genes. Our search strategy yielded several genes that were consistently enriched in normal hematopoietic GE datasets and were found to be involved in cell cycle, growth, development and hematopoiesis by functional pathway analysis. Recent studies have supported similar comparative approaches for more accurate and valid gene target discovery [21,26,35]. Two recent seminal studies searched for gene signatures of stem cells by comparing genes enriched in hematopoietic, neural and embryonic stem cells and arrived at a total of 283 and 230 common 'stemness' genes respectively [21,35]. Even though the experimental techniques and cell types in these two papers were similar, an initial comparative analysis showed that only 7 'stemness' genes were common between these two studies. Comparison to a subsequent third analysis [26] showed even less overlap, with only one gene being consistently enriched between these three independent similar studies. Repeat analysis done using different statistical methods did lead to more gene overlap, but the final conclusion was that gene array studies of stem cells are influenced by cell purity and can be contaminated by a high level of non-specific observations in the data. Consequently, the authors determined that commonly expressed genes among different studies may be better representatives of functionally important stemness genes. Thus, meta-analytical approaches may be a way to separate functionally important information from experimental noise. As the genes discovered by our analysis are common in an extremely variable dataset, they may have a high chance of being characteristic of human HSCs. Most importantly, alpha-6 integrin, the one gene that was found be enriched in all three murine stem cell studies, is similar to alpha-4 integrin that was found to be enriched in our human dataset. Both of these integrins are known to be expressed on the surface of HSCs and are implicated in cell migration and homing to the bone marrow. The functional similarities between these two integrins and the concurrence of our findings with three landmark stemness gene studies published in the literature validate our analytical approach.

Our analysis also yielded a set of genes not previously implicated in hematopoiesis. Some of these genes have interesting functions and can be potential regulators of HSC function. SMARCE (SWI/SNF related, matrix associated, actin dependent regulator of chromatin, subfamily e/BAF57) is a key member of the mammalian SWI/SNF chromatin remodeling complex that is involved in transcriptional regulation [36]. SMARCE has been shown to mediate the interaction between the chromatin remodeling complex and transcription factors and thus could be partly responsible for the unique chromatin associated with stem cells [37]. Lyn kinase is a member of the src family of kinases and has been implicated in granulopoiesis and erythropoiesis and needs further exploration as a stem cell marker [38,39]. Septin 6 is a member of a class of proteins involved in cell division, membrane trafficking and cytoskeletal organization. The roles of septins in hematopoietic stem cells remain unexplored [40]. Amyloid beta precursor protein is a cell surface protein with signal-transducing properties, and it is thought to play a role in the pathogenesis of Alzheimer's disease [41]. This protein can activate NEDD8, a ubiquitin-like protein required for cell cycle progression through the S/M checkpoint and thus can be potentially involved in cell cycle control of hematopoietic stem cells. The protein Dp-2 (E2F dimerization partner 2) belongs to a family of transcription factors that play an essential role in regulating cell cycle progression [42]. These transcription factors regulate the expression of numerous critical genes (e.g. cyclin E, CDC2, cyclin A, B-Myb, E2F1, and p107) involved in cell cycle progression as well as several enzymes (DNA polymerase α, thymidine kinase, and dihydrofolate reductase) required for DNA replication [42]. Thus Dp-2 could certainly be involved in stem cell regulation. In summary, our analytical approach provides a list of interesting genes for further scientific and functional validation. Additionally, this dataset can be used as an online resource for stem cell and hematology researchers as a control database for comparisons with disease state GE profiles done in their laboratories.

Supporting Information

Table S1

Found at: doi:10.1371/journal.pone.0002965.s001 (0.04 MB DOC)

Author Contributions

Conceived and designed the experiments: AM JMG AV. Performed the experiments: DS AY LZ PP YM TB. Analyzed the data: DS KY AV. Contributed reagents/materials/analysis tools: AP JM JB. Wrote the paper: DS AV.

References

1. Eisenstein M (2006) Microarrays: Quality control. Nature 442: 1067–1070.
2. National Center for Biotechnology Information NLoM Gene Expression Omnibus. NCBI..
3. Wheeler DL, Barrett T, Benson DA, Bryant SH, Canese K, et al. (2006) Database resources of the National Center for Biotechnology Information. Nucleic Acids Res 34: D173–180.
4. Jarvinen AK, Hautaniemi S, Edgren H, Auvinen P, Saarela J, et al. (2004) Are data from different gene expression microarray platforms comparable? Genomics 83: 1164–1168.
5. Kuo WP, Jenssen TK, Butte AJ, Ohno-Machado L, Kohane IS (2002) Analysis of matched mRNA measurements from two different microarray technologies. Bioinformatics 18: 405–412.
6. Petersen D, Chandramouli GV, Geoghegan J, Hilburn J, Paarlberg J, et al. (2005) Three microarray platforms: an analysis of their concordance in profiling gene expression. BMC Genomics 6: 63.
7. van Ruissen F, Ruijter JM, Schaaf GJ, Asgharnegad L, Zwijnenburg DA, et al. (2005) Evaluation of the similarity of gene expression data estimated with SAGE and Affymetrix GeneChips. BMC Genomics 6: 91.
8. Warnat P, Eils R, Brors B (2005) Cross-platform analysis of cancer microarray data improves gene expression based classification of phenotypes. BMC Bioinformatics 6: 265.
9. Ji Y, Coombes K, Zhang J, Wen S, Mitchell J, et al. (2006) RefSeq refinements of UniGene-based gene matching improve the correlation of expression measurements between two microarray platforms. Appl Bioinformatics 5: 89–98.
10. Pruitt KD, Tatusova T, Maglott DR (2005) NCBI Reference Sequence (RefSeq): a curated non-redundant sequence database of genomes, transcripts and proteins. Nucleic Acids Res 33: D501–504.
11. Sternberg A, Killick S, Littlewood T, Hatton C, Peniket A, et al. (2005) Evidence for reduced B-cell progenitors in early (low-risk) myelodysplastic syndrome. Blood 106: 2982–2991.
12. Oswald J, Steudel C, Salchert K, Joergensen B, Thiede C, et al. (2006) Gene-expression profiling of CD34+ hematopoietic cells expanded in a collagen I matrix. Stem Cells 24: 494–500.
13. Su AI, Wiltshire T, Batalov S, Lapp H, Ching KA, et al. (2004) A gene atlas of the mouse and human protein-encoding transcriptomes. Proc Natl Acad Sci U S A 101: 6062–6067.
14. Eckfeldt CE, Mendenhall EM, Flynn CM, Wang TF, Pickart MA, et al. (2005) Functional analysis of human hematopoietic stem cell gene expression using zebrafish. PLoS Biol 3: e254.
15. Pellagatti A, Cazzola M, Giagounidis AA, Malcovati L, Porta MG, et al. (2006) Gene expression profiles of CD34+ cells in myelodysplastic syndromes: involvement of interferon-stimulated genes and correlation to FAB subtype and karyotype. Blood 108: 337–345.
16. Breit S, Nees M, Schaefer U, Pfoersich M, Hagemeier C, et al. (2004) Impact of pre-analytical handling on bone marrow mRNA gene expression. Br J Haematol 126: 231–243.
17. Ge X, Yamamoto S, Tsutsumi S, Midorikawa Y, Ihara S, et al. (2005) Interpreting expression profiles of cancers by genome-wide survey of breadth of expression in normal tissues. Genomics 86: 127–141.

18. Gutierrez NC, Lopez-Perez R, Hernandez JM, Isidro I, Gonzalez B, et al. (2005) Gene expression profile reveals deregulation of genes with relevant functions in the different subclasses of acute myeloid leukemia. Leukemia 19: 402–409.
19. Cheok MH, Yang W, Pui CH, Downing JR, Cheng C, et al. (2003) Treatment-specific changes in gene expression discriminate in vivo drug response in human leukemia cells. Nat Genet 34: 85–90.
20. Affymetrix annotation files, provided by manufacturer, accessed from www.affymetrix.com. Affymetrix, Inc..
21. Ramalho-Santos M, Yoon S, Matsuzaki Y, Mulligan RC, Melton DA (2002) "Stemness": transcriptional profiling of embryonic and adult stem cells. Science 298: 597–600.
22. Dettling M, Buhlmann P (2002) Supervised clustering of genes. Genome Biol 3: RESEARCH0069.
23. Tusher VG, Tibshirani R, Chu G (2001) Significance analysis of microarrays applied to the ionizing radiation response. Proc Natl Acad Sci U S A 98: 5116–5121.
24. Heaney ML, Golde DW (1999) Myelodysplasia. N Engl J Med 340: 1649–1660.
25. Tan PK, Downey TJ, Spitznagel EL Jr., Xu P, Fu D, et al. (2003) Evaluation of gene expression measurements from commercial microarray platforms. Nucleic Acids Res 31: 5676–5684.
26. Fortunel NO, Otu HH, Ng HH, Chen J, Mu X, et al. (2003) Comment on " 'Stemness': transcriptional profiling of embryonic and adult stem cells" and "a stem cell molecular signature". Science 302: 393; author reply 393.
27. Marshall E (2004) Getting the noise out of gene arrays. Science 306: 630–631.
28. Ein-Dor L, Zuk O, Domany E (2006) Thousands of samples are needed to generate a robust gene list for predicting outcome in cancer. Proc Natl Acad Sci U S A 103: 5923–5928.
29. Dobbin KK, Beer DG, Meyerson M, Yeatman TJ, Gerald WL, et al. (2005) Interlaboratory comparability study of cancer gene expression analysis using oligonucleotide microarrays. Clin Cancer Res 11: 565–572.
30. Irizarry RA, Warren D, Spencer F, Kim IF, Biswal S, et al. (2005) Multiple-laboratory comparison of microarray platforms. Nat Methods 2: 345–350.
31. Larkin JE, Frank BC, Gavras H, Sultana R, Quackenbush J (2005) Independence and reproducibility across microarray platforms. Nat Methods 2: 337–344.
32. Shi L, Reid LH, Jones WD, Shippy R, Warrington JA, et al. (2006) The MicroArray Quality Control (MAQC) project shows inter- and intraplatform reproducibility of gene expression measurements. Nat Biotechnol 24: 1151–1161.
33. Choi JK, Yu U, Kim S, Yoo OJ (2003) Combining multiple microarray studies and modeling interstudy variation. Bioinformatics 19 Suppl 1: i84–90.
34. Rhodes DR, Yu J, Shanker K, Deshpande N, Varambally R, et al. (2004) Large-scale meta-analysis of cancer microarray data identifies common transcriptional profiles of neoplastic transformation and progression. Proc Natl Acad Sci U S A 101: 9309–9314.
35. Ivanova NB, Dimos JT, Schaniel C, Hackney JA, Moore KA, et al. (2002) A stem cell molecular signature. Science 298: 601–604.
36. Chen J, Archer TK (2005) Regulating SWI/SNF subunit levels via protein-protein interactions and proteasomal degradation: BAF155 and BAF170 limit expression of BAF57. Mol Cell Biol 25: 9016–9027.
37. Bernstein BE, Mikkelsen TS, Xie X, Kamal M, Huebert DJ, et al. (2006) A bivalent chromatin structure marks key developmental genes in embryonic stem cells. Cell 125: 315–326.
38. Mermel CH, McLemore ML, Liu F, Pereira S, Woloszynek J, et al. (2006) Src family kinases are important negative regulators of G-CSF-dependent granulopoiesis. Blood 108: 2562–2568.
39. Karur VG, Lowell CA, Besmer P, Agosti V, Wojchowski DM (2006) Lyn kinase promotes erythroblast expansion and late-stage development. Blood 108: 1524–1532.
40. Lindsey R, Momany M (2006) Septin localization across kingdoms: three themes with variations. Curr Opin Microbiol 9: 559–565.
41. Chen Y, Liu W, McPhie DL, Hassinger L, Neve RL (2003) APP-BP1 mediates APP-induced apoptosis and DNA synthesis and is increased in Alzheimer's disease brain. J Cell Biol 163: 27–33.
42. Ishida H, Masuhiro Y, Fukushima A, Argueta JG, Yamaguchi N, et al. (2005) Identification and characterization of novel isoforms of human DP-1: DP-1{alpha} regulates the transcriptional activity of E2F1 as well as cell cycle progression in a dominant-negative manner. J Biol Chem 280: 24642–24648.

blood
Leading the world in reporting basic and applied hematology research
JOURNAL OF THE AMERICAN SOCIETY OF HEMATOLOGY
Original Article | Current Issue | About Blood | Submissions | Subscriptions | Contact Us

Blood. 2008 Oct 15; 112(8): 3434–3443. PMCID: PMC2569182
Prepublished online 2008 May 12. doi: 10.1182/blood-2008-02-139824
Neoplasia

Inhibition of the TGF-β receptor I kinase promotes hematopoiesis in MDS

Li Zhou,[1] Aaron N. Nguyen,[2] Davendra Sohal,[1] Jing Ying Ma,[2] Perry Pahanish,[1,3] Krishna Gundabolu,[1] Josh Hayman,[1] Adam Chubak,[1] Yongkai Mo,[1] Tushar D. Bhagat,[1] Bhaskar Das,[1] Ann M. Kapoun,[2] Tony A. Navas,[2] Simrit Parmar,[3] Suman Kambhampati,[4] Andrea Pellagatti,[5] Ira Braunchweig,[1] Ying Zhang,[6] Amittha Wickrema,[7] Satyanarayana Medicherla,[2] Jacqueline Boultwood,[5] Leonidas C. Platanias,[8] Linda S. Higgins,[2] Alan F. List,[9] Markus Bitzer,[1] and Amit Verma[1,3]

[1]Albert Einstein College of Medicine, Bronx, NY;
[2]Scios, Fremont, CA;
[3]University of Texas Southwestern Medical School and Dallas Veterans Affairs Medical Center (VAMC);
[4]VAMC, Kansas City, MO;
[5]John Radcliffe Hospital, Oxford, United Kingdom;
[6]Laboratory of Cellular and Molecular Biology, National Cancer Institute, Bethesda, MD;
[7]University of Chicago, IL;
[8]Northwestern University Robert H. Lurie Cancer Center, Chicago, IL; and
[9]Moffitt Cancer Center, Tampa, FL
Corresponding author.

Received 2008 Feb 15; Accepted 2008 Apr 14.

Abstract

MDS is characterized by ineffective hematopoiesis that leads to peripheral cytopenias. Development of effective treatments has been impeded by limited insight into pathogenic pathways governing dysplastic growth of hematopoietic progenitors. We demonstrate that smad2, a downstream mediator of transforming growth factor–β (TGF-β) receptor I kinase (TBRI) activation, is constitutively activated in MDS bone marrow (BM) precursors and is overexpressed in gene expression profiles of MDS $CD34^+$ cells, providing direct evidence of overactivation of TGF-β pathway in this disease. Suppression of the TGF-β signaling by lentiviral shRNA-mediated down-regulation of TBRI leads to in vitro enhancement of hematopoiesis in MDS progenitors. Pharmacologic inhibition of TBRI (alk5) kinase by a small molecule inhibitor, SD-208, inhibits smad2 activation in hematopoietic progenitors, suppresses TGF-β–mediated gene activation in BM stromal cells, and reverses TGF-β–mediated cell-cycle arrest in BM $CD34^+$ cells. Furthermore, SD-208 treatment alleviates anemia and stimulates hematopoiesis in vivo in a novel murine model of bone marrow failure generated by constitutive hepatic expression of TGF-β1. Moreover, in vitro pharmacologic inhibition of TBRI kinase leads to enhancement of hematopoiesis in varied morphologic MDS subtypes. These data directly implicate TGF-β signaling in the pathobiology of ineffective hematopoiesis and identify TBRI as a potential therapeutic target in low-risk MDS.

Introduction

The myelodysplastic syndromes (MDSs) are clonal stem cell disorders characterized by cytologic dysplasia and ineffective hematopoiesis.[1–3] Although approximately one third of patients may progress to acute leukemia, refractory cytopenias are the principal cause of morbidity and mortality in patients with MDS.[4] In fact, approximately two-thirds of patients present with lower risk disease characterized by hypercellular marrows with increased rates of apoptosis in the progenitor and differentiated cell compartments in the marrow.[5–8] Ineffective hematopoiesis arising from abortive maturation leads to peripheral cytopenias. Higher grade or more advanced disease categories are associated with a significant risk of leukemia transformation, with a corresponding lower apoptotic index and higher percentage of marrow blasts.

Cytokines play important roles in the regulation of normal hematopoiesis, and a balance between the actions of hematopoietic growth factors and myelosuppressive factors is required for optimal production of different hematopoietic cell lineages. Excess production of inhibitory cytokines amplifies ineffective hematopoiesis inherent to the MDS clone. Transforming growth factor–β (TGF-β) is a myelosuppressive cytokine that has been implicated in the hematopoietic suppression in MDS. The plasma levels of TGF-β have been reported to be elevated in some[9–13] but not all studies[14–17] and are supported by greater TGF-β immunohistochemical staining in selected studies. In addition to direct myelosuppressive effects, TGF-β has also been implicated in the autocrine production of other myelosuppressive cytokines (TNF, IL-6, and IFNγ) in MDS.[18] Conflicting data may arise from technical limitations of bone marrow immunohistochemical analyses of a secreted protein as well as the biologic heterogeneity of the disease itself. In addition, plasma levels of TGF-β may not be an accurate reflection of the biologic effects of this cytokine in the MDS bone marrow microenvironment. Thus we investigated the role of TGF-β in MDS by direct examination of receptor signal activation to conclusively determine its role in the pathogenesis of ineffective hematopoiesis in MDS.

Our previous studies have shown that signaling pathways activated by myelosuppressive cytokines can serve as therapeutic targets in low-risk MDS. We showed that interferons (IFNα, IFNβ, and IFNγ), TGF-β, and tumor necrosis factor α (TNFα) can all activate the p38 mitogen-activated protein kinase (MAPK) in primary human hematopoietic progenitors and that activation of p38 is required for myelosuppressive actions of these cytokines on hematopoiesis.[19,20] We subsequently confirmed overactivation of p38 MAPK in the bone marrow progenitors of low-risk MDS patients. Our data showed that inhibition of this cytokine-stimulated p38 MAPK pathway partially rescues hematopoiesis in MDS progenitors. This led to a clinical trial of a p38 inhibitor, SCIO-469, in low-risk MDS; the preliminary results have shown modest clinical activity in some cases of lower-risk MDS.[21] Having demonstrated that intracellular signaling pathways can serve as therapeutic targets in MDS, we decided to directly evaluate TGF-β signaling in MDS. We determined that the smad2 protein is heavily phosphorylated in MDS bone marrow progenitors and is found to be up-regulated in meta-analysis of MDS $CD34^+$ cell gene expression studies, thereby demonstrating sustained TGF-β signal activation in this disease. We showed that inhibition of the TGF-β receptor I kinase (TBRI) by shRNA suppression or by small molecule inhibitors abrogates smad2 activation and reverses the suppressive effects of TGF-β on hematopoiesis. Most importantly, TBRI inhibition stimulated in vitro hematopoiesis from a variety of MDS progenitors, thus providing a therapeutic rationale for inhibiting TGF-β signaling in this disease.

Methods

Cells lines and reagents human

$CD34^+$ cells were isolated from bone marrows of healthy or MDS patients, after obtaining informed

consent approved by the institutional review boards of University of Texas (UT) Southwestern Medical School (Dallas, TX), the Dallas VAMC, the University of Arizona College of Medicine (Phoenix, AZ), and the University of South Florida (Tampa, FL), and in accordance with the Declaration of Helsinki. Some bone marrow $CD34^+$ cells from various healthy donors were also obtained from Cambrex (Atlanta, GA). KG-1, K562, and HS-5 cell lines were purchased from ATCC (Manassas, VA). Erythroid progenitors at the colony-forming unit–erythroid (CFU-E) stage of differentiation were grown in cytokine-enriched Iscove modified Dulbecco medium (IMDM) media, similar to our previous studies.[19,20,22] Briefly, bone marrow or peripheral blood mobilized $CD34^+$ cells were immunomagnetically selected and cultured in 15% fetal bovine serum, 15% human serum, IMDM, 10 ng/mL IL-3, 2 units/mL erythropoietin (Epo), and 50 ng/mL stem cell factor (SCF). The cells were fed on days 3 and 6 to maintain an Epo concentration of 2 units/mL. The cells were sorted for glycophorin positivity on day 8 of culture and used for biochemical studies. SCF, thrombopoietin (TPO), Flt-3–ligand (FLT-3L), erythropoietin, and TGF-β1 were bought from R&D Systems (Minneapolis, MN). The phos-Smad2 (S465/467), Cdc2, and PCNA antibodies were from Cell Signaling Technology (Beverly, MA); cyclin E2 and Cdc6 antibodies were from Santa Cruz Biotechnology (Santa Cruz, CA); and smad2 antibody was from Invitrogen (Carlsbad, CA). TBRI inhibitor SD-208 was provided by Scios (Fremont, CA). SD-208 is a selective 2,4-disubstituted pteridine-derived TGF-β receptor I (TGF-βI) kinase inhibitor[23–28] that exhibits an in vitro specificity for TGF-βRI kinase of more than 100-fold compared with TGF-βRII kinase and at least 20-fold more than members of a panel of related protein kinases. SD-208 was diluted in dimethyl sulfoxide (DMSO; 20 mM stock solution) and kept at −20°C until use.

Cell lysis and immunoblotting

Cells were lysed in phosphorylation lysis buffer as previously described.[20] In the experiments in which the effects of SD-208 were studied, DMSO (diluent)–treated cells were used as control. Immunoblotting was performed as previously described.[20]

Immunohistochemistry

Paraffin-mounted bone marrow core biopsy sections from MDS patients and controls were obtained after informed consent. Controls had anemia from non–MDS-related causes. Slides were deparaffinized and hydrated. Mercury pigments from B5 fixative were removed by iodine-sodium thiosulfate sequences. After rinsing 3 times in PBS, all sections were immersed in 3% hydrogen peroxide for 20 minutes at room temperature to completely block endogenous peroxidases. Antigen retrieval (citrate buffer, pH 6.0) was used for all these antibodies. To prevent nonspecific binding with primary antibodies, sections were pretreated with 15% normal goat serum. After 3 washes with PBS, the sections were incubated with primary antibodies overnight at 4°C. The primary antibodies used in this study were rabbit phospho-smad2 polyclonal antibody diluted at 1:1000 dilution (Cell Signaling Technology). After 3 washes with PBS, the sections were then incubated with biotinylated goat antirabbit (Chemicon International, Temecula, CA) secondary antibody at 1:2000 dilution at room temperature for 30 minutes. Normal rabbit or mouse IgGs (Santa Cruz Biotechnology) were used as negative controls. All sections were then treated with avidin-biotin-horseradish peroxidase reagents (Vector, Burlingame, CA) and finally stained with diaminobenzidine (Research Genetic, Carlsbad, CA). After several more rinses, the sections were counterstained with hematoxylin and subsequently mounted with Permount (Fisher Scientific) mounting medium. The quantification of p-smad2 staining was analyzed by counting the total number of positively stained cells and by measuring the intensity of the positively stained cells in 5 hot fields (hot field is

defined as area of high density of p-smad2 staining) for each patient sample under 400× magnification aided by Image Pro Plus (Media Cybernetics, Bethesda, MD) software. The results were expressed as mean numbers of positively stained cells per field and mean intensity per field for each individual patient sample.

ShRNA knockdown experiments

The human lentiviral shRNAmir (pCMV-GIN-Zeo) containing the hairpin sequence TGCTGTTGACAGTGAGCGAGGTACTACGTTGAAAGACTTATAGTGAAGCCACAGATGTATAAGTC targeting TGF-βRI was obtained from Open Biosystems (Huntsville, AL). The scrambled control shRNAmir was cut out from pSM retroviral vector (Open Biosystems) by *Xho*I and *Eco*RI and ligated into lentiviral vector and used as a control. Recombinant lentiviruses were produced by transient transfection of the 293T cells with the transducing vector and 2 packaging vectors: pVSVg, a plasmid expressing the VSVg envelope gene, and pΔ8.9, a plasmid expressing the HIV-1 gag/pol gene. The supernatants were collected 48 hours after transfection. Cell lines HS-5 and K562 were transduced with the virus supernatant in the presence of 8 μg/mL polybrene, and transduced cells were identified by expression of green fluorescent protein (GFP) and sorted by fluorescence-activated cell sorting (FACS). Nucleofection of $CD34^+$ cells or MDS BM mononuclear cells (MNCs) was performed according to the manufacturer's instructions, using the Nucleofector machine (Amaxa, Cologne, Germany). The $CD34^+$ cells were thawed and cultured for 2 hours; 2×10^6 cells were resuspended in 100 μL human $CD34^+$ nucleofection solution (Amaxa). Samples were transferred into cuvettes and transfected using program U08. $CD34^+$ cells were collected, dispensed in the wells of a 24-well plate containing 1 mL prewarmed StemSpan (StemCell Technologies, Vancouver, BC), and supplemented with 100 ng/mL human FLt-3, SCF, and TPO. The lentiviral transfected $CD34^+$ cells were sorted 24 hours later according to the GFP intensity using Moflow (Becton Dickinson, San Jose, CA). Quantitative reverse-transcription–polymerase chain reaction (RT-PCR) for TBRI expression was done on total RNA from HS-5 and K562 cells obtained by RNAeasy mini kit (Qiagen, Valencia, CA). cDNA was synthesized with SuperScript Reverse Transcriptase III (Invitrogen). Real-time PCR was performed with SYBR green PCR Master Mix (Applied Biosystems, Foster City, CA), and TBRI and *GAPDH* (control) were simultaneously amplified with specific primers.

Primers for *GAPDH* were forward, 5′-cgaccactttgtcaagctca-3′ and reverse, 5′-ccctgttgctgtagccaaat-3′. Primers for TBRI were forward, 5′-tcgtctgcatctcactcat and reverse, 5′-gataaatctctgcctcacg-3′.

Meta-analysis

National Center for Biotechnology Information's (NCBI, Bethesda, MD) GEO database[29] was searched for gene expression studies on MDS and normal CD34 cells. A total of 2 MDS datasets with 69 unique MDS $CD34^+$ studies[30,31] and 57 normal $CD34^+$ datasets from 6 studies[30–34] were identified and downloaded. Fifty-nine MDS samples belonged to low-grade risk group, whereas 10 belonged to high-grade International Prognostic Scoring System (IPSS) risk group. The data were integrated using UniGene IDs.[35] Studies were done using Affymetrix U133A/B and Plus 2.0 platforms (Santa Clara, CA). After interarray quantile normalization, smad2 expression was assessed and visually represented as a heat map using R statistical software (http://www.r-project.org/).

$CD34^+$ cell proliferation and cell-cycle assays

$CD34^+$ cells, cultured in IMDM medium (Mediatech, Manassas, VA) containing 15% fetal bovine serum

(FBS; HyClone, Logan, UT) and cytokines (50 ng/mL each of SCF, TPO, and FLT-3L), were pretreated with DMSO or 0.5 μM SD-208 for 1 hour before TGF-β1 (0.5 ng/mL final concentration) was added. Cells were cultured for 7 days at 37°C/5% CO_2. On days 3, 5, and 7, cell aliquots were taken and viable cell concentration was determined using Guava ViaCount (Guava Technologies, Hayward, CA). The experiment was repeated at least 3 times (using multiple donors of $CD34^+$ cells) with similar results. Cell-cycle distribution of $CD34^+$ cells (gated with PE-conjugated CD34 antibody [BD Biosciences, San Jose, CA]) was determined on day 7 using the APC BrdU Flow Kit and the LSR-II flow cytometer (BD Biosciences) according to the manufacturer's instructions.

cDNA microarray analysis

$CD34^+$ cells were treated with DMSO or SD-208 in the presence or absence of TGF-β1. After 24 hours, total $CD34^+$ RNA was extracted using Qiagen's RNeasy kit. Details of microarray and data analysis have been described previously.[36] The data were lowess normalized[37] using the maNorm function in microarray package of Bioconductor version 1.5.8 (Fred Hutchinson Cancer Research Center, Seattle, WA). Differential expression values were expressed as the ratio of the median of background-subtracted fluorescent intensity of the experimental RNA to the median of background-subtracted fluorescent intensity of the control RNA.

Murine experiments

Transgenic mice expressing a fusion gene (Alb/TGF) consisting of modified porcine TGF-β1 cDNA under the control of the regulatory elements of the mouse albumin gene[38] were used under animal institute–approved protocol. Mice were given SD-208 in 1% methylcellulose solution by gastric lavage using a curved 14-G needle. Blood counts were analyzed by Advia (Bayer) machine. Mice femurs were flushed and bone marrows cells were used for clonogenic assays. Methocult GF M3534 (StemCell Technologies) was used to assess myeloid (granulocyte/macrophage colony-forming unit [CFU-GM]) colony formation, and Methocult SF M3436 was used for erythroid colony (erythroid burst-forming unit [BFU-E]) assessment.

TGF-β gene reporter assay

HS-5 cells were plated in 6-well plates 24 hours before transfection. Cells were transfected in triplicate with SuperFect (Qiagen) according to the manufacturer's instruction using the reporter plasmid (pGL2-3TP-Lux); plasmids that contain kinase-null TBRI (pRK5-TBRI-KR) were used as positive control.[39] pSV-B-Gal was used to normalize the transfection efficiency. After an overnight incubation, the medium was replaced with serum-free medium with or without SD-208 as necessary for the experiment. After 48 hours, cells were treated with 10 ng/mL TGF-β1. Cells were harvested 24 hours later in reporter lysis buffer (Promega, Madison, WI), and luciferase and β-galactosidase activities were determined using Dual Luciferase System (Promega).

Hematopoietic progenitor cell assays

Hematopoietic progenitor colony formation was determined by clonogenic assays in methylcellulose, as in our previous studies.[19,20] All participants in the study signed informed consent, approved by the institutional review board of UT Southwestern and Dallas VA Medical Center. Mononuclear cells were isolated from MDS patient bone marrow aspirates by Ficoll-Hypaque density gradient separation. These cells were cultured in methylcellulose media (Methocult GF H4434; StemCell Technologies) containing

recombinant human stem cell factor, granulocyte-macrophage colony-stimulating factor (GM-CSF), IL-3 and erythropoietin. Granulocyte/macrophage colony-forming units (CFU-GMs) and erythroid burst-forming units (BFU-Es) were scored on day 14 of culture.

Results

smad2 is activated in MDS bone marrow precursors

Bone marrows of 20 patients with MDS were assessed for the activation/phosphorylation state of smad2 by immunohistochemistry. Most (16 of 20) patients belonged to lower (low and Int-1 IPSS) risk category of MDS. MDS bone marrow samples were compared with age-matched controls with non-MDS causes of cytopenias (iron deficiency anemia [1], chemotherapy-related anemia [1], hyperplenism [1], drug-induced marrow suppression [1], autoimmune anemia [1], myelofibrosis [1], and unexplained cytopenias in the absence of any dysplasia [2]). Notable activation of smad2 was seen in bone marrow cells of all patients with MDS, (Figure 1A) with a greater number of positively staining cells (Figure 1B) and significantly higher intensity of nuclear staining (Figure 1C) compared with controls. Activation of smad2 was seen in all subtypes of MDS examined (7 with refractory anemia [RA]), 11 with refractory cytopenias with multilineage dysplasia [RCMD], and 2 with refractory anemia with excess blasts [RAEB]). Because smad2 is ubiquitously expressed, we also investigated the phenotypes of bone marrow cells that expressed the activated kinase. Histologic examination revealed that smad2 was activated in hematopoietic progenitors of all lineages including erythroid and myeloid precursors and even megakaryocytes.

Because sustained TGF-β signaling can also lead to up-regulation of smad2 protein, we decided to analyze its expression in a meta-analysis of publicly available microarray studies in MDS. A total of 69 unique MDS patient $CD34^+$ gene expression profiles were obtained from published studies,[30,31] integrated using UniGene protein IDs,[35] subjected to interarray normalization, and then used for analysis (Figures S1,S2 and Table S1 showing schema of meta-analysis, available on the *Blood* website; see the Supplemental Materials link at the top of the online article). Fifty-seven normal $CD34^+$ gene expression profiles were also obtained from a total of 6 studies[30–34,40] and used as controls. This strategy was shown to be a biologically valid strategy for analysis as it was able to cluster datasets based on their cell of origin and phenotype (D.S. and A.V., manuscript submitted). Our analysis of this integrated dataset demonstrated that smad2 gene was greatly up-regulated in low-grade MDS $CD34^+$ cells compared with normal cells (Figure 1D, $P < .001$). This result is based on other independent studies and confirms our histologic findings, while offering further evidence of overactivated TGF-β signaling in a large number of MDS samples.

Down-regulation of TGF β receptor I can inhibit smad2 activation in hematopoietic cells and stimulate MDS hematopoiesis

Because smad2 is phosphorylated by TGF-beta receptor I kinase (alk5 kinase, TBRI), lentiviral vectors containing shRNA targeting TBRI were developed (Figure 2A) to determine the biologic role of TGF-smad2 pathway activation in MDS hematopoiesis. The anti–TBRI-shRNA was successfully able to inhibit TBRI expression compared with scrambled control in hematopoietic (K562) and bone marrow stromal (HS-5) cell lines with stable expression of GFP^+ lentiviral construct (Figure 2B). Down-regulation of TBRI also led to inhibition of TGF-mediated smad2 activation (Figure 2C), demonstrating a functional level of TBRI inhibition with the shRNA. Further functional validation showed that introduction of anti–TBRI-shRNA in primary $CD34^+$ hematopoietic progenitors led to their resistance to TGF-β–mediated

suppression of erythroid colony formation (Figure 2D). Hematopoietic progenitors with GFP TBRI-shRNA expression also formed bigger colonies, again demonstrating resistance to TGF-β–mediated antiproliferative signals (Figure 2E).

After demonstrating TBRI as a functionally important mediator of TGF-smad2 signaling, we expressed anti–TBRI-shRNA in 5 primary MDS bone marrow patient samples and performed clonogenic assays in methycellulose. Three patients belonged to RCMD subtype, and 1 each belonged to RA and RAEB subtype. The patient with RAEB had moderate marrow fibrosis. All MDS samples demonstrated an increase in erythroid and myeloid colony formation after anti–TBRI-shRNA expression compared with scrambled control, demonstrating an important functional role of this kinase in hematopoietic suppression seen in MDS (Figure 2F).

SD-208 is an effective and functionally active inhibitor of TGF-β signaling in hematopoietic cells

Having demonstrated an important role of TBRI in TGF-smad signaling in hematopoiesis, we next wanted to test the efficacy of SD-208, a novel small molecule pyridopyrimidine inhibitor of TBRI. We first demonstrated that SD-208 was able to potently inhibit smad2 activation in myeloid hematopoietic cell lines KG-1 and K562 as well as in erythroid progenitors derived from primary BM $CD34^+$ cells (Figure 3A-C). Because the bone marrow microenvironment plays an important role in cytokine signaling and production in bone marrow failure states, we next tested the efficacy of SD-208 in human bone marrow stromal cells. SD-208 was also able to effectively inhibit TGF-smad2/3–mediated gene transcription in the bone marrow stromal cell line, HS-5. (Figure 3D) Furthermore, functional testing revealed that SD-208 was also able to abrogate the suppressive affects of TGF-β on primary human CD34 proliferation (Figure 4A). These effects were dependent on its ability to block TGF-mediated G0/G1 cell-cycle arrest in these hematopoietic progenitors (Figure 4B,C). Gene expression analysis also supported these findings by demonstrating that cell- cycle progression proteins were not down-regulated by TGF-β in the presence of SD-208 (Table 1). Immunoblotting validated these microarray finings (Figure 4E), thus demonstrating the functional ability of TBRI inhibitor in reversing TGF-mediated actions in hematopoiesis.

TBRI inhibition can improve anemia in a model of bone marrow failure

To further examine the effects of TGF-β on bone marrow function, we evaluated the hematopoietic effects of constitutive TGF secretion in a transgenic mouse expressing a fusion gene (Alb/TGF) consisting of modified porcine TGF-β cDNA under the control of the regulatory elements of the mouse albumin gene.[38] We determined that these mice become anemic at an early age (3 weeks), and histologic examination of their bone marrows reveals dysplastic megakaryocytes and focal marrow reticulin fibrosis, features commonly seen in human bone marrow failure states such as MDS (Figure 5A,B). These mice were used to determine the specificity and efficacy of SD-208 in an in vivo setting. Mice were randomized into treatment or placebo groups on the basis of pretreatment hematocrits. Blood counts were measured after 14 days of oral administration of SD-208 or vehicle. TBRI inhibitor treatment led to significant increase in hematocrit in these mice, demonstrating the specificity of SD-208 in inhibiting TGF-β signaling. (Figure 5 C). Furthermore, bone marrow progenitors of treated mice showed increased erythroid and myeloid colony forming ability compared with placebo control, thus demonstrating the efficacy of the TBRI inhibitor in rescuing hematopoietic activity in vivo (Figure 5D).

Pharmacologic inhibition of TBRI kinase can stimulate MDS hematopoiesis

Finally, we tested the ability of SD-208 in vitro in 15 MDS bone marrow samples. Most of the patients had

low-grade MDS and did not have increased blast counts (Table 2). Mononuclear cells were grown in methylcellulose with cytokines in the presence and absence of various doses of SD-208. Consistent with results seen with siRNAs, treatment with the TBRI inhibitor (Figure 6) resulted in a significant increase in erythroid (BFU-E) and myeloid (CFU–granulocytic monocytic) colony numbers (Figure 6A) These results point to a high therapeutic potential of TBRI inhibition in low-grade MDS.

Discussion

Progress in the discovery of disease-selective treatments for MDS has been challenged by the limited insight into molecular pathogenesis of the ineffective hematopoiesis seen in these disorders. Our work has shown that TGF-smad2 pathway is commonly overactivated in a variety of subtypes of MDS. Inhibition of the TGF-β receptor I kinase (TBRI) blocks smad2 activation and promotes MDS hematopoiesis in vitro, suggesting that TGF-β–smad2 signaling pathway is a functionally important inhibitory pathway in MDS.

Transforming growth factor–beta (TGF-β) is an important physiologic regulator of cell proliferation and differentiation.[41] TGF-β has been shown to affect both early and late stages of hematopoiesis and generally leads to suppressive effects on erythroid and myeloid cell proliferation[41] Deregulation of TGF-β signaling has been implicated in a variety of carcinogenesis and metastasis models, illustrating an important biologic role in oncogenesis. Because MDS is a preleukemic condition characterized by dysplastic hematopoiesis, earlier studies have also examined the role of TGF-β in this disease. Most reports to date have relied upon immunohistochemical detection of TGF-β in patient bone marrows or measurement of TGF-β levels in patient plasma. Some of these studies showed increased TGF-β in MDS,[10–13] whereas some did not observe any correlation.[14–17] As local concentrations of cytokines can be more informative than serum concentrations and immunohistochemical detection of cell surface proteins in bone marrow sections has technical limitations, we focused our studies on direct evaluation of nuclear smad2 phosphorylation in MDS bone marrows. Smad2 activation and nuclear translocation are specific and accurate markers of TGF-β signaling, and Smad2 up-regulation occurs with sustained TGF-β signaling. Thus, our results are the first to directly show evidence that TGF-β signaling is a common pathway activated in MDS and indicate that a downstream signaling biomarker can identify a valid therapeutic target.

Because MDS is a heterogeneous disease, we validated our findings in a larger number of MDS samples. We devised a meta-analytic approach using publicly available gene expression data to test our hypothesis. Recent publications have concluded that microarray data generated in different laboratories and different platforms can be compared after adequate integration and normalization.[42–47] Our database covered 6 independent studies[30–34,40] and provides further validation of our findings that is hard to achieve with single-center studies in a complex disease such as MDS. We hope that creation of this database will also help other MDS investigators.

Our findings are consistent with other work that has been done in defining molecular pathways in MDS. Our earlier data demonstrated that cytokine signaling cascades such as p38 MAPK can be functionally important in regulating hematopoietic failure in MDS.[48] It has also been shown that TGF-β can activate p38 and other MAP kinase pathways.[19,41,49] Thus our earlier results can in part be explained by overactivated TGF-β signaling in MDS. A recent clinical trial evaluating thalidomide in MDS observed that patients with increased red cell counts after treatment had a significant decrease in TGF-β levels.[9] Even though this was a small study it reinforces our findings, suggesting an important role of TGF-β signaling in ineffective hematopoiesis. In addition, our data point to a greater role of TGF-β–suppressive

signaling in low-grade MDS. The bone marrow at this stage of the disease is hypercellular and is characterized by increased rates of apoptosis. At this stage of the disease, both normal and cytogenetically abnormal hematopoietic clones are found to exist in the marrow.[50] With disease progression toward high-risk stages, normal progenitors gradually diminish, resulting in a bone marrow composed mainly of the resistant abnormal clones with an increased percentage of myeloblasts. These observations in combination with our data may allude to a pathogenic role of TGF-β signaling in suppressing hematopoiesis in normal clonal progenitors in low-grade MDS. As preponderance of leukemic clones seen in higher grade MDS is characterized by relative resistance to suppressive effects of TGF-β,[41,51–53] the therapeutic efficacy of TBRI inhibitors may be greater in low-grade disease subtypes.

Ineffective hematopoiesis is the cause of most of morbidity in patients with low-risk MDS. Two-thirds of all MDS cases are at the low-risk stage, have a lower chance of progressing to leukemia, and suffer problems mainly associated with low blood counts. Thus strategies aimed at raising blood counts are needed at this stage. The erythroid lineage is the most commonly affected hematopoietic lineage in MDS. TGF-β has recently been shown to regulate both primitive and late stages of erythropoiesis.[54] by distinct molecular processes. After smad2/3 phosphorylation by the TBRI kinase, these proteins associate with partner smads and other proteins to bind distinct DNA sequences and regulate different biologic functions. It has recently been shown that smad2-smad4 complex enters the nucleus and negatively regulates suppression of primitive erythropoiesis, whereas the smad2-TIFγ complex can regulate late stages of erythroid differentiation.[54] Thus TBRI-dependent smad2 overactivation in MDS can affect different facets of erythropoiesis and can be abrogated by inhibition of the alk5 kinase.

In addition to MDS, TGF-β has also been implicated in the pathobiology of idiopathic myelofibrosis (IMF). Due to the fibrogenic actions of TGF-β, oversecretion of this cytokine has been correlated with marrow fibrosis seen in IMF.[55,56] In addition, myelofibrosis seen after thrombopoietin overexpression in mice can be abrogated by depletion of TGF-β1 by a soluble receptor, suggesting that TGF-β secretion is an important downstream effector of marrow fibrosis in various cytokine-induced models of hematopoietic failure.[57] These data coupled with our findings provide a rationale for using inhibitors of TGF-β signaling (including TBRI inhibitors) in other bone marrow failure syndromes. TBRI selectively participates in TGF-β signaling, whereas other activin-like and TGF-β receptors can also participate in BMP and activin ligand signaling[49,58] and thus provide selective therapeutic efficacy. SD-208 is a selective 2,4-disubstituted pteridine-derived TGF-βRI kinase inhibitor[23–28] that has demonstrated specificity for this kinase. In addition, other TBRI inhibitors are in development[27,59] for various other indications such as chronic renal diseases. Our findings provide a preclinical rationale for bringing these agents into clinical trials for MDS.

Supplementary Material

[Supplemental Table and Figures]

Acknowledgments

This work was supported by National Institutes of Health (NIH, Bethesda, MD) 1R01HL082946-01 and Community Foundation of Southeastern Michigan (Detroit) J. P. McCarthy fund award (A.V.); by NIH RO1 AG029138 (L.C.P.); and by Immunooncology Training Program T32 CA009173 (L.Z.).

Footnotes

An Inside *Blood* analysis of this article appears at the front of this issue.

The online version of this article contains a data supplement.

The publication costs of this article were defrayed in part by page charge payment. Therefore, and solely to indicate this fact, this article is hereby marked “advertisement” in accordance with 18 USC section 1734.

Authorship

Contribution: L.Z. and A.N.N. designed and performed experiments and wrote the paper; D.S., J.Y.M., P.P., K.G., J.H., A.C., Y.M., T.D.B., B.D., A.M.K., T.A.N., and A.P. performed experiments; S.P., S.K., I.B., Y.Z., A.W., J.B., A.F.L., and M.B. contributed samples; S.M., L.C.P, and L.S.H. participated in design of studies; and A.V. designed experiments and wrote the paper.

Conflict-of-interest disclosure: A.N.N., J.Y.M., A.M.K., T.A.N., S.M., and L.S.H. are employees of Scios, Inc. The remaining authors declare no competing financial interests.

Correspondence: Amit Verma, Chanin 302B, Albert Einstein Cancer Center, 1300 Morris Park Ave, Bronx, NY 10461; e-mail: llun@ved:otliam.

References

1. Heaney ML, Golde DW. Myelodysplasia. N Engl J Med. 1999;340:1649–1660. [PubMed: 10341278]

2. Sanz GF, Sanz MA, Greenberg PL. Prognostic factors and scoring systems in myelodysplastic syndromes. Haematologica. 1998;83:358–368. [PubMed: 9592987]

3. Greenberg PL. Biologic nature of the myelodysplastic syndromes. Acta Haematol. 1987;78(suppl 1):94–99. [PubMed: 2829490]

4. Greenberg P, Cox C, LeBeau MM, et al. International scoring system for evaluating prognosis in myelodysplastic syndromes. Blood. 1997;89:2079–2088. [PubMed: 9058730]

5. Raza A, Gezer S, Mundle S, et al. Apoptosis in bone marrow biopsy samples involving stromal and hematopoietic cells in 50 patients with myelodysplastic syndromes. Blood. 1995;86:268–276. [PubMed: 7795232]

6. Greenberg PL. Apoptosis and its role in the myelodysplastic syndromes: implications for disease natural history and treatment. Leuk Res. 1998;22:1123–1136. [PubMed: 9922076]

7. Westwood NB, Mufti GJ. Apoptosis in the myelodysplastic syndromes. Curr Hematol Rep. 2003;2:186–192. [PubMed: 12901339]

8. Ohshima K, Karube K, Shimazaki K, et al. Imbalance between apoptosis and telomerase activity in myelodysplastic syndromes: possible role in ineffective hemopoiesis. Leuk Lymphoma. 2003;44:1339–1346. [PubMed: 12952227]

9. Zorat F, Shetty V, Dutt D, et al. The clinical and biological effects of thalidomide in patients with myelodysplastic syndromes. Br J Haematol. 2001;115:881–894. [PubMed: 11843822]

10. Allampallam K, Shetty V, Mundle S, et al. Biological significance of proliferation, apoptosis, cytokines, and monocyte/macrophage cells in bone marrow biopsies of 145 patients with myelodysplastic syndrome. Int J Hematol. 2002;75:289–297. [PubMed: 11999358]

11. Allampallam K, Shetty V, Hussaini S, et al. Measurement of mRNA expression for a variety of cytokines and its receptors in bone marrows of patients with myelodysplastic syndromes. Anticancer Res. 1999;19:5323–5328. [PubMed: 10697556]

12. Powers MP, Nishino H, Luo Y, et al. Polymorphisms in TGFbeta and TNFalpha are associated with the myelodysplastic syndrome phenotype. Arch Pathol Lab Med. 2007;131:1789–1793. [PubMed: 18081437]

13. Akiyama T, Matsunaga T, Terui T, et al. Involvement of transforming growth factor-beta and thrombopoietin in the pathogenesis of myelodysplastic syndrome with myelofibrosis. Leukemia. 2005;19:1558–1566. [PubMed: 16034467]

14. Taketazu F, Miyagawa K, Ichijo H, et al. Decreased level of transforming growth factor-beta in blood lymphocytes of patients with aplastic anemia. Growth Factors. 1992;6:85–90. [PubMed: 1591018]

15. Gyulai Z, Balog A, Borbenyi Z, Mandi Y. Genetic polymorphisms in patients with myelodysplastic syndrome. Acta Microbiol Immunol Hung. 2005;52:463–475. [PubMed: 16400883]

16. Aguayo A, Kantarjian H, Manshouri T, et al. Angiogenesis in acute and chronic leukemias and myelodysplastic syndromes. Blood. 2000;96:2240–2245. [PubMed: 10979972]

17. Yoon SY, Li CY, Lloyd RV, Tefferi A. Bone marrow histochemical studies of fibrogenic cytokines and their receptors in myelodysplastic syndrome with myelofibrosis and related disorders. Int J Hematol. 2000;72:337–342. [PubMed: 11185990]

18. Verma A, List AF. Cytokine targets in the treatment of myelodysplastic syndromes. Curr Hematol Rep. 2005;4:429–435. [PubMed: 16232378]

19. Verma A, Deb DK, Sassano A, et al. Activation of the p38 mitogen-activated protein kinase mediates the suppressive effects of type I interferons and transforming growth factor-beta on normal hematopoiesis. J Biol Chem. 2002;277:7726–7735. [PubMed: 11773065]

20. Verma A, Deb DK, Sassano A, et al. Cutting edge: activation of the p38 mitogen-activated protein kinase signaling pathway mediates cytokine-induced hemopoietic suppression in aplastic anemia. J Immunol. 2002;168:5984–5988. [PubMed: 12055203]

21. Sokol L, Cripe L, Kantarjian H, et al. Phase I/II, randomized, multicenter multicenter, dose, dose-ascension study of the p38 MAPK inhibitor ascension study of the p38 MAPK inhibitor Scio-469 in patients with myelodysplastic syndromes (MDS) 469. American Society of Hematology. 2006;108 Abstract no. 2657.

22. Wickrema A, Uddin S, Sharma A, et al. Engagement of Gab1 and Gab2 in erythropoietin signaling. J Biol Chem. 1999;274:24469–24474. [PubMed: 10455108]

23. Uhl M, Aulwurm S, Wischhusen J, et al. SD-208, a novel transforming growth factor beta receptor I kinase inhibitor, inhibits growth and invasiveness and enhances immunogenicity of murine and human glioma cells in vitro and in vivo. Cancer Res. 2004;64:7954–7961. [PubMed: 15520202]

24. Leung SY, Niimi A, Noble A, et al. Effect of transforming growth factor-beta receptor I kinase inhibitor 2,4-disubstituted pteridine (SD-208) in chronic allergic airway inflammation and remodeling. J Pharmacol Exp Ther. 2006;319:586–594. [PubMed: 16888081]

25. Gaspar NJ, Li L, Kapoun AM, et al. Inhibition of transforming growth factor beta signaling reduces pancreatic adenocarcinoma growth and invasiveness. Mol Pharmacol. 2007;72:152–161. [PubMed: 17400764]

26. Ge R, Rajeev V, Ray P, et al. Inhibition of growth and metastasis of mouse mammary carcinoma by selective inhibitor of transforming growth factor-beta type I receptor kinase in vivo. Clin Cancer Res. 2006;12:4315–4330. [PubMed: 16857807]

27. Akhurst RJ. Large- and small-molecule inhibitors of transforming growth factor-beta signaling. Curr Opin Investig Drugs. 2006;7:513–521.

28. Hayashi T, Hideshima T, Nguyen AN, et al. Transforming growth factor beta receptor I kinase inhibitor down-regulates cytokine secretion and multiple myeloma cell growth in the bone marrow microenvironment. Clin Cancer Res. 2004;10:7540–7546. [PubMed: 15569984]

29. National Center for Biotechnology Information. Gene Expression Omnibus. [Accessed March 1, 2008]. http://www.ncbi.nlm.nih.gov/geo/

30. Pellagatti A, Cazzola M, Giagounidis AA, et al. Gene expression profiles of CD34+ cells in myelodysplastic syndromes: involvement of interferon-stimulated genes and correlation to FAB subtype and karyotype. Blood. 2006;108:337–345. [PubMed: 16527891]

31. Sternberg A, Killick S, Littlewood T, et al. Evidence for reduced B-cell progenitors in early (low-risk) myelodysplastic syndrome. Blood. 2005;106:2982–2991. [PubMed: 16076868]

32. Su AI, Wiltshire T, Batalov S, et al. A gene atlas of the mouse and human protein-encoding transcriptomes. Proc Natl Acad Sci U S A. 2004;101:6062–6067. [PMCID: PMC395923] [PubMed: 15075390]

33. Oswald J, Steudel C, Salchert K, et al. Gene-expression profiling of CD34+ hematopoietic cells expanded in a collagen I matrix. Stem Cells. 2006;24:494–500. [PubMed: 16166251]

34. Eckfeldt CE, Mendenhall EM, Flynn CM, et al. Functional analysis of human hematopoietic stem cell gene expression using zebrafish. PLoS Biol. 2005;3:e254. [PMCID: PMC1166352] [PubMed: 16089502]

35. National Center for Biotechnology Information. UniGene. [Accessed March 1, 2008]. http://www.ncbi.nlm.nih.gov/sites/entrez?db=unigene.

36. Kapoun AM, Liang F, O'Young G, et al. B-type natriuretic peptide exerts broad functional opposition to transforming growth factor-beta in primary human cardiac fibroblasts: fibrosis, myofibroblast conversion, proliferation, and inflammation. Circ Res. 2004;94:453–461. [PubMed: 14726474]

37. Yang YH, Dudoit S, Luu P, et al. Normalization for cDNA microarray data: a robust composite method addressing single and multiple slide systematic variation. Nucleic Acids Res. 2002;30:e15. [PMCID: PMC100354] [PubMed: 11842121]

38. Sanderson N, Factor V, Nagy P, et al. Hepatic expression of mature transforming growth factor beta 1 in transgenic mice results in multiple tissue lesions. Proc Natl Acad Sci U S A. 1995;92:2572–2576. [PMCID: PMC42260] [PubMed: 7708687]

39. Yu L, Hebert MC, Zhang YE. TGF-beta receptor-activated p38 MAP kinase mediates Smad-independent TGF-beta responses. EMBO J. 2002;21:3749–3759. [PMCID: PMC126112]

[PubMed: 12110587]

40. Bhatia M. Molecular Signatures Orchestrating fate of Human Hematopoietic Stem Cells Originating From Different Stages of Ontogeny. http://www.ncbi.nlm.nih.gov/projects/geo/query/acc.cgi?acc=GSE3823.

41. Isufi I, Seetharam M, Zhou L, et al. Transforming growth factor-beta signaling in normal and malignant hematopoiesis. J Interferon Cytokine Res. 2007;27:543–552. [PubMed: 17651015]

42. Irizarry RA, Warren D, Spencer F, et al. Multiple-laboratory comparison of microarray platforms. Nat Methods. 2005;2:345–350. [PubMed: 15846361]

43. Dobbin KK, Beer DG, Meyerson M, et al. Interlaboratory comparability study of cancer gene expression analysis using oligonucleotide microarrays. Clin Cancer Res. 2005;11:565–572. [PubMed: 15701842]

44. Larkin JE, Frank BC, Gavras H, Sultana R, Quackenbush J. Independence and reproducibility across microarray platforms. Nat Methods. 2005;2:337–344. [PubMed: 15846360]

45. Shi L, Reid LH, Jones WD, et al. The MicroArray Quality Control (MAQC) project shows inter- and intraplatform reproducibility of gene expression measurements. Nat Biotechnol. 2006;24:1151–1161. [PMCID: PMC3272078] [PubMed: 16964229]

46. Rhodes DR, Barrette TR, Rubin MA, Ghosh D, Chinnaiyan AM. Meta-analysis of microarrays: interstudy validation of gene expression profiles reveals pathway dysregulation in prostate cancer. Cancer Res. 2002;62:4427–4433. [PubMed: 12154050]

47. Rhodes DR, Yu J, Shanker K, et al. Large-scale meta-analysis of cancer microarray data identifies common transcriptional profiles of neoplastic transformation and progression. Proc Natl Acad Sci U S A. 2004;101:9309–9314. [PMCID: PMC438973] [PubMed: 15184677]

48. Navas TA, Mohindru M, Estes M, et al. Inhibition of overactivated p38 MAPK can restore hematopoiesis in myelodysplastic syndrome progenitors. Blood. 2006;108:4170–4177. [PMCID: PMC1895446] [PubMed: 16940419]

49. Shi Y, Massague J. Mechanisms of TGF-beta signaling from cell membrane to the nucleus. Cell. 2003;113:685–700. [PubMed: 12809600]

50. Legare RD, Gilliland DG. Myelodysplastic syndrome. Curr Opin Hematol. 1995;2:283–292. [PubMed: 9372009]

51. Hu X, Zuckerman KS. Transforming growth factor: signal transduction pathways, cell cycle mediation, and effects on hematopoiesis. J Hematother Stem Cell Res. 2001;10:67–74. [PubMed: 11276360]

52. Imai Y, Kurokawa M, Izutsu K, et al. Mutations of the Smad4 gene in acute myelogeneous leukemia and their functional implications in leukemogenesis. Oncogene. 2001;20:88–96. [PubMed: 11244507]

53. Wolfraim LA, Fernandez TM, Mamura M, et al. Loss of Smad3 in acute T-cell lymphoblastic leukemia. N Engl J Med. 2004;351:552–559. [PubMed: 15295048]

54. He W, Dorn DC, Erdjument-Bromage H, Tempst P, Moore MA, Massague J. Hematopoiesis controlled by distinct TIF1gamma and Smad4 branches of the TGFbeta pathway. Cell. 2006;125:929–941.

[PubMed: 16751102]

55. Tefferi A. Myelofibrosis with myeloid metaplasia. N Engl J Med. 2000;342:1255–1265. [PubMed: 10781623]

56. Ciurea SO, Merchant D, Mahmud N, et al. Pivotal contributions of megakaryocytes to the biology of idiopathic myelofibrosis. Blood. 2007;110:986–993. [PMCID: PMC1924766] [PubMed: 17473062]

57. Gastinne T, Vigant F, Lavenu-Bombled C, et al. Adenoviral-mediated TGF-beta1 inhibition in a mouse model of myelofibrosis inhibit bone marrow fibrosis development. Exp Hematol. 2007;35:64–74. [PubMed: 17198875]

58. Massague J, Seoane J, Wotton D. Smad transcription factors. Genes Dev. 2005;19:2783–2810. [PubMed: 16322555]

59. Yingling JM, Blanchard KL, Sawyer JS. Development of TGF-beta signalling inhibitors for cancer therapy. Nat Rev Drug Discov. 2004;3:1011–1022. [PubMed: 15573100]

Figures and Tables

Figure 1

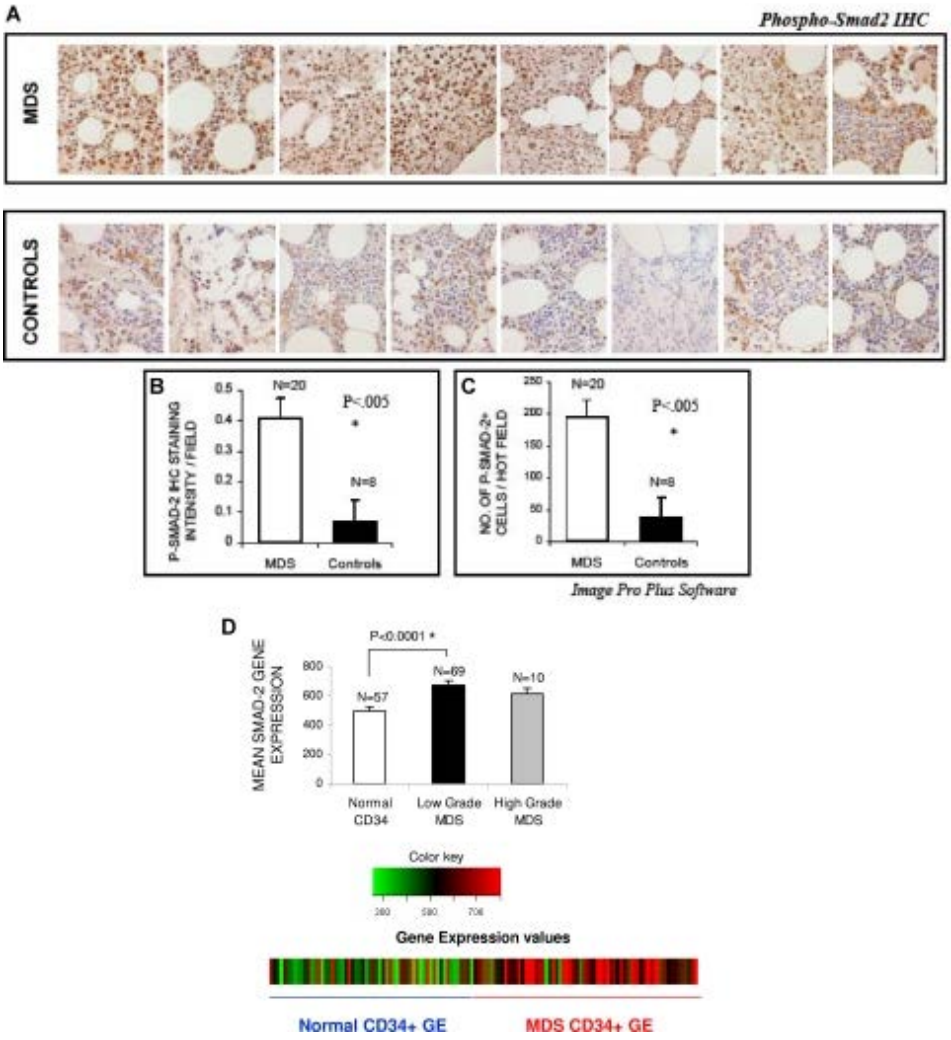

smad2 is activated in MDS. Bone marrow (BM) biopsies from patients with MDS and controls with non-MDS causes

of cytopenias were fixed and immunostained with antibody against phospho-smad2 (A). Histologic examination reveals more intense staining in MDS samples. Eight representative samples of MDS and controls are shown in panel A. The quantification of p-smad2 staining was analyzed by counting the total number of positively stained cells (B) and by measuring intensity of the positively stained cells (C) in 5 hot fields (which is defined as area of high density of p-p38 staining) and aided by Image Pro Plus (Nikon, 400×). Two-tailed *t* test shows significantly higher smad2 activation/field in MDS samples. Differences in smad2 expression were also evaluated in normalized meta-analysis of MDS $CD34^+$ (69 cases)– and normal $CD34^+$ (57 cases)–cell–derived gene expression microarray studies. Smad2 gene expression was significantly up-regulated in low-grade MDS bone marrow $CD34^+$ cells (2-tailed *t* test) (D). Error bars represent SEM.

Figure 2

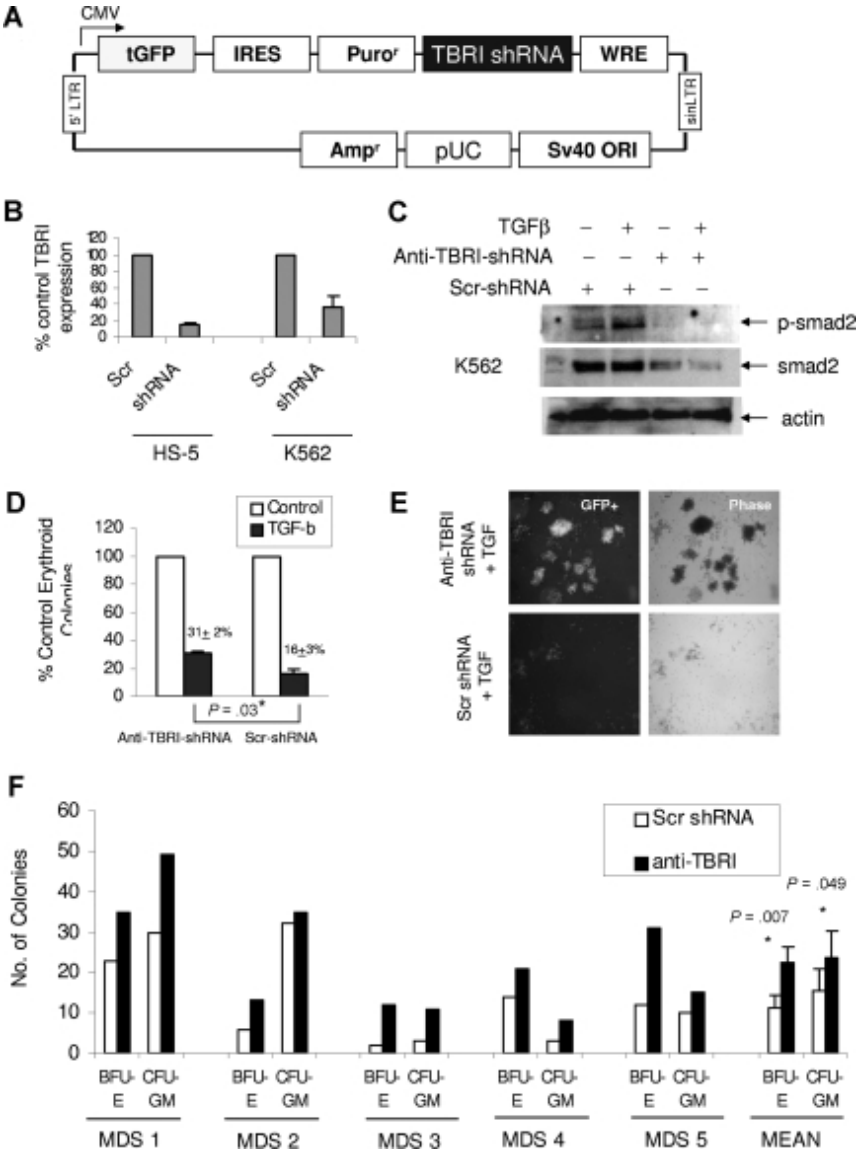

Down-regulation of TGF beta receptor I (TBRI) can inhibit smad2 activation in hematopoietic cells and stimulate MDS hematopoiesis. GFP-expressing lentiviral-based shRNA against TBRI (A) was used to knock down TBRI in hematopoietic cells. qPCR shows decrease in TBRI mRNA expression after lentiviral shRNA-TBRI infection in bone marrow stromal (HS-5) and leukemia cells (K562) compared with scrambled control (B). K562 cells with stable expression of TBRI-shRNA lentivirus show decreased smad2 phosphorylation after TGF stimulation (C). Primary $CD34^+$ progenitors were electroporated with GFP coexpressing anti–TBRI-shRNA construct and sorted after 48 hours. GFP-positive cells were grown in methylcellulose with cytokines, and erythroid colonies were counted after 14 days. TBRI-shRNA–transfected progenitors were less inhibited by TGF-β compared with cells transfected with scrambled control

shRNA (31% colonies/control vs 16% colonies/control). Expressed as means (± SEM) of 4 independent experiments (*P* = .03, 2-tailed *t* test) (D). $CD34^+$ cells transfected with anti–TBRI-shRNA also formed bigger colonies in the presence of TGF-β1 compared with controls (E; Nikon, 40×). Primary bone marrow–derived mononuclear cells from 5 patients with MDS were transfected with shRNA targeting TBRI and control, and equal numbers of cells (for each individual patient) were grown in methylcellulose with cytokines. Erythroid (BFU-E) and myeloid (CFU-GM) colonies were counted after 14 days of culture and demonstrated an increase after anti–TBRI-shRNA transfection (significance between means calculated by 2-tailed *t* test) (F).

Figure 3

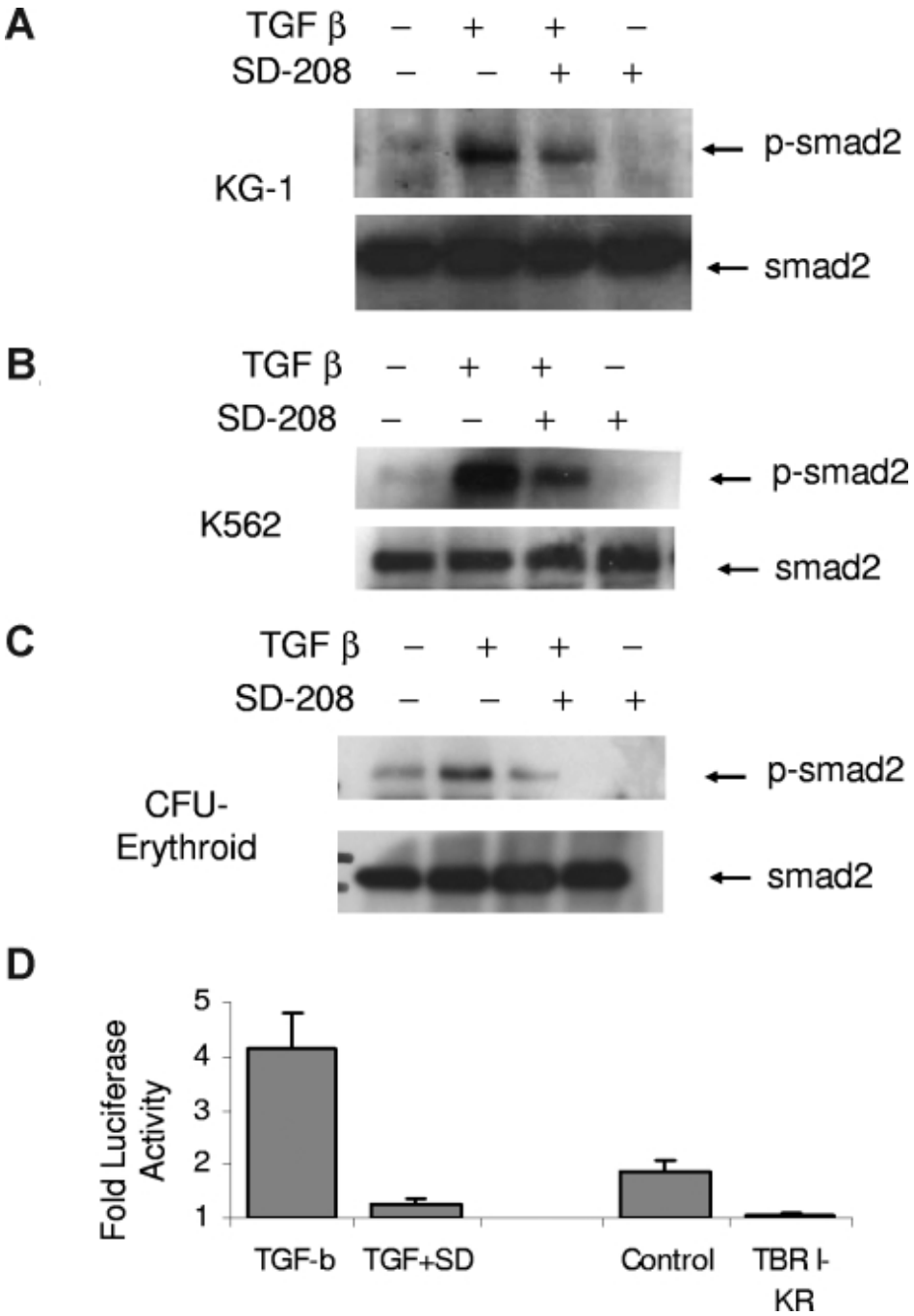

SD-208 is an inhibitor of TGF-β signaling in hematopoietic cells. Leukemic cells (K562 and KG-1) and primary hematopoietic progenitors at the colony-forming unit–erythroid stage of maturation (CFU-E) were treated with TGF-β1 (20 ng/mL) in the presence and absence of SD-208 (.5 μM) and assessed for smad2 phosphorylation by immunoblotting. SD-208 pretreament (1 hour) led to attenuation of activation/phosphorylation of smad2 (A-C). Bone marrow stroma–

derived cells (HS-5) were transfected with plasmids expressing smad binding 3TP-luciferase and β-galactisidose (transfection control) and stimulated with TGF-β1 in the presence and absence of SD-208 (dose .5 μM). TGF-β1–induced control-normalized luciferase activity was potently inhibited by SD-208. A kinase-null mutant of TGF-β receptor I (TBRI-KR) was used a positive control (D). Error bars represent SEM.

Figure 4

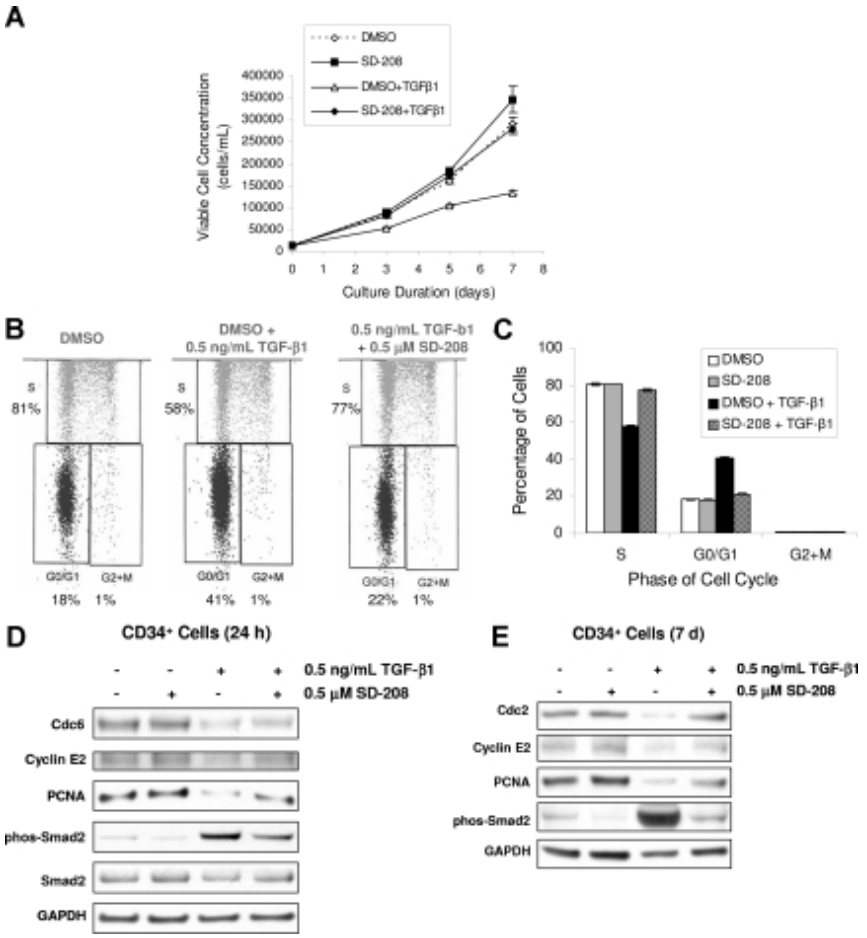

TBRI inhibition can inhibit TGF-β–mediated cell-cycle arrest of CD34$^+$ cells. Equal numbers of BM CD34$^+$ cells were grown in the presence of SCF, TPO, and FLT-3L and were pretreated with DMSO or 0.5 μM SD-208 for 1 hour before TGF-β1 (0.5 ng/mL final concentration) was added. On days 3, 5, and 7, cell aliquots were taken and viable cell concentration was determined using Guava ViaCount. The experiment was repeated at least 3 times (using multiple donors of CD34$^+$ cells) and means plus or minus SEM is shown (A). CD34$^+$ cells were treated with DMSO or SD-208 in the presence or absence of TGF-β1 for 7 days. Cell-cycle distribution of CD34$^+$ cells (gated with PE-conjugated CD34 antibody) was determined on day 7 using the APC BrdU Flow Kit and the LSR-II flow cytometer (BD Biosciences; B; representative sample, C). Error bars represent SEM. CD34$^+$ cells were treated with DMSO or SD-208 in the presence or absence of TGF-β1 as described above. After 24 hours, cDNA was prepared and hybridized on a cDNA microarray. Selected cell-cycle progression genes that were down-regulated by TGF-β by 2-fold were validated at the protein level by Western blotting. CD34$^+$ cells were treated with DMSO or SD-208 in the presence or absence of TGF-β1 as described above. Cells were collected at the indicated time points and lysed in radioimmunoprecipitation assay (RIPA) buffer. Equal protein was separated on a 10% Bis-Tris sodium dodecyl sulfate–polyacrylamide gel electrophoresis (SDS-PAGE) gel and transferred to nitrocellulose membrane and immunoblotted with the antibodies (D). GAPDH levels were used as protein loading controls, and p-smad2 was used as positive control for TGF-β1 stimulation.

Table 1

Cell-cycle progression genes down-regulated by TGF-β

Clone ID	TGF-β1 (24 h)*	SD-208 plus TGF-β1 (24 h)	Symbol	Name
P01125_G01	−2.3	1.8	CDC2	Cell division cycle 2
P01066_F04	−2.6	2.0	CDC6	Cell division cycle 6
P01091_D07	−2.0	2.2	CDC7	Cell division cycle 7
P01108_D07	−2.0	1.9	CDC45L	Cell division cycle 45-like
P01077_E02	−3.0	2.2	CCNA2	Cyclin A2
P01093_D10	−1.9	1.9	CCNE1	Cyclin E1
P01113_A07	−2.1	2.0	CCNE2	Cyclin E2
P01071_H02	−2.3	2.1	PCNA	Proliferating cell nuclear antigen
P01071_E06	−1.9	2.0	RFC3	Replication factor C3
P01102_D08	−2.1	1.8	E2F1	E2F transcription factor 1

*Fold change of gene expression over control unstimulated $CD34^+$ cells.

Figure 5

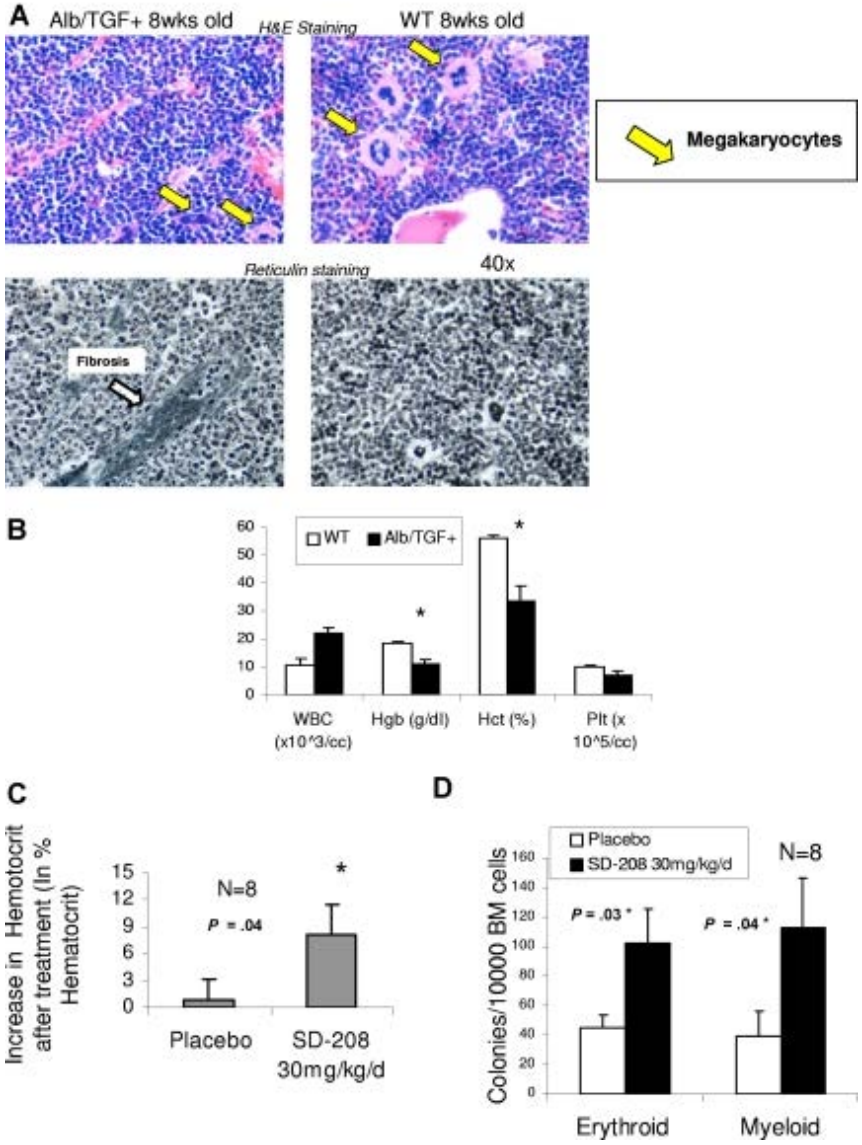

SD-208 can improve anemia in a murine model of TGF-β1–driven bone marrow failure. Mice transgenic for alb/TGF-β were killed at 8 weeks of age and their bone marrows were stained for histology (hematoxylin and eosin and reticulin stain). Transgenic mice demonstrated dysplastic micromegakaryocytes and patchy fibrosis. (A) Blood counts were analyzed at 3 weeks by Advia (Bayer) counter, and alb/TGF$^+$ transgenic mice were found to be significantly anemic compared with WT controls (n = 4; means ± SEM; Nikon, 40×) (B). alb/TGF$^+$ mice were treated with either SD-208 (30 mg/kg per day) or vehicle (placebo, daily) by gastric lavage for 14 days. Blood counts were done on the 14th day and revealed a significant rise in hematocrit after SD-208 treatment (C). The mice were killed and bone marrow cells were plated in methylcellulose with Epo (for BFU-E colonies) and IL-3, IL-6, and SCF (for CFU-GM colonies). SD-208 treatment led to a significant increase in both erythroid and myeloid colony-forming potential compared with placebo (n = 8; means ± SEM; 2-tailed *t* test; D).

Table 2

Patient characteristics

Age, y/sex	WBC count, $\times 10^9$/L	Hgb level, g/dL	Plt count, $\times 10^9$/L	Cytogenetics	Path	IPSS	Risk
89/M	4.6	9.2	169	N	CMML	0	Low
71/M	3.9	8.1	154	N	RA	0	Low
76/M	6	7	137	N	RA	0	Low

55/M	3.4	10	146	N	RA	0	Low
69/M	2.1	9.6	120	N	RCMD	0.5	Int-1
65/M	2.4	10.8	90	N	RCMD	0.5	Int-1
58/M	3	12	106	N	RA	0.5	Int-1
88/M	2.4	8.3	155	N	RCMD	0.5	Int-1
77/M	2	12	174	N	RCMD	0.5	Int-1
76/M	5.2	9.4	41	t(11:14)	RCMD	1	Int-1
70/M	4.7	12	20	del 20q	RAEB	1	Int-1
78/M	0.6	6	30	del 16 (q22)	RCMD	1.5	Int-2
48/F	5.2	8.4	95	−1q, −11q	RAEB	1.5	Int-2
73/M	1.2	9.4	88	−20q, iso 17q	RCMD	2	Int-2
65/F	3.1	8.3	54	N	RAEB	1.5	Int-2

WBC indicates white blood cell; Hgb, hemmoglobin; Plt, platelet; Path, pathological condition; and CMML, chronic myelomonocytic leukemia

Figure 6

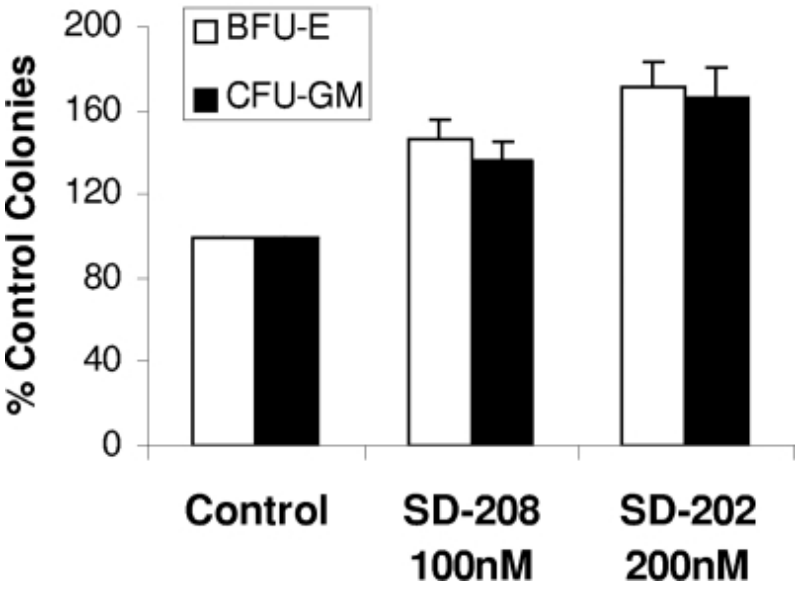

TBRI inhibition stimulates hematopoiesis in MDS. MDS bone marrow–derived MNCs from 15 patients were plated in methylcellulose and cytokines in the presence and absence of TBRI inhibitor SD-208 (100 nM and 200 nM). Colonies were scored at day 14 and results were expressed as means (± SEM) of 15 independent experiments.

blood
Leading the world in reporting basic and applied hematology research
JOURNAL OF THE AMERICAN SOCIETY OF HEMATOLOGY
Original Article | Current Issue | About Blood | Submissions | Subscriptions | Contact Us

Blood. 2013 Apr 11; 121(15): 2875–2881. PMCID: PMC3624935
Prepublished online 2013 Feb 6. doi: 10.1182/blood-2011-12-397067

miR-21 mediates hematopoietic suppression in MDS by activating TGF-β signaling

Tushar D. Bhagat,[1] Li Zhou,[1] Lubomir Sokol,[2] Rachel Kessel,[1] Gisela Caceres,[2] Krishna Gundabolu,[1] Roni Tamari,[1] Shanisha Gordon,[1] Ioannis Mantzaris,[1] Tomasz Jodlowski,[1] Yiting Yu,[1] Xiaohong Jing,[1] Rahul Polineni,[1] Kavi Bhatia,[1] Andrea Pellagatti,[3] Jacqueline Boultwood,[3] Suman Kambhampati,[4] Ulrich Steidl,[1] Cy Stein,[1] Wenjun Ju,[5] Gang Liu,[6] Paraic Kenny,[1] Alan List,[2] Markus Bitzer,[✉1,5] and Amit Verma[✉1]

[1]Albert Einstein College of Medicine, Bronx, NY;
[2]Moffitt Cancer Center, Tampa, FL;
[3]LLR Molecular Haematology Unit, NDCLS, John Radcliffe Hospital, Oxford, UK;
[4]VA Medical Center/University of Kansas Medical Center, Kansas City, MO;
[5]University of Michigan, Ann Arbor, MI; and
[6]University of Alabama, Birmingham, AL
[✉]Corresponding author.
T.D.B., L.Z., and L.S. contributed equally to this study.

Received 2011 Dec 16; Accepted 2013 Jan 24.

Key Points

- We observed that *SMAD7*, a negative regulator of TGF-β receptor-I kinase, is markedly reduced in MDS, and leads to ineffective hematopoiesis.
- Increased levels of microRNA-21 are seen in MDS and reduce *SMAD7* levels, thus overactivating TGF-β signaling.

Abstract

Myelodysplastic syndromes (MDS) are characterized by ineffective hematopoiesis that leads to peripheral cytopenias. We observed that *SMAD7*, a negative regulator of transforming growth factor–beta (TGF-β) receptor-I kinase, is markedly reduced in MDS and leads to ineffective hematopoiesis by overactivation of TGF-β signaling. To determine the cause of *SMAD7* reduction in MDS, we analyzed the 3′UTR of the gene and determined that it contains a highly conserved putative binding site for microRNA-21. We observed significantly elevated levels of miR-21 in MDS marrow samples when compared with age-matched controls. miR-21 was shown to directly bind to the 3′UTR of *SMAD7* and reduce its expression in hematopoietic cells. Next, we tested the role of miR-21 in regulating TGF-β signaling in a TGF-β–overexpressing transgenic mouse model that develops progressive anemia and dysplasia and thus serves as a model of human bone marrow failure. Treatment with a chemically modified miR-21 inhibitor led to significant increases in hematocrit and led to an increase in *SMAD7* expression in vivo. Inhibition of miR-21 also led to an increase in erythroid colony formation from primary MDS bone marrow progenitors, demonstrating its ability in stimulating hematopoiesis in vitro. Taken together, these studies demonstrate

the role of miR-21 in regulating overactivated TGF-β signaling in MDS.

Introduction

The myelodysplastic syndromes (MDS) are clonal stem cell disorders characterized by cytologic dysplasia and ineffective hematopoiesis.[1-3] Although approximately one-third of patients' disease may progress to acute leukemia, refractory cytopenias are the principal cause of morbidity and mortality in patients with MDS.[4] In fact, approximately two-thirds of patients present with lower-risk disease characterized by hypercellular marrows, with increased rates of apoptosis in the progenitor and differentiated cell compartments in the marrow.[5-8] Ineffective hematopoiesis arising from abortive maturation leads to peripheral cytopenias. Higher grade or more advanced disease categories are associated with a significant risk of leukemia transformation with a corresponding lower apoptotic index and higher percentage of marrow blasts.

Cytokines play important roles in the regulation of normal hematopoiesis, and a balance between the actions of hematopoietic growth factors and myelosuppressive factors is required for optimal production of different hematopoietic cell lineages. Excess production of inhibitory cytokines amplifies ineffective hematopoiesis inherent to the MDS clone. Transforming growth factor-beta (TGF-β) is a myelosuppressive cytokine that has been implicated in the hematopoietic suppression in MDS. The plasma levels of TGF-β have been reported to be elevated in some[9-13] but not all studies[14-17] and are supported by greater TGF-β immunohistochemical staining in selected studies. Conflicting data may arise from technical limitations of bone marrow immunohistochemical analyses of a secreted protein, as well as the biological heterogeneity of the disease itself. Thus, we investigated the role of TGF-β in MDS by direct examination of receptor signal activation to conclusively determine its role in the pathogenesis of ineffective hematopoiesis in MDS. We determined that the *SMAD2* is upregulated and overactivated in MDS bone marrow progenitors, thereby demonstrating sustained TGF-β signal activation in this disease. Because there is conflicting data about upregulation of extracellular TGF-β levels in MDS, we next sought to determine the molecular basis of TGF-β receptor-I overactivation and subsequent *SMAD2* phosphorylation/activation in this disease. We observed that *SMAD7*, a negative regulator of TGF-β receptor-I kinase, is markedly decreased in MDS and this leads to overactivation of TGF-β signal transduction, even in the absence of increased levels of extracellular TGF-β.[18] Thus, we wanted to focus on the molecular alterations that lead to *SMAD7* reduction in MDS. In the present study, we were able to show that miR-21 is increased in MDS, binds to the 3′UTR of the *SMAD7* gene, and leads to consequent upregulation of the TGF-β pathway in MDS. We were also able to show that inhibition of this microRNA is able to abrogate TGF-β signaling both in vitro and in vivo and stimulates hematopoiesis in MDS.

Materials and methods

Cells lines and reagents

Human CD34+ cells were isolated from the bone marrow of normal or MDS patients after obtaining informed consent in accordance with the Declaration of Helsinki and approval by the institutional review board of Albert Einstein College of Medicine. Bone marrow CD34+ cells from various normal donors were also obtained from AllCells (Emeryville, CA). HS-5 cell line (CRL-11882) was purchased from ATCC (Manassas, VA). TGF-β1 was bought from R&D Systems (Minneapolis, MN). The phos-SMAD2 (S465/467) and actin antibodies were from Cell Signaling Technology (Beverly, MA), and SMAD2 antibody was from Invitrogen (Carlsbad, CA), SMAD7 antibody was from ABcam (Cambridge, MA).

Locked nucleic acid (LNA)-modified miR-21 inhibitor was provided by Exiqon (Woburn, MA).

Cell lysis and immunoblotting

Cells were lysed in phosphorylation lysis buffer as previously described.[19] Immunoblotting was performed as previously described.[19]

Gene expression analysis

Gene expression data were obtained from 183 MDS CD34+ cells and 17 controls.[20] Clinical information for the cases was provided by the authors. *SMAD7* and *SMAD2* expression was represented as box plots using R statistical software.

qPCR for miR-21

Quantitative reverse-transcriptase polymerase chain reaction (RT-PCR) was done for miR-21 and endogenous control, *RNU44*, on MDS and age-matched control bone marrow mononuclear cells (MNCs) after obtaining informed consent approved by the institutional review board of Moffitt Cancer Center. Reverse-transcriptase reactions and real-time PCR were performed on Applied Biosystems Real-Time PCR instruments (Applied Biosystems, Foster City, CA) according to the manufacturer's protocols as described elsewhere.[21,22]

Murine experiments

TGF-β1 transgenic mice expressing a fusion gene (Alb/TGF) consisting of modified porcine TGF-β1 cDNA under the control of the regulatory elements of the mouse albumin gene[23] were used under animal institute–approved protocol. Mice were given LNA miR-21 inhibitors (Exiqon) at a dose of 25 mg/kg given intraperitoneally on alternate days for a total of 5 doses. Mismatched oligos were used as controls at similar doses. Blood counts were analyzed by Advia machine (Siemens, Princeton, NJ).

SMAD7 gene reporter assay

HS-5 cells were plated in 6-well plates 24 hours before transfection. Cells were transfected in triplicate with SuperFect (Qiagen, Alameda, CA) according to the manufacturer's instructions.[24] To generate SMAD7 3′UTR mutants containing mutations in the conserved miR-21 binding site, site-directed mutagenesis was performed using the wild-type 3′UTR as the template. In the 3′UTR mutant, the nucleotide sequence complementary to nt 2–5 of miR-21 was mutated to the same sequence as that in miR-21 (from AGCT to TCGA). Luciferase reporters containing wild-type and mutant 3′UTR of *SMAD7* gene were used for transfection with Pre-miR miR-21 precursors (Ambion, Invitrogen) or controls (30 nM). The generation of wild-type and mutant constructs has been described previously.[25] Cells were harvested 24 hours later in reporter lysis buffer, and luciferase and renilla activities were determined using Dual Luciferase System (Promega, Madison, WI).

miR-21 overexpression

A plasmid-encoding miR-21 and green fluorescent protein (GFP) in the pMIF-cGFP-Zeo lentiviral vector (Systems Biosciences, Mountain View, CA) was introduced into cells by nucleofection. The empty pMIF-cGFP-Zeo vector, encoding only GFP, was used as a negative control.

Hematopoietic progenitor cell assays

Hematopoietic progenitor colony formation was determined by clonogenic assays in methylcellulose, as in our previous studies.[19,26] All participants in the study signed informed consent, approved by the institutional review board of Albert Einstein College of Medicine. Granulocyte/macrophage colony-forming units (CFU-GM) and erythroid burst-forming units (BFU-E) from bone marrow samples were scored on day 14 of the culture.

Fluorescence in situ hybridization

After 14 days of methylcellulose culture, cells were isolated from the plates and cytospun on microscopic slides. The cells on the slides were fixed in Carnoy's solution. The following dual color probes (Abbott Molecular, Abbott Park, IL) were used to detect 7q deletions and 5q deletions: LSI D7S522 (7q31) SpectrumOrange/CEP7 SpectrumGreen, EGR-1 SpectrumOrange/D5S721/D5S23 SpectrumGreen. Fluorescence in situ hybridization was performed according to the manufacturer's instructions. Cells were counterstained with 4′6-diamidino-2-phenylindole and examined on a Zeiss Axioplan 2 fluorescence microscope (Zeiss, North Chesterfield, VA).

Results

SMAD7 is reduced in bone marrow progenitors in MDS

SMAD7 is a negative regulator of the TGF-β signaling pathway and inhibits the activity of the TGF-β receptor-I kinase. We analyzed the expression of *SMAD7* in a large gene expression dataset obtained from bone marrow CD34+–selected samples from MDS patients[20] We found that *SMAD7* is significantly reduced in these samples when compared with healthy controls (Figure 1, mean log2 expression 8.31 in controls vs 6.32 in MDS samples, false discovery rate < 0.1, Benjamin Hochberg correction multiple testing, Student's *t*-test < 0.001). Furthermore, *SMAD2*, the effector SMAD protein for TGF-β signaling was found to be increased in the same samples (Figure 1B, mean log2 expression 8.4 in controls vs 8.8 in MDS samples, false discovery rate < 0.1, Benjamin Hochberg correction multiple testing, Student's *t*-test < 0.001), demonstrating the sustained activation of TGF-β pathway in these samples. Subset analysis revealed striking *SMAD7* reduction in all subsets of MDS examined (Figure 1A). Correlation of *SMAD7* levels with clinical parameters did not reveal any associations with age, sex, or cytogenetics, revealing it to be a pervasive finding in MDS.

microRNA-21 is increased in MDS and has a putative binding site on the *SMAD7* 3′UTR

microRNAs have been implicated in the pathogenesis of cancer[27] and have also recently been shown to be dysregulated in cases of MDS.[21] To evaluate whether any of these aberrantly expressed microRNAs could target *SMAD7*, we evaluated the 3′UTR of the transcript and found putative binding sites for various microRNAs (Figure 2A). miR-21 was found to have a highly conserved binding site in the 3′UTR of *SMAD7* and was also one of the microRNAs aberrantly expressed in a genome-wide analysis of 41 MDS samples (Figure 2B).[21] Thus, we evaluated the expression of miR-21 in primary MDS bone marrow samples (N = 19; 10 low-risk, 9 high-risk MDS, supplemental Table 1) by quantitative RT-PCR and compared it with age-matched controls (N = 13). miR-21 levels were significantly increased in MDS when compared with controls, and the mean expression was more than fourfold higher (Student's *t*-test, $P = .03$) (Figure 2C). Both lower-risk MDS (low and Int-1 International Prognostic Scoring System) and higher-risk MDS (Int-2 and high International Prognostic Scoring System) had significantly higher expression when compared with controls (Student's *t*-test, $P < .05$).

miR-21 binds directly to 3′UTR of *SMAD7*, reduces the expression of *SMAD7*, and inhibits erythroid colony formation

We next wanted to determine whether miR-21 expression can decrease *SMAD7* expression and whether this effect is caused by direct interaction of miR-21 with the *SMAD7* 3′UTR. A luciferase reporter containing the 3′UTR segment containing predicted microRNA interaction sites was used to analyze the effect of miR-21 on *SMAD7* gene transcription in bone marrow stromal HS-5 cells. The nucleotide sequence complementary to nts 2–5 of miR-21 binding site in the 3′UTR of *SMAD7* was mutated to the same sequence as that in miR-21 (from AGCT to TCGA)[25] (Figure 3A). Dual luciferase activity was measured and showed decreased SMAD7 luciferase activity caused by expression of miR-21 compared with cells transfected with control mimics. This was abrogated by mutation in its binding site on the UTR (Student's *t*-test, $P = .001$), demonstrating a direct effect of miR-21 on the 3′UTR of *SMAD7* (Figure 3A).

Subsequently, the effect of miR-21 on *SMAD7* expression was tested by using a chemically modified LNA inhibitor that led to decreased levels of miR-21 transcripts (Figure 4A) when compared with mismatched control. We observed that inhibition of miR-21 led to an increase in *SMAD7* protein expression in leukemic cell lines and in primary MDS patient samples (Figure 4B). Inhibition of miR-21 also led to decreased phosphorylation/activation of *SMAD2* in a MDS patient sample (Figure 4C). Next, we tested the functional role of miR-21 in regulating the effects of TGF-β on normal hematopoiesis and the role of *SMAD7* in regulating these effects. CD34+ cells were transfected with shRNAs against *SMAD7* and controls as performed previously,[18] sorted for GFP expression, and then treated with TGF-β in the presence and absence of the miR-21 inhibitor. We observed that miR-21 inhibition was able to abrogate the inhibitory responses of TGF-β on erythroid colony formation from primary human CD34+ stem cells that were transfected with scrambled control shRNAs (Figure 4D). This effect was not seen in cells transfected with shRNAs against SMAD7.

Furthermore, we also overexpressed miR-21 in separate experiments by using lentiviral vector-encoding miR-21 precursors (pMIF-cGFP-Zeo), along with a control vector that expressed only GFP. Overexpression of miR-21 led to decreased *SMAD7* protein levels in leukemic cells (Figure 4E) and led to quantitative and qualitative reduction in erythroid colony formation from primary CD34+ cells (Figure 4F-G). Taken together, these data demonstrate that miR-21 potentiates TGF-β signaling in hematopoietic cells via downregulation of SMAD7.

Inhibition of miR-21 can improve anemia in a model of TGF-β–driven bone marrow failure

To test the role of miR-21 in regulating TGF-β signaling in vivo, we used chemically modified inhibitors of miR-21 and tested them in a transgenic mouse expressing a fusion gene (Alb/TGF) consisting of modified porcine TGF-β cDNA under the control of the regulatory elements of the mouse albumin gene.[23] We have shown that these mice constitutively secrete TGF-β, become anemic, and have histologic marrow findings that mimic human MDS, thus serving as an in vivo model of bone marrow failure.[28] These mice were randomized into a treatment or placebo group on the basis of pretreatment hemotocrit levels. Blood counts were measured after administration of miR-21 inhibitor or control. miR-21 inhibitor treatment led to increased expression of *SMAD7* and inhibition of constitutive *SMAD2* activation in murine bone marrow (see Figure 5C). Mice treated with miR-21 inhibitor had a significant increase in hematocrit (Figure 5A) and were able to form more erythroid colonies from marrow-derived cells (Figure 5B) when compared with control (Student's *t*-test, $P < .05$). These results demonstrate the role of miR-21 inhibition in inhibiting TGF-β signaling in vivo.

Inhibition of miR-21 can stimulate MDS hematopoiesis

Finally, we tested the ability of chemically modified (LNA) miR-21 inhibitor in vitro in 5 primary MDS bone marrow samples. These included different subtypes of MDS (Table 1). Mononuclear cells from the bone marrow were grown in methylcellulose with cytokines in the presence of miR-21 inhibitor and control. Treatment with the miR-21 inhibitor resulted in a significant increase in erythroid (BFU-E) colony numbers in all patients (results depicted as means in Figure 6A and Table 1). miR-21 inhibitor treatment did not result in any significant increase in colony formation from healthy controls (Figure 6B). Karyotypic analysis of colonies from 2 MDS samples revealed a reduction in percentage of cells, with cytogenetic alterations in miR-21 inhibitor–treated cells when compared with controls (20% in treated vs 29% in controls for 5q- deletion; 3% in treated vs 11% in controls for 7q- deletion). In addition to confirming the findings from our studies in mice, these results point to the potential stimulatory effect of miR-21 inhibition on MDS hematopoiesis.

Discussion

The discovery of effective treatments for MDS has been challenged by the limited insight into molecular pathogenesis of the ineffective hematopoiesis seen in these disorders. Even though TGF-β levels have been shown to be elevated in a subset of MDS cases, our previous work has shown that intracellular signaling is activated in a large proportion of cases. Furthermore, we demonstrated that *SMAD7* downregulation may be the key mechanism driving the suppression of hematopoiesis in MDS via overactivation of the TGF-*SMAD2* pathway. This would also explain increased TGF-β signal transduction even in the absence of large amounts of circulating TGF-β that have been observed in various studies in MDS patients.[14-17] In the present study, we determined the reasons for downregulation of *SMAD7* in MDS and observed that miR-21 can bind to the 3′UTR region of the *SMAD7* gene, reduce its expression, and potentiate TGF-β signaling in hematopoietic cells. Furthermore, inhibition of miR-21 can stimulate hematopoiesis in vitro and in vivo, thus demonstrating a critical role of this microRNA in regulation of myelosuppresive pathways in MDS.

SMAD7 is an important regulator of TGF-β signaling and its dysregulation has been implicated in many disease and cancer models.[29] Genome-wide association studies have shown that polymorphisms in the *SMAD7* gene are some of the most significant genetic alterations[30] in colorectal cancer. A recent study showed that decreased *SMAD7* is also seen in idiopathic pulmonary fibrosis and contributes to TGF-β–mediated fibrosis seen in this disease.[25] Our study demonstrates that *SMAD7* reduction is seen in a large number of MDS samples and points to its role in hematopoietic failure seen in this disease. The bone marrow at earlier stages of MDS is hypercellular and is characterized by ineffective hematopoiesis affecting both stem and progenitor cells. Because TGF-β is a critical regulator of hematopoiesis and affects both proliferation and differentiation of stem cells,[31] an aberrant increase in TGF-β signaling can potentially explain the changes seen in MDS.

There could be many possible reasons for *SMAD7* reduction in MDS. Even though the deletion of chromosome 18/18q, where the *SMAD7* gene is located, was noticed to be a common deletion in MDS,[32] it is only seen in a small proportion of patients with the disease. Furthermore, even though splicing mutations have recently been discovered in MDS,[33] it is possible that splicing abnormalities can also affect *SMAD7* transcripts, even though this information is not yet available. Because microRNAs are important regulators of genes, we decided to examine miR-mediated degradation of *SMAD7* in MDS. We were able to show that miR-21 directly binds to the *SMAD7* 3′UTR region and regulated TGF-β signaling. miR-21 has been

well studied in cancer and has been shown to influence a variety of targets including PTEN, PLAG1, and NFIB among others. A recent study demonstrated that miR-21–mediated degradation of *SMAD7* was seen in pulmonary tissue and led to increased TGF-β–mediated fibrosis in idiopathic lung fibrosis.[25] We show that this phenomenon can be seen in a hematologic disease and can explain the reduced SMAD7 levels seen in bone marrow progenitors. Our findings also raise the question of why miR-21 is found to be upregulated in MDS. In recent studies, the miR-21 gene locus has been shown to contain STAT3 binding sites.[34] Furthermore, STAT3 has also been shown to directly lead to miR-21 upregulation in immune cells.[34] Our genomic analysis of hematopoietic stem cells in MDS demonstrated that STAT3 is selectively upregulated in these cells. Thus, it is possible that this leads to miR-21 upregulation seen by us in MDS that in turn enhances TGF-β signaling that leads to ineffective hematopoiesis.

Most importantly, our results demonstrate that the activation of the TGF-β pathway by *SMAD7* reduction in MDS can be abrogated by miR-21 inhibition both in vitro and in vivo. Ineffective hematopoiesis and anemia cause most of the morbidity in patients with MDS. Two-thirds of all MDS patients are at the low-risk stage of disease, have a lower chance of the disease progressing to leukemia, and have problems associated primarily with low red blood cell counts. Because TGF-β has been specifically shown to regulate both the early and late stages of erythropoiesis,[31] miR-21 can be predicted to affect red cell production in particular, as was seen in the present study. Thus, taken together our findings support the exploration of miR-21 inhibitors in future preclinical and clinical studies in MDS.

Supplementary Material

Supplemental Table:

Acknowledgments

This work was supported by a Leukemia and Lymphoma Society Translational Research grant, the American Cancer Society (RSG-09-037), the Gabrielle Angel foundation, the Immunology and Immunooncology Training Program (T32 CA009173), the Partnership for Cures, the Department of Defense, National Institutes of Health (R01HL082946, R01HL116336), Leukaemia and Lymphoma Research UK, and a Carl Gottschalk Research Scholarship from the American Society of Nephrology.

Footnotes

The online version of this article contains a data supplement.

The publication costs of this article were defrayed in part by page charge payment. Therefore, and solely to indicate this fact, this article is hereby marked “advertisement” in accordance with 18 USC section 1734.

Authorship

Contribution: T.D.B., L.Z., L.S., R.K., G.C., K.G., R.T., S.G., I.M., T.J., X.J., R.P., and K.B. performed research; Y.Y. analyzed the data and provided statistical support; A.P., J.B., and S.K. contributed samples and gene expression data; U.S., C.S., W.J., G.L., P.K., and A.L. contributed samples and reagents; and T.D.B., M.B., and A.V. wrote the paper.

Conflict-of-interest disclosure: The authors declare no competing financial interests.

Correspondence: Amit Verma, Chanin 302B, Albert Einstein Cancer Center, 1300 Morris Park Ave, Bronx,

NY 10461; e-mail: llun@ved:otliam; or Markus Bitzer, Internal Medicine/Nephrology, University of Michigan, MSRB 2, 1570C, 1150 W. Medical Center Dr, Ann Arbor, MI 48105-5676; e-mail: llun@ved:otliam.

References

1. Heaney ML, Golde DW. Myelodysplasia. N Engl J Med. 1999;340(21):1649–1660. [PubMed: 10341278]

2. Sanz GF, Sanz MA, Greenberg PL. Prognostic factors and scoring systems in myelodysplastic syndromes. Haematologica. 1998;83(4):358–368. [PubMed: 9592987]

3. Greenberg PL. Biologic nature of the myelodysplastic syndromes. Acta Haematol. 1987;78(Suppl 1):94–99. [PubMed: 2829490]

4. Greenberg P, Cox C, LeBeau MM, et al. International scoring system for evaluating prognosis in myelodysplastic syndromes. Blood. 1997;89(6):2079–2088. [PubMed: 9058730]

5. Raza A, Gezer S, Mundle S, et al. Apoptosis in bone marrow biopsy samples involving stromal and hematopoietic cells in 50 patients with myelodysplastic syndromes. Blood. 1995;86(1):268–276. [PubMed: 7795232]

6. Greenberg PL. Apoptosis and its role in the myelodysplastic syndromes: implications for disease natural history and treatment. Leuk Res. 1998;22(12):1123–1136. [PubMed: 9922076]

7. Westwood NB, Mufti GJ. Apoptosis in the myelodysplastic syndromes. Curr Hematol Rep. 2003;2(3):186–192. [PubMed: 12901339]

8. Ohshima K, Karube K, Shimazaki K, et al. Imbalance between apoptosis and telomerase activity in myelodysplastic syndromes: possible role in ineffective hemopoiesis. Leuk Lymphoma. 2003;44(8):1339–1346. [PubMed: 12952227]

9. Zorat F, Shetty V, Dutt D, et al. The clinical and biological effects of thalidomide in patients with myelodysplastic syndromes. Br J Haematol. 2001;115(4):881–894. [PubMed: 11843822]

10. Allampallam K, Shetty V, Mundle S, et al. Biological significance of proliferation, apoptosis, cytokines, and monocyte/macrophage cells in bone marrow biopsies of 145 patients with myelodysplastic syndrome. Int J Hematol. 2002;75(3):289–297. [PubMed: 11999358]

11. Allampallam K, Shetty V, Hussaini S, et al. Measurement of mRNA expression for a variety of cytokines and its receptors in bone marrows of patients with myelodysplastic syndromes. Anticancer Res. 1999;19(6B):5323–5328. [PubMed: 10697556]

12. Powers MP, Nishino H, Luo Y, et al. Polymorphisms in TGFbeta and TNFalpha are associated with the myelodysplastic syndrome phenotype. Arch Pathol Lab Med. 2007;131(12):1789–1793. [PubMed: 18081437]

13. Akiyama T, Matsunaga T, Terui T, et al. Involvement of transforming growth factor-beta and thrombopoietin in the pathogenesis of myelodysplastic syndrome with myelofibrosis. Leukemia. 2005;19(9):1558–1566. [PubMed: 16034467]

14. Taketazu F, Miyagawa K, Ichijo H, et al. Decreased level of transforming growth factor-beta in blood

lymphocytes of patients with aplastic anemia. Growth Factors. 1992;6(1):85–90. [PubMed: 1591018]

15. Gyulai Z, Balog A, Borbényi Z, et al. Genetic polymorphisms in patients with myelodysplastic syndrome. Acta Microbiol Immunol Hung. 2005;52(3-4):463–475. [PubMed: 16400883]

16. Aguayo A, Kantarjian H, Manshouri T, et al. Angiogenesis in acute and chronic leukemias and myelodysplastic syndromes. Blood. 2000;96(6):2240–2245. [PubMed: 10979972]

17. Yoon SY, Li CY, Lloyd RV, et al. Bone marrow histochemical studies of fibrogenic cytokines and their receptors in myelodysplastic syndrome with myelofibrosis and related disorders. Int J Hematol. 2000;72(3):337–342. [PubMed: 11185990]

18. Zhou L, McMahon C, Bhagat T, et al. Reduced SMAD7 leads to overactivation of TGF-beta signaling in MDS that can be reversed by a specific inhibitor of TGF-beta receptor I kinase. Cancer Res. 2011;71(3):955–963. [PMCID: PMC3032816] [PubMed: 21189329]

19. Verma A, Deb DK, Sassano A, et al. Cutting edge: activation of the p38 mitogen-activated protein kinase signaling pathway mediates cytokine-induced hemopoietic suppression in aplastic anemia. J Immunol. 2002;168(12):5984–5988. [PubMed: 12055203]

20. Pellagatti A, Cazzola M, Giagounidis A, et al. Deregulated gene expression pathways in myelodysplastic syndrome hematopoietic stem cells. Leukemia. 2010;24(4):756–764. [PubMed: 20220779]

21. Sokol L, Caceres G, Volinia S, et al. Identification of a risk dependent microRNA expression signature in myelodysplastic syndromes. Br J Haematol. 2011;153(1):24–32. [PMCID: PMC4294220] [PubMed: 21332710]

22. Bitzer M, Ju W, Jing X, et al. Quantitative analysis of miRNA expression in epithelial cells and tissues. Methods Mol Biol. 2012;820:55–70. [PubMed: 22131025]

23. Sanderson N, Factor V, Nagy P, et al. Hepatic expression of mature transforming growth factor beta 1 in transgenic mice results in multiple tissue lesions. Proc Natl Acad Sci U S A. 1995;92(7):2572–2576. [PMCID: PMC42260] [PubMed: 7708687]

24. Yu L, Hébert MC, Zhang YE. TGF-beta receptor-activated p38 MAP kinase mediates Smad-independent TGF-beta responses. EMBO J. 2002;21(14):3749–3759. [PMCID: PMC126112] [PubMed: 12110587]

25. Liu G, Friggeri A, Yang Y, et al. miR-21 mediates fibrogenic activation of pulmonary fibroblasts and lung fibrosis. J Exp Med. 2010;207(8):1589–1597. [PMCID: PMC2916139] [PubMed: 20643828]

26. Verma A, Deb DK, Sassano A, et al. Activation of the p38 mitogen-activated protein kinase mediates the suppressive effects of type I interferons and transforming growth factor-beta on normal hematopoiesis. J Biol Chem. 2002;277(10):7726–7735. [PubMed: 11773065]

27. Croce CM. Causes and consequences of microRNA dysregulation in cancer. Nat Rev Genet. 2009;10(10):704–714. [PMCID: PMC3467096] [PubMed: 19763153]

28. Zhou L, Nguyen AN, Sohal D, et al. Inhibition of the TGF-beta receptor I kinase promotes hematopoiesis in MDS. Blood. 2008;112(8):3434–3443. [PMCID: PMC2569182] [PubMed: 18474728]

29. Akhurst RJ. TGF beta signaling in health and disease. Nat Genet. 2004;36(8):790–792.

[PubMed: 15284845]

30. Tenesa A, Farrington SM, Prendergast JG, et al. Genome-wide association scan identifies a colorectal cancer susceptibility locus on 11q23 and replicates risk loci at 8q24 and 18q21. Nat Genet. 2008;40(5):631–637. [PMCID: PMC2778004] [PubMed: 18372901]

31. He W, Dorn DC, Erdjument-Bromage H, et al. Hematopoiesis controlled by distinct TIF1gamma and Smad4 branches of the TGFbeta pathway. Cell. 2006;125(5):929–941. [PubMed: 16751102]

32. Haase D, Germing U, Schanz J, et al. New insights into the prognostic impact of the karyotype in MDS and correlation with subtypes: evidence from a core dataset of 2124 patients. Blood. 2007;110(13):4385–4395. [PubMed: 17726160]

33. Yoshida K, Sanada M, Shiraishi Y, et al. Frequent pathway mutations of splicing machinery in myelodysplasia. Nature. 2011;478(7367):64–69. [PubMed: 21909114]

34. Iliopoulos D, Jaeger SA, Hirsch HA, et al. STAT3 activation of miR-21 and miR-181b-1 via PTEN and CYLD are part of the epigenetic switch linking inflammation to cancer. Mol Cell. 2010;39(4):493–506. [PMCID: PMC2929389] [PubMed: 20797623]

Figures and Tables

Figure 1

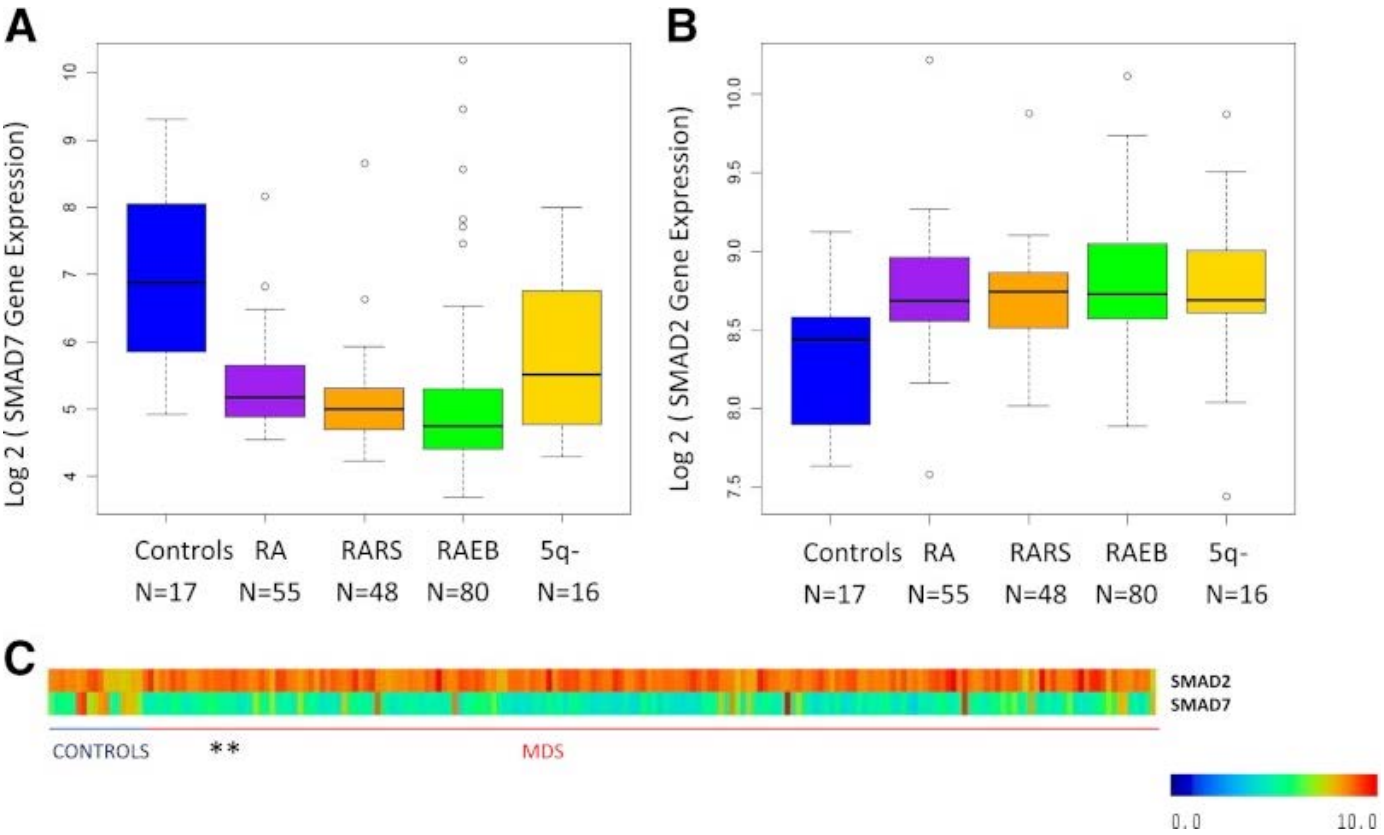

***SMAD7* expression is significantly decreased in MDS CD34+ cells.** (A) SMAD7 expression in 183 samples of MDS CD34+ cells and 17 healthy controls reveals reduction in all subsets of MDS. (false discovery rate < 0.1, Benjamin Hochberg correction multiple testing). (B) *SMAD2*, the effector SMAD protein for TGF-β signaling, was found to be increased in the same samples. (C) Heatmaps showing expression values for both genes. (The 5q- patients were a subset

of the RA patient cohort.)

Figure 2

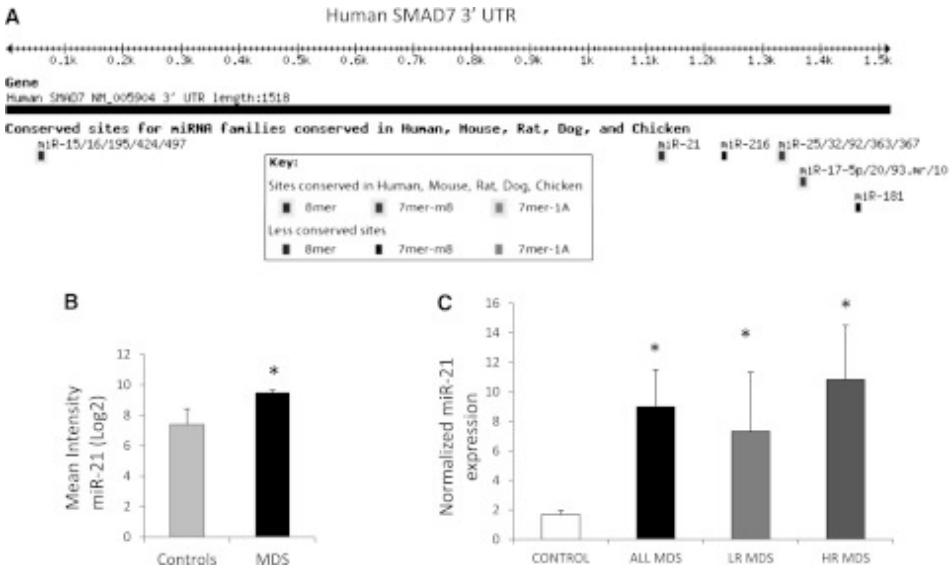

miR-21 has a putative binding site on the *SMAD7* 3′UTR and is overexpressed in MDS. (A) Targetscan software predicts a strong possibility of miR-21 binding site at position 1122 of the *SMAD7* 3′UTR with a highly conserved site. (B) Microarray analysis of 41 untreated MDS marrow samples were compared with 10 age-matched controls[21] and demonstrate upregulation of miR-21 (mean intensity ± SEM, Student's *t*-test, *P* = .001). (C) Quantitative RT-PCR was done for miR-21 and endogenous control, *RNU44*, on 19 MDS and 13 age-matched control bone marrow MNCs using the Ambion Taqman miroRNA assay kit. MDS samples had significantly higher expression of miR-21 (*Student's *t*-test, *P* = .04). Both lower- and higher-risk MDS (low-risk MDS, N = 10, *P* value = .04; high-risk MDS, N = 9, *P* = .03, Student's *t*-test) had higher mean expression when compared with controls.

Figure 3

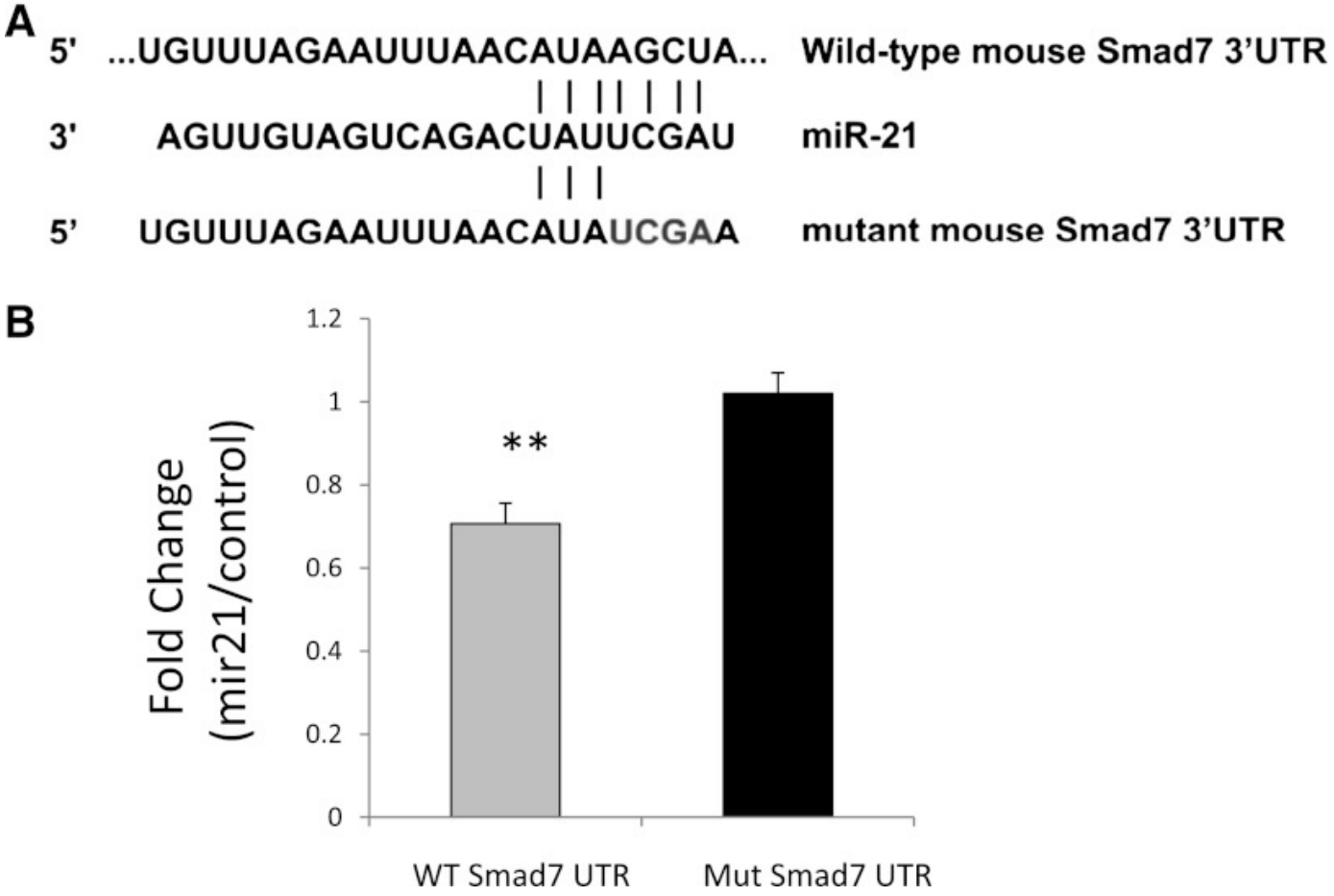

miR-21 binds to *SMAD7* 3′UTR. (A) The nucleotide sequence complementary to nt 2–5 of miR-21 in the 3′UTR of *SMAD7* was mutated to the same sequence as that in miR-21 (from AGCT to TCGA). (B) Luciferase reporters containing wild-type and mutant 3′UTR of the *SMAD7* gene were used for transfection with control miRNA or miR-21 precursors into bone marrow stromal HS-5 cells. Dual luciferase activity was measured and shows decreased luciferase activity caused by miR-21 that is abrogated by mutation in its binding site on the UTR (Student's *t*-test, $P = .001$) compared with cells transfected with control mimics.

Figure 4

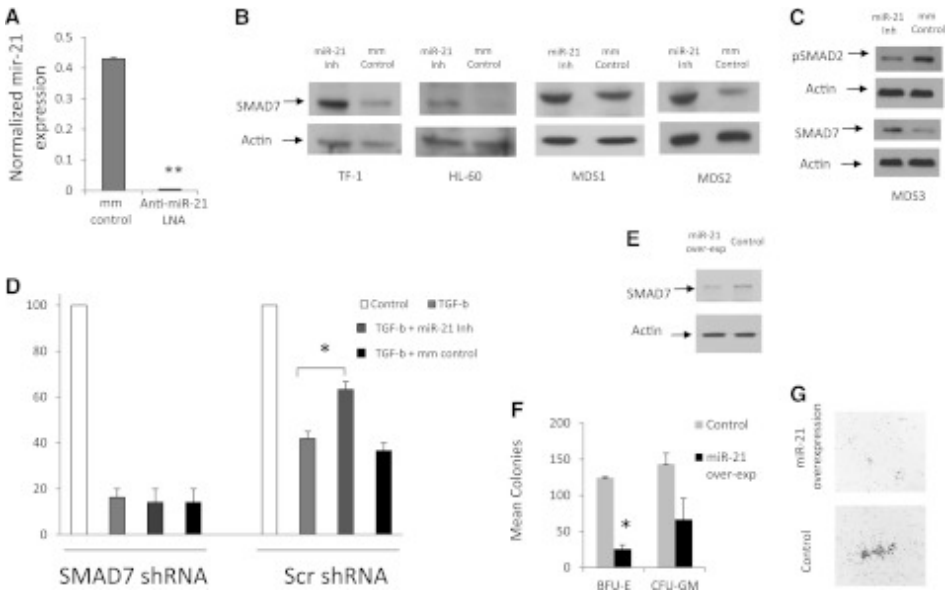

Inhibition of miR-21 can abrogate the effects of TGF-β on hematopoietic cells. miR-21 levels were measured in leukemic K562 cells after 48-hour treatment with LNA inhibitor of miR-21 and compared with mismatched control (mm control). miR-21 transcripts were significantly decreased after LNA treatment (50 mM) as measured by quantitative RT-PCR (mean ± SEM of 2 experiments, Student's *t*-test, $P < .001$). (B) SMAD7 protein expression is increased after miR-21 inhibition (50 mM, 48-hour treatment) in HL-60, TF-1 cell lines and in leukocytes from 2 MDS patients, as shown by immunoblotting. Actin was used as a protein-loading control. (C) miR-21 inhibitor treatment leads to decreased *p*-SMAD2 in MDS leukocytes when compared with mismatched-control LNAs (50 mM). (D) Primary CD34+ progenitors were nucleofected with GFP coexpressing anti-SMAD7 (or scrambled control) shRNA constructs[18] and sorted after 24 hours. GFP-positive cells were grown in methylcellulose in the presence and absence of TGF-β (20 ng/mL) and miR-21 inhibitor (50 mM), and erythroid colonies were counted after 14 days. miR-21 inhibitor treatment abrogates the inhibitory effects of TGF-β on erythroid colonies (mean ± SEM of 2 independent experiments, Student's *t*-test, $P = .04$) in cells that were transfected with scrambled shRNA controls. SMAD7 shRNA–transfected progenitors did not demonstrate any reversal of TGF-β–induced inhibition after miR-21 inhibitor treatment. (E) miR-21 and GFP were co-overexpressed in leukemic K562 cells using the pMIF-cGFP-Zeo vector, leading to decreased levels of *SMAD7* as detected by immunoblotting when compared with the GFP-only control. (F) Primary CD34+ progenitors were nucleofected with miR-21and GFP or with the GFP-only control and sorted after 24 hours. GFP-positive cells were grown in methylcellulose in the presence of TGF-β (20 ng/mL) and hematopoietic colonies were counted after 14 days. (G) miR-21 overexpression led to decreased erythroid colony formation (mean ± SEM of 2 independent experiments, Student's *t*-test, $P = .01$) and also led to qualitative reductions in colony sizes.

Figure 5

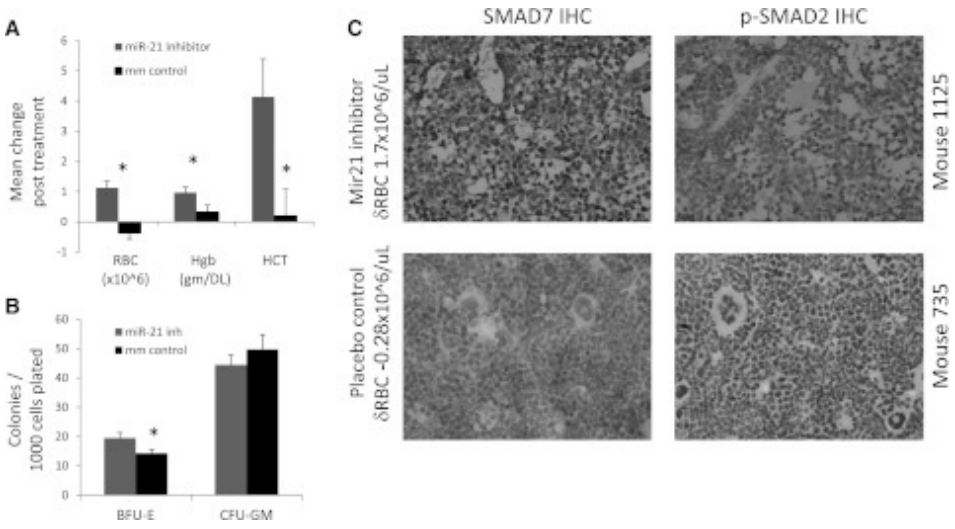

Treatment with mir21 inhibitor leads to an increase in red blood cells in TGF-β transgenic mice. (A) Mice expressing TGF-β (Alb/TGFβ+) were treated with LNA-modified anti–miR-21 (n = 7) or mismatched placebo controls (n = 6) for 5 doses. Mice treated with anti–miR-21 oligos had a significant increase in hematocrit (HCT, Student's *t*-test, $P = .03$), hemoglobin (Hgb [gm/DL], Student's *t*-test, $P = .049$), and red blood cells (RBCs [$\times 10^6$], Student's *t*-test, $P = .0005$). (B) Equal numbers of bone marrow cells were grown in methylcellulose and demonstrated increased erythroid colony formation in the mice treated with miR-21 inhibitor (n = 5 in each group, Student's *t*-test, $P = .04$. (C) Representative bone marrow biopsy samples from both groups show an increase in *SMAD7* levels in the treatment group with a corresponding decrease in phospho-SMAD2.

Table 1

MDS patient characteristics and response to miR-21 inhibition

N	Age/Sex	WBC 3	Hgb	Plt 3	Subtype	Cytogenetics	Colonies post treatment	Colonies post treatment

		(10 /mL)	(g/dL)	(10 /mL)			with mismatched control		with miR-21 inhibitor	
							BFU-E	CFU-GM	BFU-E	CFU-GM
1	63/M	1.2	9	14	RCMD	+11	204	12	259	24
2	79/f	2.9	9.6	29	RAEB	−7q	22	4	26	5
3	68/F	3.5	9.3	35	RAEB	−5q, −18	20	37	49	46
4	70/M	18.2	8.5	84	RAEB	Nml	91	93	121	86
5	69/F	5.2	8.8	75	RCMD	Nml	62	26	98	25

WBC, white blood cells; plt, platelets; Hgb, hemoglobin.

Figure 6

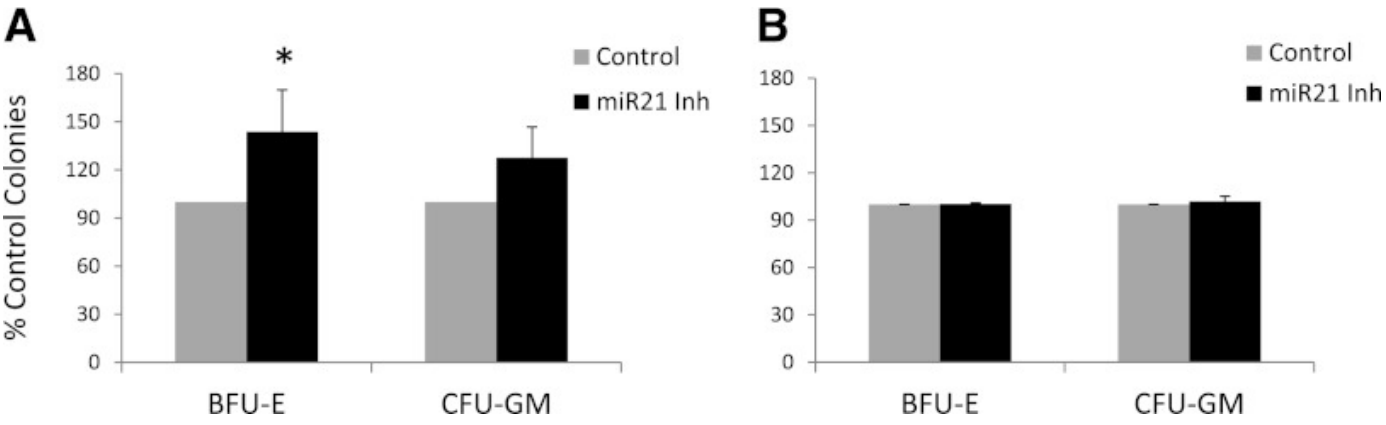

Inhibition of miR-21 stimulates erythropoiesis in MDS. MDS bone marrow–derived MNCs from 5 patients with MDS (A) and 3 controls (B) were plated in methylcellulose and cytokines in the presence and absence of miR-21 inhibitor (50 nM). Colonies were scored at Day 14 and results were expressed as means ± SEM of independent experiments.

The Journal of Biological Chemistry
JBC
ASBMB
About JBC | This Article | Submissions | Subscriptions | Contact

J Biol Chem. 2011 Jul 15; 286(28): 25211–25223.
Published online 2011 Apr 30. doi: 10.1074/jbc.M111.235028
PMCID: PMC3137092

Aberrant Epigenetic and Genetic Marks Are Seen in Myelodysplastic Leukocytes and Reveal *Dock4* as a Candidate Pathogenic Gene on Chromosome 7q*

Li Zhou,[a] Joanna Opalinska,[a] Davendra Sohal,[a] Yiting Yu,[a] Yongkai Mo,[a] Tushar Bhagat,[a] Omar Abdel-Wahab,[b] Melissa Fazzari,[a] Maria Figueroa,[c] Cristina Alencar,[a] Jinghang Zhang,[a] Suman Kambhampati,[d] Simrit Parmar,[e] Sangeeta Nischal,[a] Christoph Hueck,[a] Masako Suzuki,[a] Ellen Freidman,[a] Andrea Pellagatti,[f] Jacqueline Boultwood,[f] Ulrich Steidl,[a] Yogen Saunthararajah,[g] Vijay Yajnik,[h] Christine Mcmahon,[a] Steven D. Gore,[i] Leonidas C. Platanias,[j] Ross Levine,[b] Ari Melnick,[c] Amittha Wickrema,[k] John M. Greally,[a,1] and Amit Verma[a,2]

From the [a]Albert Einstein College of Medicine, Bronx, New York 10461,
the [b]Memorial Sloan-Kettering Cancer Center, New York, New York 10065,
the [c]Weill Cornell Medical School, New York, New York 10065,
the [d]Kansas City Veterans Affairs Medical Center, Kansas City, Kansas 64128,
the [e]M.D. Anderson Cancer Center, Houston, Texas 77030,
the [f]John Radcliffe Hospital, Oxford OX3 9DU, United Kingdom,
the [k]University of Chicago Medical School, Chicago, Illinois 60637,
the [g]Cleveland Clinic, Cleveland, Ohio 44195,
the [h]Massachusetts General Hospital, Boston, Massachusetts 02114,
the [i]Sidney Kimmel Comprehensive Cancer Center, The Johns Hopkins Hospital, Baltimore, Maryland 21287, and
the [j]Robert H. Lurie Comprehensive Cancer Center, Northwestern University Medical School and Jesse Brown Veterans Affairs Medical Center, Chicago, Illinois 60611

[1] To whom correspondence may be addressed. E-mail: llun@ved:otliam.
[2] To whom correspondence may be addressed. E-mail: llun@ved:otliam.

Received 2011 Mar 8; Revised 2011 Apr 29

Abstract

Myelodysplastic syndromes (MDS) are characterized by abnormal and dysplastic maturation of all blood lineages. Even though epigenetic alterations have been seen in MDS marrow progenitors, very little is known about the molecular alterations in dysplastic peripheral blood cells. We analyzed the methylome of MDS leukocytes by the HELP assay and determined that it was globally distinct from age-matched controls and was characterized by numerous novel, aberrant hypermethylated marks that were located mainly outside of CpG islands and preferentially affected GTPase regulators and other cancer-related pathways. Additionally, array comparative genomic hybridization revealed that novel as well as previously characterized deletions and amplifications could also be visualized in peripheral blood leukocytes, thus potentially reducing the need for bone marrow samples for future studies. Using integrative analysis, potentially pathogenic genes silenced by genetic deletions and aberrant hypermethylation in different patients were identified. *DOCK4*, a GTPase regulator located in the commonly deleted 7q31 region, was identified by this unbiased approach. Significant hypermethylation and reduced expression of DOCK4 in MDS bone marrow stem cells was observed in two large independent datasets, providing further validation

of our findings. Finally, *DOCK4* knockdown in primary marrow CD34 stem cells led to decreased erythroid colony formation and increased apoptosis, thus recapitulating the bone marrow failure seen in MDS. These findings reveal widespread novel epigenetic alterations in myelodysplastic leukocytes and implicate *DOCK4* as a pathogenic gene located on the 7q chromosomal region.

Keywords: Epigenetics, Gene Expression, Gene Silencing, Microarray, Stem Cell

Introduction

The myelodysplastic syndromes (MDS)[3] are collections of heterogeneous hematological diseases characterized by refractory cytopenias due to ineffective hematopoiesis. Recent evidence suggests that stem cells in MDS are characterized by aberrant transcriptional profiles and that deregulation of gene expression may account for abnormal growth and differentiation of these progenitors (1, 2). One of the ways that gene expression may be dysregulated is through aberrant DNA methylation. Methylation of cytosine has been implicated as a way to silence genes epigenetically and indicates an attractive target for potential therapeutics (3). Aberrant methylation of promoters of genes such as *p15*,*DAPK*, and others has been reported in MDS (4, 5). Even though these are important cell cycle and apoptosis genes, methylation of their promoter CpGs has not correlated very well with clinical responses after treatment with DNA methyltransferase inhibitors in most studies (7, 8). It is possible that global studies of the DNA methylome in MDS may yield an epigenetic signature that is better as a diagnostic and prognostic tool than single locus studies. Early attempts at global methylation analysis of MDS using a microarray covering 1,505 CpG islands have shown aberrant hypermethylation of selected genes in MDS and their involvement in progression to AML (9). Their study opened up the possibility that assays with better resolution and coverage not restricted to CpG islands alone may yield more informative insights into the MDS methylome.

Several experimental approaches are available to determine genome-wide DNA methylation levels. Most of these techniques are based on restriction enzyme digestion or DNA immunoprecipitation with antibodies that bind to methylated CpGs (10). Among the restriction enzyme-based methods, some involve comparing the profiles from digestion of DNA with methylation-sensitive and -insensitive restriction enzymes (11, 12). The HELP (HpaII tiny fragment enrichment by ligation-mediated PCR) assay is based on this principle and relies on differential digestion by a pair of enzymes, HpaII and MspI, that differ on the basis of their methylation sensitivity. These enzymes cut at the same CpG-containing sites (CCGG), but HpaII is unable to cleave the sites that are methylated. Thus, the DNA segments generated by these two digestions will vary in composition based on the amount of methylation. The HpaII and MspI genomic representations can be cohybridized to a custom microarray and their ratio used to indicate the methylation of particular CCGG sites at these loci. The HELP assay has been shown to be a robust discovery tool for flagging loci for subsequent quantitative and nucleotide resolution bisulfite analyses (MassArray and Pyrosequencing) that represent the gold standard tests for cytosine methylation (13–15).

In addition to epigenetic alterations, MDS is also characterized by many cytogenetic abnormalities that may contribute to its pathogenesis. Recent studies have shown that higher resolution microarray-based technologies such as comparative genomic hybridization (aCGH) and single nucleotide polymorphism microarrays can reveal cytogenetic abnormalities not seen by conventional methods (16–18). In this study, we tested whether it is important to study the effect of genetic and epigenetic abnormalities together to obtain a comprehensive insight into MDS pathogenesis. We have developed an integrated genomics and epigenomics platform based on the combination of the HELP assay and aCGH and have used it on MDS samples. We have used MDS peripheral blood cells as very little is known about the molecular and

epigenetic makeup of these dysplastic cells. We wanted to determine whether aberrant epigenetic marks can be observed in MDS peripheral blood cells and whether these cells could be used for these studies instead of hard to obtain marrow samples. Our studies showed that methylation changes could be seen in peripheral blood leukocytes and were of sufficient magnitude to discriminate MDS leukocytes from age-matched controls. Similarly, both novel and well characterized genomic copy number changes were also found in these peripheral blood cells. Using integrative analysis, common sets of genes were identified that were affected in different patients by genetic deletion events and the epigenetic events of aberrant methylation. One of the genes identified by this unbiased approach was *DOCK4*, which is located in the commonly deleted chromosome 7q31 region. *DOCK4* was found to be epigenetically silenced in both peripheral leukocytes and marrow stem cells in MDS. We determined that *Dock4* knockdown leads to ineffective hematopoiesis, thus implicating it as a potential candidate gene in MDS and underscoring the power of genome-wide integrative analysis in gene discovery in MDS.

MATERIALS AND METHODS

Patient Samples and Nucleic Acid Extraction Specimens were obtained from 21 patients diagnosed with MDS and from controls after signed informed consent was approved by the Albert Einstein College of Medicine Institutional Review Board. MDS subtypes included refractory cytopenias with multilineage dysplasia, refractory anemia, refractory anemia with excess blasts, and chronic myelomonocytic leukemia. Peripheral blood leukocytes were isolated after red cell lysis and used for DNA and RNA extraction. Genomic DNA was extracted by a standard phenol-chloroform protocol followed by an ethanol precipitation and resuspension in 10 mM Tris-HCl, pH 8.0. Total RNA was extracted using an RNeasy mini kit from Qiagen (Valencia, CA) and subjected to amplification using the MessageAmp II aRNA kit from Ambion (Foster City, CA).

DNA Methylation Analysis by HELP The HELP assay was carried out as published previously (14). Intact DNA of high molecular weight was corroborated by electrophoresis on 1% agarose gel in all cases. One microgram of genomic DNA was digested overnight with either HpaII or MspI (New England Biolabs, Ipswich, MA). The following day, the reactions were extracted once with phenol-chloroform and resuspended in 11 μl of 10 mM Tris-HCl, pH 8.0, and the digested DNA was used to set up an overnight ligation of the JHpaII adapter using T4 DNA ligase. The adapter-ligated DNA was used to carry out the PCR amplification of the HpaII- and MspI-digested DNA as described previously (14). Both amplified fractions were submitted to Roche-NimbleGen, Inc. (Madison, WI), for labeling and hybridization onto a human hg17 custom-designed oligonucleotide array (50-mers) covering 25,626 HpaII-amplifiable fragments located at gene promoters. HpaII-amplifiable fragments are defined as genomic sequences contained between two flanking HpaII sites found within 200–2,000 bp from each other. Each fragment on the array is represented by 15 individual probes distributed randomly and spatially across the microarray slide. Thus, the microarray covers 50,000 CpGs corresponding to 14,000 gene promoters.

Quantitative DNA Methylation Analysis by Mass Array Epityping Validation of HELP microarray findings was carried out by MALDI-TOF mass spectrometry using EpiTYPER^{TM} by MassArray (Sequenom) on bisulfite-converted DNA as described previously (19, 20). MassArray primers were designed to cover the flanking HpaII sites for a given HpaII-amplifiable fragment, as well as any other HpaII sites found up to 2,000 bp upstream of the downstream site and up to 2,000 bp downstream of the upstream site, to cover all possible alternative sites of digestion. The primers used were as follows: KLF3_1, forward 5′-AGGAAGAGAGTATTTTAAAGATGAAGTTTATGGGATAGT-3′ and reverse 5′-

CAGTAATACGACTCACTATAGGGAGAAGGCTAAACCCTTTAAATTAACCCATCTC-3′; KLF3_2, forward 5′-AGGAAGAGAGTTGAAGGTTATTGAGTTTAGGG-3′ and reverse 5′-CAGTAATACGACTCACTATAGGGAGAAGGCTCTCAACTCACTACAAAAAAAAAA-3′; Dock4-294-593, number 1, forward AGGAAGAGAGGGAGAAAATGTTATGGAATGGTTTTT and reverse CAGTAATACGACTCACTATAGGGAGAAGGCTTCACCTCAACCACAAACTAAACAAA; and Dock4–1299-1597, number 2, forward AGGAAGAGAGGGGTTATTAGTTTAAGATTTAAATTGGTG and reverse CAGTAATACGACTCACTATAGGGAGAAGGCTAAATCATAACTCACCACAACCTCC.

Quantitative Real Time PCR The expression values of *DOCK4* were validated by quantitative RT-PCR. cDNA was synthesized from DNase I-treated total RNA extracted from patient samples using the Superscript III first strand kit from Invitrogen (Superscript III) following the manufacturer's protocol. Real time PCR was performed using SYBR Green PCR master mix from Applied Biosystems (Foster City, CA) with primers specific for *DOCK4* and a DNA Engine Opticon 2 real time thermocycler from Bio-Rad. *GAPDH* was simultaneously amplified with specific primers as housekeeping genes to normalize the *DOCK4* expression. The primer sequences are as follows: DOCK4, forward 5′-GGATACCTACGGAGCACGAG-3′ and reverse 5′-AGCCATCACACTTCTCCAGG-3′; glyceraldehyde-3-phosphate dehydrogenase, forward 5′-CGACCACTTTGTCAAGCTCA-3′ and reverse 5′-CCCTGTTGCTGTAGCCAAAT-3′.

Microarray Quality Control All microarray hybridizations were subjected to extensive quality control using the following strategies. First, uniformity of hybridization was evaluated using a modified version of a previously published algorithm (15) adapted for the NimbleGen platform, and any hybridization with strong regional artifacts was discarded and repeated. Second, normalized signal intensities from each array were compared against a 20% trimmed mean of signal intensities across all arrays in that experiment, and any arrays displaying a significant intensity bias that could not be explained by the biology of the sample were excluded.

HELP Data Processing and Analysis Signal intensities at each HpaII-amplifiable fragment were calculated as a robust (25% trimmed) mean of their component probe-level signal intensities. Any fragments found within the level of background MspI signal intensity, measured as 2.5 mean-absolute-differences above the median of random probe signals, were categorized as “failed.” These failed loci therefore represent the population of fragments that did not amplify by PCR, whatever the biological (*e.g.* genomic deletions and other sequence errors) or experimental cause. However, “methylated” loci were so designated when the level of HpaII signal intensity was similarly indistinguishable from background. PCR-amplifying fragments (those not flagged as either methylated or failed) were normalized using an intra-array quantile approach wherein HpaII/MspI ratios are aligned across density-dependent sliding windows of fragment size-sorted data. The $\log_2$(HpaII/MspI) was used as a representative for methylation and analyzed as a continuous variable. For most loci, each fragment was categorized as either methylated, if the centered log HpaII/MspI ratio was less than zero, or hypomethylated, if the log ratio was greater than zero.

Microarray Data Analysis Unsupervised clustering of HELP data by hierarchical clustering was performed using the statistical software R version 2.6.2. A two-sample *t* test was used for each gene to summarize methylation differences between groups. Genes were ranked on the basis of this test statistic and a set of top differentially methylated genes with an observed log fold change of >1 between group means was identified. Genes were further grouped according to the direction of the methylation change (hypomethylated *versus* hypermethylated in MDS), and the relative frequencies of these changes were computed among the top candidates to explore global methylation patterns. Extensive validations (shown for *KLF3* promoter regions) with MassArray showed good correlation with the data generated by the HELP

assay. MassArray analysis validated significant quantitative differences in methylation for differentially methylated genes selected by our approach.

Array-based Comparative Genomic Hybridization (aCGH) Gene copy number changes were analyzed by high resolution (6 kb) microarray-based comparative genomic hybridization (aCGH) performed on Roche-NimbleGen 385K whole genome tiling arrays (2006–11-01_HG17_WG_CGH). Pooled DNA from healthy cases was used as controls during hybridization. These arrays contain 50–75-mer probes at average spacing of 6270 bp (6 kb). This probe-level aCGH data were analyzed by DNA copy algorithm (Nimblescan software package, Roche-Nimblegen) using five adjacent oligonucleotides and confirmed by circular binary segmentation algorithm (22). Significant DNA copy number changes were cross-referenced from the HapMap data base from NCBI to remove normal variants.

Pathway Analysis and Transcription Factor-binding Site Analysis Using the Ingenuity Pathway Analysis software (Redwood City, CA), we carried out an analysis of the biological information retrieved by each of the individual platforms alone, and we compared it with the information obtained by the integrated analysis of all three platforms. Enrichment of genes associated with specific canonical pathways was determined relative to the ingenuity knowledge data base for each of the individual platforms and the integrated analysis at a significance level of $p < 0.01$. Biological networks captured by the different microarray platforms were generated using Ingenuity Pathway Analysis software and scored based on the relationship between the total number of genes in the specific network and the total number of genes identified by the microarray analysis. The list of hypermethylated genes was examined for enrichment of conserved gene-associated transcription factor-binding sites using the Molecular Signatures Database (MSigDB) (23). Their functional gene sets were obtained from Gene Ontology (GO) (24).

This analysis was performed by Gene Set Enrichment Analysis (GSEA) (23), a computational method that determines whether an *a priori* defined set of genes (commonly hypermethylated genes in MDS) shows statistically significant, concordant differences between two biological states. GSEA calculates an enrichment score (ES) for a given gene set using a rank of genes and infers statistical significance of each ES against ES background distribution calculated by permutation of the original data set. The ES is the maximum deviation from zero of the cumulative sum and can be interpreted as a weighted Kolmogorov-Smirnov statistic. When an entire data base of gene sets is scored, an adjustment was made to the resulting *p* values to account for multiple hypotheses testing. In this study, the javaGSEA implementation was used for GSEA analysis. The list of differentially methylated HpaII fragments was analyzed using GSEA "pre-ranked" algorithm, which is used when a pre-ordered ranked list is to be analyzed with GSEA. 1,000 permutations were applied to sample labels to test if genes from each *a priori* defined positional gene sets were randomly distributed along the gene list.

The same method was applied to determine whether transcription-binding sites are randomly distributed in the differentially methylated genes. The *a priori* defined gene sets used in this analysis is transcription factor target, which contains genes that share a transcription factor-binding site defined in the TRANSFAC (version 7.4) database (25). Using GSEA pre-ranked algorithm, 1000 permutations were applied to sample labels to test if genes from each transcription factor target gene sets were randomly distributed along the differentially methylated gene list. The result shows significant over-representation of binding sites for *SP1, AHR, FOXO4, LEF1, NF1,* and *SOX9* and other transcription factors.

Meta-analysis of MDS and Normal CD34$^+$ Gene Expression Studies A human bone marrow gene expression dataset, including profiles of 89 cases of MDS CD34$^+$ cells and 61 normal CD34$^+$ profiles was constructed.

Individual datasets were obtained from seven independent studies (2, 26–31) from NCBI Gene Expression Omnibus database, an on-line repository of all gene expression profiles reported in the literature (26). Methods to find and extract data have been described previously (32, 33). The datasets were integrated based on UniGene identifications and were quantile-normalized to ensure cross-study comparability, based on our previous approach (32, 33). Analyses were performed using SAS (SAS Institute, Cary, NC) and the R language.

shRNA Gene Knockdown The human GIPZ lentiviral shRNAmir individual clones targeting *DOCK4* (catalog nos. RHS4430-98480907, RHS4430-99166546, and RHS4430-98521322) and the nonsilencing control (catalog no. RHS4346) were obtained from OpenBiosystems (Huntsville, AL). Nucleofection of $CD34^+$ cells was performed according to the manufacturer's instruction using the Nucleofector machine (Amaxa, Cologne, Germany). 10^6 $CD34^+$ cells (AllCells) were thawed, cultured for 2 h, resuspended in 100 μl of human $CD34^+$ Nucleofection solution (Amaxa), then transferred into cuvettes, and electroporated using program U008. $CD34^+$ cells were collected and cultured in 24-well plates containing 1 ml of prewarmed Stemspan (Stemcell Technologies, Vancouver, British Columbia, Canada), supplemented with 100 ng/ml human Flt-3, stem cell factor, and Tpo for another 24 h before the analysis.

Hematopoietic Colony Assays 24 h after gene knockdown, $CD34^+$ cells were collected, and the shRNA-transfected cells were sorted according to the GFP intensity using Moflow (BD Biosciences). The same numbers of GFP-positive cells were culture in MethoCult GF4434 (StemCell Technologies) containing recombinant human stem cell factor, granulocyte-macrophage colony-stimulating factor (GM-CSF), IL-3, and erythropoietin. Granulocyte/macrophage colony-forming units and erythroid burst-forming units were scored on day 14 of culture.

Apoptosis Assay To detect apoptotic cells, annexin V-APC staining was performed 24 h after the lentiviral transfection using the annexin V-APC apoptosis detection kit (eBioscience) according to the manufacturer's instructions. 7-Aminoactinomycin D was used for the viability staining. Apoptotic cells were analyzed using a FACScan (BD Biosciences).

Immunohistochemistry on Bone Marrow Tissue Microarray Tissue microarrays were constructed from formalin-fixed, paraffin-embedded bone marrow core biopsies from patients with MDS and control patients with anemia whose bone marrow showed no evidence of neoplasia. The tissue blocks were procured from Jacobi Hospital (Bronx, NY) after approval by the Internal Review Board. For each patient, three 0.5-mm cores were placed in a tissue array using a manual arrayer (Chemicon International, Temecula, CA). Sections of the tissue microarrays were cut to a 5-μm thickness, placed on positively charged slides, and heated to 60 °C for 1 h. They were then deparaffinized in xylene and rehydrated with graded alcohols. Endogenous peroxidase activity was quenched with 3% hydrogen peroxide. Antigen retrieval was accomplished by microwaving the slides in Dako Target Retrieval Solution, pH 6.0 (Dako Cytomation, Dako, Carpinteria, CA), and subsequently steaming them in a vegetable steamer for 30 min. The slides were stained using a rabbit polyclonal anti-DOCK4 antibody, provided by Yajnik and co-workers (34), at 1:200 dilution, followed by Dako EnVision labeled polymer-HRP anti-rabbit antibody. Antibody binding was detected using 3,3-diaminobenzidine chromogen (Cell Marque, Rocklin, CA). The slides were lightly counterstained with hematoxylin, dehydrated with graded alcohols, cleared with xylene, and coverslipped using Cytoseal 60 (Thermo Scientific, Waltham, MA). The tissue cores were then scored for weak *versus* strong staining for DOCK4 by a hematopathologist who was blinded to the patient identities. Tissue cores that did not contain at least 10% evaluable marrow were excluded from the analysis.

RESULTS

Methylation Profiling on Peripheral Blood Leukocytes Separates Distinct Subsets of MDS from Normal Controls Even though the hallmark of myelodysplastic syndromes is dysplastic appearance of peripheral blood cells, epigenetic and other molecular alterations in these cells have not been examined in detail. We wanted to determine the methylome of these cells by the HELP assay, which is an unbiased high resolution-based assay that has led to the discovery of novel epigenetic alterations in leukemias and other cancers (13, 35, 37). DNA methylation profiles were generated from 21 MDS patient peripheral leukocyte samples and 9 age-matched controls. The MDS samples included all subtypes of this disease (Table 1). The controls included six elderly healthy cases and three patients with anemia of chronic disease. Unsupervised hierarchal clustering showed that the controls formed a cluster that was distinct from MDS samples, demonstrating epigenetic dissimilarity between these groups. Interestingly, a sample from a patient with a 5q syndrome clustered with normals (Fig. 1). The MDS samples formed two clusters with epigenomic similarity to each other (groups 1 and 2), in addition to the rest of samples that demonstrated greater epigenetic heterogeneity (group 3). Because we used peripheral blood leukocytes for these analyses, we wanted to determine whether these epigenetic clusters were due the differing myeloid and lymphoid cell percentages in these samples. We observed that most of the MDS samples had lymphoid and neutrophil percentages that were in the normal range, and clustering was not found be dependent on their relative ratios (Table 1 showing sample characteristics, no significant differences between myeloid and lymphoid percentages between the cases $p > 0.05$, Proportions Test). Furthermore, epigenetic similarity between clusters of samples was neither dependent on the histological subtypes of MDS nor cytogenetic alterations within these samples. These data demonstrate that significant changes in DNA methylation are seen in MDS leukocytes and are sufficient to clearly distinguish these cases from controls (Fig. 1).

Most Differentially Methylated Genes Are Hypermethylated in MDS Leukocytes Having demonstrated epigenetic dissimilarity between MDS and control samples, we next determined the qualitative epigenetic differences between these groups by performing a supervised analysis of the respective DNA methylation profiles. A volcano plot comparing the differences between mean methylation of individual loci in MDS *versus* control samples plotted against the significance (log (*p* value) based on *t* test) of the difference is used to represent these data in Fig. 2*A*. We observed that most significantly differentially methylated loci were hypermethylated in all cases of MDS ($n = 152$) when compared with controls (p value < 0.05; Fig. 2 and supplemental Tables 1 and 2 listing all genes). This is consistent with previous reports demonstrating hypermethylation of selected loci in MDS bone marrow progenitors (38). The two subgroups of MDS samples based on unsupervised clustering (Fig. 1) also had predominantly hypermethylated genes, although group 2 had a slightly higher proportion of significantly hypomethylated genes when compared with controls (Fig. 2, *B* and *C*). Most interestingly, only 28% (43/153) of the commonly differentially hypermethylated CCGG loci (Fig. 2*A*) were located in the CpG islands (Fig. 2*D*). This was significant even after the correction for the proportion of non-CpG island probes present in the HELP array and shows that these non-CpG island loci are preferentially dysregulated in this disease (Fig. 2*D*).

A transcription factor, *KLF3* (39, 40), that was significantly methylated in MDS was chosen for validation. Promoter regions of the Kruppel-like factor-3 (*KLF-3*) (supplemental Fig. 1) was examined by MALDI-TOF-based quantitative methods (MassArray, Sequenom). DNA was bisulfite-converted, and primers were designed to amplify regions of interest, and quantitative assessment of methylation was performed by mass spectroscopic analysis. We observed a strong correlation of quantitative methylation obtained from MassArray with the findings of our HELP microarrays, demonstrating the validity of our findings

(supplemental Fig. 1). Furthermore, MassArray analysis of CG dinucleotides surrounding the assayed HpaII sites revealed distinct hypermethylation of these cytosines in MDS samples when compared with controls (supplemental Fig. 1), potentially pointing to their role as potential biomarkers in this disease, as shown for the *KLF3* gene promoter.

Genes Hypermethylated in MDS Display Specific Functional and Genomic Characteristics A gene ontology analysis of the 152 commonly hypermethylated genes (p <0.05 and methylation change >1 log fold) showed specific enrichment of GTPase regulators with *DOCK4*, *DOCK2*, *ARHGEF4*, *CDC42SE1*, *FARP1*, *GIT2*, *IQGAP2*, and *RALGPS1* as the genes that were hypermethylated in MDS (Table 2). Other gene pathways with significant involvement of hypermethylated genes included those regulating calcium-dependent cell-cell adhesion, spermatid development, small nuclear ribonucleoprotein complex, and nuclear organization. Table 2 shows the genes associated with each of these enriched GO categories, which include many potentially novel relevant candidate genes such as *DOCK4* as well as genes already implicated in hematological malignancies such as *HOXB3* and *RUNX3*. Further functional pathway analysis revealed cancer as the top functional pathway affected by hypermethylation in MDS (supplemental Fig. 2). Involvement of these important pathways by genes commonly affected by hypermethylation even in this heterogeneous mix of patients supports the biological validity of our dataset.

Aberrant methylation was not distributed randomly across chromosomes. Differentially methylated HpaII fragments showed significant regional differences on chromosomes 11 and 16 compared with the genomic distribution of all HpaII fragments from the HELP array. Furthermore, to determine whether these hypermethylated genes shared any common DNA elements, we performed a search for transcription factor-binding sites enriched in these genes. Significant over-representation of binding sites for *SP1*, *AHR*, *FOXO4*, *LEF1*, *NF1*, and *SOX9* and other transcription factors was seen in MDS (Table 3).

Array CGH Detects Copy Number Variations in MDS Leukocytes Because chromosomal deletions and amplifications have been seen in MDS bone marrow progenitors, we next wanted to determine whether these can also be seen in dysplastic leukocytes. We also wanted to test the potential of high resolution aCGH in detecting novel copy number variations in the peripheral blood. aCGH performed at a 6-kb resolution demonstrated that cytogenetic changes can be seen in peripheral blood leukocytes (Fig. 3 and Tables 4 and 5). The changes seen in peripheral blood are very similar to those seen in the bone marrow progenitors (Fig. 3*A*). Furthermore, both small and large chromosomal changes were successfully observed in peripheral leukocytes (Fig. 3, *B* and *C*). Next, we used aCGH data from 20 samples to uncover cryptic changes not seen by conventional karyotyping. We observed five common deletions and nine common chromosomal amplifications affecting 25% or more cases with our analysis (Tables 4 and 5). These included novel areas of deletion (1q32 and 14q11) and amplification (1q41–42, 15q11, 19q13, and 22q22) that were not seen by conventional karyotypic analysis. Interestingly, the 17q21-21 region found to be amplified in our analysis was also described as a novel MDS amplification in a recent report (18), thus confirming the applicability of our findings to other patient cohorts.

Integrative Analysis Can Reveal Novel Pathogenic Genes We hypothesized that genes silenced by both deletion and methylation are likely to be involved in disease pathogenesis as they are being silenced by distinct mechanisms in separate cases. Therefore, an integrative analysis of epigenetic and genetic lesions could prioritize candidate lesions for functional validation. Using this strategy, we selected five genes (*DOCK4*, *PRES*, *KCNN2*, *PGGT1B*, and *TNFAIP9*) that were targeted by both genetic deletion and epigenetic silencing in our dataset. These genes were selected on the basis of being deleted in at least 25% of cases and differentially methylated in the others. One of these genes, *DOCK4* (dedicator of cytokinesis-4) has

been postulated as a tumor suppressor (41) and is located on chromosome 7q31, a frequently deleted segment in MDS (Fig. 4*A*) (42). *DOCK4* was found to be hypermethylated by the HELP assay (Fig. 4*B*), and the methylation was validated quantitatively by MassArray EpiTYPER^{TM} analysis, demonstrating significantly increased methylation in MDS samples when compared with controls (Fig. 4*C*). To determine the effect of *DOCK4* methylation on transcription, we measured its expression in these samples by quantitative RT-PCR and found it to be significantly reduced in the MDS leukocyte samples (Fig. 4*D*). Furthermore, DOCK4 expression was significantly down-regulated by both promoter methylation and 7q deletion in MDS samples illustrating that it is affected by both genetic and epigenetic alterations (Fig. 4*E*).

DOCK4 Is Hypermethylated and Reduced in Expression in MDS Bone Marrows in Independent Datasets To validate these findings in bone marrow samples, we examined DOCK4 methylation in an independent cohort of 15 MDS and secondary AML patients enrolled in a clinical trial (38). Analysis of these HELP DNA methylation profiles revealed striking hypermethylation of the DOCK4 promoter in MDS/AML patients when compared with normal bone marrow controls (*t* test, *p* value <0.01) (Fig. 5*A*). To further test DOCK4 expression in a larger set of MDS-derived bone marrow $CD34^+$ cells, we utilized a recently constructed meta-analytical data base of MDS bone marrow gene expression profiles (32, 33). DOCK4 was significantly underexpressed in 89 MDS $CD34^+$ cell samples when compared with 61 normal bone marrow $CD34^+$ cells (p value = 4.3×10^{-8}, *t* test) Significantly reduced levels of DOCK4 were seen in all subtypes of MDS examined (Fig. 5*B, right panel, box plots*), thus demonstrating a potential important role in the pathobiology of this disease. Finally, we also determined DOCK4 protein expression in bone marrow biopsies by immunohistochemistry in 9 cases of MDS and compared these with 19 cases of age-matched controls with anemia due to various other etiologies (chronic disease, nutrient deficiency, and HIV). Only a minority of MDS samples (2/9, 22%) showed strong expression of DOCK4 in the bone marrow progenitors as compared with most of the controls (19/22, 86% with strong staining, *p* value = 0.001, Fisher's exact test) as is shown in representative cases in Fig. 5*C*. These data obtained from different laboratories support a potential role of *DOCK-4* in MDS pathogenesis.

DOCK4 Knockdown Leads to Ineffective Hematopoiesis MDS is characterized by ineffective hematopoiesis. Increased progenitor and stem cell apoptosis coupled with dysplastic maturation of blood cells is seen in MDS. To determine the functional role of DOCK4 in hematopoiesis, we tested three different shRNAs against *DOCK4* and demonstrated specific knockdown of the gene with all three constructs (Fig. 6*A*). These were then used to knock down DOCK4 in primary bone marrow-derived $CD34^+$ stem cells that were subsequently used for hematopoietic colony assays. DOCK4 shRNA led to significantly decreased erythroid and myeloid colony formation demonstrating an important role in hematopoiesis. Furthermore, DOCK4 knockdown led to significant increase in apoptosis of $CD34^+$ cells, demonstrating similarity with phenotypic changes seen in MDS bone marrows and validating the potential of our integrative platform in gene discovery in this disease.

DISCUSSION

MDS is a stem cell disorder that responds to treatment with cytosine analogues, azacytidine and decitabine, agents that deplete DNA methyltransferases, suggesting a role of aberrant methylation in the pathobiology of this disease. Even though most studies have looked at the methylation status of selected genes in MDS, recent studies have started exploring epigenetic aberrations in an unbiased manner across the genome (9). Most of these studies have focused on marrow samples that are hard to obtain and frequently limited by poor quality and quantity of derived nucleic acid. We used an unbiased global assay to look for epigenomic

disturbances in peripheral blood cells in MDS. Our aim was to evaluate whether high resolution assays would be able to reveal epigenetic and genetic disturbances in these cells and thus could be used for future gene discovery and biomarker studies. Our studies revealed aberrations in DNA methylation that clearly distinguished MDS from normal controls, even when total leukocyte populations were used for analysis. These results also suggest that aberrant methylation marks are stable and can be seen at the level of differentiated and heterogeneous cell populations, when examined by high resolution assays. Furthermore, by combining epigenomic assays with genetic assays, we could find novel genes that may play roles in the pathogenesis of this disease.

Our epigenetic studies were based on the HELP assay that examines cytosine methylation at CCGG (HpaII) sites, some of which lie outside of CpG islands (13). In fact, we found that the majority of common differentially hypermethylated cytosines in MDS samples are not located in CpG islands. Recent work has also shown that non-CpG island cytosine methylation can be important in controlling gene transcription and can be involved in normal development and carcinogenesis (20, 43). These findings will be important for future predictive biomarker studies in MDS and underscore the importance of using unbiased high resolution assays not restricted to CpG islands for these studies.

A problem with genomic assays is the large number of candidate genes that are discovered during analysis. It is difficult to rank these targets by their functional importance, and it is thus challenging to conclude which of these are the actual drivers of disease pathophysiology. We tried to use our integrative platform to address this issue by hypothesizing that genuinely important pathogenic genes may be disrupted by different mechanisms in different patient samples. Using this approach, we found five genes that were targeted by hypermethylation and deletions in different MDS samples. One of these genes, *DOCK4*, happens to reside within the chromosome 7q31 region that has been found to be a common region deleted in poor prognosis MDS (42). DOCK4 is a member of family of guanine exchange factors that can activate GTPases Rap and Rac (34). DOCK4 is a multidomain protein and is a part of the DOCK superfamily of 11 unconventional guanine exchange factors, characterized by the presence of DHR1 and DHR2 (DOCK homology regions 1 and 2) domains. *DOCK4* deletions have been seen in murine tumor models, and missense mutations have been described in prostate and ovarian cancer cell lines (41). DOCK4 is required for Rap GTPAse activation that controls formation and maintenance of adherens junctions. Loss of DOCK4 function leads to loss of cell adherence and can support tumorigenicity, implicating it as a tumor suppressor gene. GTPases such as Rac and Rap also play important roles in cytokine signaling during hematopoiesis (6, 44, 45), and so modulation of their activation can impact this process. Additionally, DOCK4 has also been shown to interact molecularly with the β-catenin pathway, specifically with GSK-3, pathways that play important roles in regulating stem cell function in hematopoiesis (34). Chromosome 7 is frequently deleted in MDS and leads to a worse prognosis in this disease. Studies have shown that 7q31 may be the commonly deleted segment in this disease (36). Our identification of DOCK4 in an unbiased manner using our integrative platform shows the potential of combining different genomic assays to prioritize identification of important genes in this heterogeneous disease.

Supplementary Material

Supplemental Data:

*

This work was supported, in whole or in part, by National Institutes of Health Grants RO1HL082846, RO1AG02913801, and CA009173. This work was also supported by American Cancer Society, Partnership for Cures grant and the Gabrielle Angel Foundation.

S The on-line version of this article (available at http://www.jbc.org/) contains supplemental Tables 1 and 2 and Figs. 1 and 2.

[3]The abbreviations used are:

MDS myelodysplastic syndrome
CGH comparative genomic hybridization
aCGH array CGH
GSEA gene set enrichment analysis
ES enrichment score
AML acute myeloid leukemia.

REFERENCES

1. Pellagatti A., Jädersten M., Forsblom A. M., Cattan H., Christensson B., Emanuelsson E. K., Merup M., Nilsson L., Samuelsson J., Sander B., Wainscoat J. S., Boultwood J., Hellström-Lindberg E. (2007) Proc. Natl. Acad. Sci. U.S.A. 104, 11406–11411 [PMCID: PMC1892786] [PubMed: 17576924]

2. Pellagatti A., Cazzola M., Giagounidis A. A., Malcovati L., Porta M. G., Killick S., Campbell L. J., Wang L., Langford C. F., Fidler C., Oscier D., Aul C., Wainscoat J. S., Boultwood J. (2006) Blood 108, 337–345 [PubMed: 16527891]

3. Jones P. A., Baylin S. B. (2002) Nat. Rev. Genet. 3, 415–428 [PubMed: 12042769]

4. Christiansen D. H., Andersen M. K., Pedersen-Bjergaard J. (2003) Leukemia 17, 1813–1819 [PubMed: 12970781]

5. Aggerholm A., Holm M. S., Guldberg P., Olesen L. H., Hokland P. (2006) Eur. J. Haematol. 76, 23–32 [PubMed: 16343268]

6. Cancelas J. A., Lee A. W., Prabhakar R., Stringer K. F., Zheng Y., Williams D. A. (2005) Nat. Med. 11, 886–891 [PubMed: 16025125]

7. Issa J. P., Garcia-Manero G., Giles F. J., Mannari R., Thomas D., Faderl S., Bayar E., Lyons J., Rosenfeld C. S., Cortes J., Kantarjian H. M. (2004) Blood 103, 1635–1640 [PubMed: 14604977]

8. Kantarjian H., Oki Y., Garcia-Manero G., Huang X., O'Brien S., Cortes J., Faderl S., Bueso-Ramos C., Ravandi F., Estrov Z., Ferrajoli A., Wierda W., Shan J., Davis J., Giles F., Saba H. I., Issa J. P. (2007) Blood 109, 52–57 [PubMed: 16882708]

9. Jiang Y., Dunbar A., Gondek L. P., Mohan S., Rataul M., O'Keefe C., Sekeres M., Saunthararajah Y., Maciejewski J. P. (2009) Blood 113, 1315–1325 [PMCID: PMC2637194] [PubMed: 18832655]

10. Esteller M. (2003) Adv. Exp. Med. Biol. 532, 39–49 [PubMed: 12908548]

11. Schumacher A., Kapranov P., Kaminsky Z., Flanagan J., Assadzadeh A., Yau P., Virtanen C., Winegarden N., Cheng J., Gingeras T., Petronis A. (2006) Nucleic Acids Res. 34, 528–542 [PMCID: PMC1345696] [PubMed: 16428248]

12. Weber M., Davies J. J., Wittig D., Oakeley E. J., Haase M., Lam W. L., Schübeler D. (2005) Nat.

Genet. 37, 853–862 [PubMed: 16007088]

13. Figueroa M. E., Lugthart S., Li Y., Erpelinck-Verschueren C., Deng X., Christos P. J., Schifano E., Booth J., van Putten W., Skrabanek L., Campagne F., Mazumdar M., Greally J. M., Valk P. J., Löwenberg B., Delwel R., Melnick A. (2010) Cancer Cell 17, 13–27 [PMCID: PMC3008568] [PubMed: 20060365]

14. Khulan B., Thompson R. F., Ye K., Fazzari M. J., Suzuki M., Stasiek E., Figueroa M. E., Glass J. L., Chen Q., Montagna C., Hatchwell E., Selzer R. R., Richmond T. A., Green R. D., Melnick A., Greally J. M. (2006) Genome Res. 16, 1046–1055 [PMCID: PMC1524864] [PubMed: 16809668]

15. Thompson R. F., Reimers M., Khulan B., Gissot M., Richmond T. A., Chen Q., Zheng X., Kim K., Greally J. M. (2008) Bioinformatics 24, 1161–1167 [PubMed: 18353789]

16. Gondek L. P., Tiu R., O'Keefe C. L., Sekeres M. A., Theil K. S., Maciejewski J. P. (2008) Blood 111, 1534–1542 [PMCID: PMC2214746] [PubMed: 17954704]

17. Mohamedali A., Gäken J., Twine N. A., Ingram W., Westwood N., Lea N. C., Hayden J., Donaldson N., Aul C., Gattermann N., Giagounidis A., Germing U., List A. F., Mufti G. J. (2007) Blood 110, 3365–3373 [PubMed: 17634407]

18. Starczynowski D. T., Vercauteren S., Telenius A., Sung S., Tohyama K., Brooks-Wilson A., Spinelli J. J., Eaves C. J., Eaves A. C., Horsman D. E., Lam W. L., Karsan A. (2008) Blood 112, 3412–3424 [PubMed: 18663149]

19. Figueroa M. E., Reimers M., Thompson R. F., Ye K., Li Y., Selzer R. R., Fridriksson J., Paietta E., Wiernik P., Green R. D., Greally J. M., Melnick A. (2008) PLoS ONE 3, e1882 [PMCID: PMC2266992] [PubMed: 18365023]

20. Figueroa M. E., Wouters B. J., Skrabanek L., Glass J., Li Y., Erpelinck-Verschueren C. A., Langerak A. W., Löwenberg B., Fazzari M., Greally J. M., Valk P. J., Melnick A., Delwel R. (2009) Blood 113, 2795–2804 [PMCID: PMC2945920] [PubMed: 19168792]

21. Deleted in proof.

22. Olshen A. B., Venkatraman E. S., Lucito R., Wigler M. (2004) Biostatistics 5, 557–572 [PubMed: 15475419]

23. Subramanian A., Tamayo P., Mootha V. K., Mukherjee S., Ebert B. L., Gillette M. A., Paulovich A., Pomeroy S. L., Golub T. R., Lander E. S., Mesirov J. P. (2005) Proc. Natl. Acad. Sci. U.S.A. 102, 15545–15550 [PMCID: PMC1239896] [PubMed: 16199517]

24. Ashburner M., Ball C. A., Blake J. A., Botstein D., Butler H., Cherry J. M., Davis A. P., Dolinski K., Dwight S. S., Eppig J. T., Harris M. A., Hill D. P., Issel-Tarver L., Kasarskis A., Lewis S., Matese J. C., Richardson J. E., Ringwald M., Rubin G. M., Sherlock G. (2000) Nat. Genet. 25, 25–29 [PMCID: PMC3037419] [PubMed: 10802651]

25. Quandt K., Frech K., Karas H., Wingender E., Werner T. (1995) Nucleic Acids Res. 23, 4878–4884 [PMCID: PMC307478] [PubMed: 8532532]

26. Edgar R., Domrachev M., Lash A. E. (2002) Nucleic Acids Res. 30, 207–210 [PMCID: PMC99122] [PubMed: 11752295]

27. Breit S., Nees M., Schaefer U., Pfoersich M., Hagemeier C., Muckenthaler M., Kulozik A. E. (2004) Br. J. Haematol. 126, 231–243 [PubMed: 15238145]

28. Eckfeldt C. E., Mendenhall E. M., Flynn C. M., Wang T. F., Pickart M. A., Grindle S. M., Ekker S. C., Verfaillie C. M. (2005) PLoS Biol. 3, e254 [PMCID: PMC1166352] [PubMed: 16089502]

29. Oswald J., Steudel C., Salchert K., Joergensen B., Thiede C., Ehninger G., Werner C., Bornhäuser M. (2006) Stem Cells 24, 494–500 [PubMed: 16166251]

30. Sternberg A., Killick S., Littlewood T., Hatton C., Peniket A., Seidl T., Soneji S., Leach J., Bowen D., Chapman C., Standen G., Massey E., Robinson L., Vadher B., Kaczmarski R., Janmohammed R., Clipsham K., Carr A., Vyas P. (2005) Blood 106, 2982–2991 [PubMed: 16076868]

31. Li Y., Sassano A., Majchrzak B., Deb D. K., Levy D. E., Gaestel M., Nebreda A. R., Fish E. N., Platanias L. C. (2004) J. Biol. Chem. 279, 970–979 [PubMed: 14578350]

32. Sohal D., Yeatts A., Ye K., Pellagatti A., Zhou L., Pahanish P., Mo Y., Bhagat T., Mariadason J., Boultwood J., Melnick A., Greally J., Verma A. (2008) PLoS ONE 3, e2965 [PMCID: PMC2495035] [PubMed: 18698424]

33. Zhou L., Nguyen A. N., Sohal D., Ying Ma J., Pahanish P., Gundabolu K., Hayman J., Chubak A., Mo Y., Bhagat T. D., Das B., Kapoun A. M., Navas T. A., Parmar S., Kambhampati S., Pellagatti A., Braunchweig I., Zhang Y., Wickrema A., Medicherla S., Boultwood J., Platanias L. C., Higgins L. S., List A. F., Bitzer M., Verma A. (2008) Blood 112, 3434–3443 [PMCID: PMC2569182] [PubMed: 18474728]

34. Upadhyay G., Goessling W., North T. E., Xavier R., Zon L. I., Yajnik V. (2008) Oncogene 27, 5845–5855 [PMCID: PMC4774646] [PubMed: 18641688]

35. Figueroa M. E., Abdel-Wahab O., Lu C., Ward P. S., Patel J., Shih A., Li Y., Bhagwat N., Vasanthakumar A., Fernandez H. F., Tallman M. S., Sun Z., Wolniak K., Peeters J. K., Liu W., Choe S. E., Fantin V. R., Paietta E., Löwenberg B., Licht J. D., Godley L. A., Delwel R., Valk P. J., Thompson C. B., Levine R. L., Melnick A. (2010) Cancer Cell 18, 553–567 [PMCID: PMC4105845] [PubMed: 21130701]

36. Greenberg P., Cox C., LeBeau M. M., Fenaux P., Morel P., Sanz G., Sanz M., Vallespi T., Hamblin T., Oscier D., Ohyashiki K., Toyama K., Aul C., Mufti G., Bennett J. (1997) Blood 89, 2079–2088 [PubMed: 9058730]

37. Alvarez H., Opalinska J., Zhou L., Sohal D., Fazzari M., Yu Y., Montagna C., Montgomery E., Canto M., Dunbar K., Wang J., Roa J., Mo Y., Bhagat T., Ramesh K., Cannizzaro L., Mollenhauer J., Thompson R., Suzuki M., Meltzer S., Melnick A., Greally J. M., Maitra A., Verma A. (2011) PLoS Genet. 7, e1001356 [PMCID: PMC3069107] [PubMed: 21483804]

38. Figueroa M. E., Skrabanek L., Li Y., Jiemjit A., Fandy T. E., Paietta E., Fernandez H., Tallman M. S., Greally J. M., Carraway H., Licht J. D., Gore S. D., Melnick A. (2009) Blood 114, 3448–3458 [PMCID: PMC2765680] [PubMed: 19652201]

39. Soderholm J., Kobayashi H., Mathieu C., Rowley J. D., Nucifora G. (1997) Leukemia 11, 352–358 [PubMed: 9067573]

40. Eaton S. A., Funnell A. P., Sue N., Nicholas H., Pearson R. C., Crossley M. (2008) J. Biol. Chem. 283, 26937–26947 [PMCID: PMC2556010] [PubMed: 18687676]

41. Yajnik V., Paulding C., Sordella R., McClatchey A. I., Saito M., Wahrer D. C., Reynolds P., Bell D. W., Lake R., van den Heuvel S., Settleman J., Haber D. A. (2003) Cell 112, 673–684 [PubMed: 12628187]

42. Liang H., Castro P. D., Ma J., Nagarajan L. (2005) Cancer Genet. Cytogenet. 162, 151–159 [PubMed: 16213364]

43. Irizarry R. A., Ladd-Acosta C., Wen B., Wu Z., Montano C., Onyango P., Cui H., Gabo K., Rongione M., Webster M., Ji H., Potash J. B., Sabunciyan S., Feinberg A. P. (2009) Nat. Genet. 41, 178–186 [PMCID: PMC2729128] [PubMed: 19151715]

44. Verma A., Deb D. K., Sassano A., Kambhampati S., Wickrema A., Uddin S., Mohindru M., Van Besien K., Platanias L. C. (2002) J. Immunol. 168, 5984–5988 [PubMed: 12055203]

45. Verma A., Deb D. K., Sassano A., Uddin S., Varga J., Wickrema A., Platanias L. C. (2002) J. Biol. Chem. 277, 7726–7735 [PubMed: 11773065]

Figures and Tables

TABLE 1

MDS patient characteristics

The following abbreviations are used: HGB, GM/DL, NML, normal; RAEB, refractory anemia with excess blasts; RCMD, refractory cytopenias with multilineage dysplasia; RA, refractory anemia; CMML, chronic myelomonocytic leukemia;.

Sample ID	Subtype	HGB (GM/DL)	WBC ($\times 10^3$)	Platelets ($\times 10^3$)	Cytogenetics	Lymphocytes	Neutrophils
						%	%
MDS 1	RAEB	7.7	1	24	−7, −5	33	44
MDS 2	RCMD	11.7	1.7	32	−20q	40	45
MDS 3	RAEB	9.6	3.8	1	Complex	39	29
MDS 4	RAEB	9	1.4	19	+8	47	51
MDS 5	RCMD	14	2.1	126	NML	26	59
MDS 6	RCMD	12.6	2.1	85	NML	27	56
MDS 7	RAEB	9.9	2.1	5	Complex	57	32
MDS 8	RCMD	8.2	4.5	101	NML	36	54
MDS 9	RCMD	11.2	5.1	170	NML	15	76
MDS 10	RA	9	6.7	335	NML	38	45
MDS 11	RCMD	8.1	2.9	131	NML	37	49
MDS 12	RAEB	8.9	2.2	26	NML	32	49
MDS 13	RA	9.8	5.8	165	NML	42	41
MDS 14	RCMD	9.3	4.1	67	−7, +1	38	8
MDS 15	CMML	12.8	60	468	NML	5	81
MDS 16	RCMD	7.3	11.6	123	−5q, −1	30	56
MDS 17	RAEB	4.6	9.2	169	NML	42	39

MDS 18	RAEB	8.4	44	89	+8	10	89
MDS 19	RA	8.9	6.3	181	+8	45	39
MDS 20	RAEB	8.1	0.8	51	Complex	73	25
5q Syndrome	RA	6.6	11.6	562	−5q	16	74

FIGURE 1.

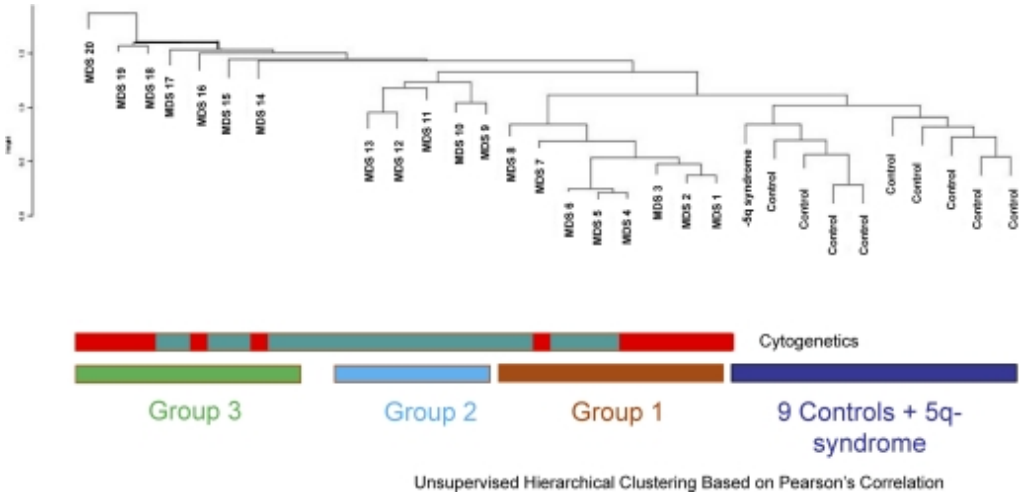

Methylation profiling on peripheral blood leukocytes separates distinct subsets of MDS from normals. Methylation profiles generated by the HELP assay were used to cluster 21 MDS and 9 control samples by hierarchical clustering. The controls formed a cluster that was distinct from MDS samples. The MDS samples included two clusters (groups 1 and 2) of epigenetically similar samples with a greater amount of resemblance to controls. The remaining seven MDS samples demonstrated greater heterogeneity. No correlation with cytogenetics (normal represented as *green* and abnormal as *red*) was seen.

FIGURE 2.

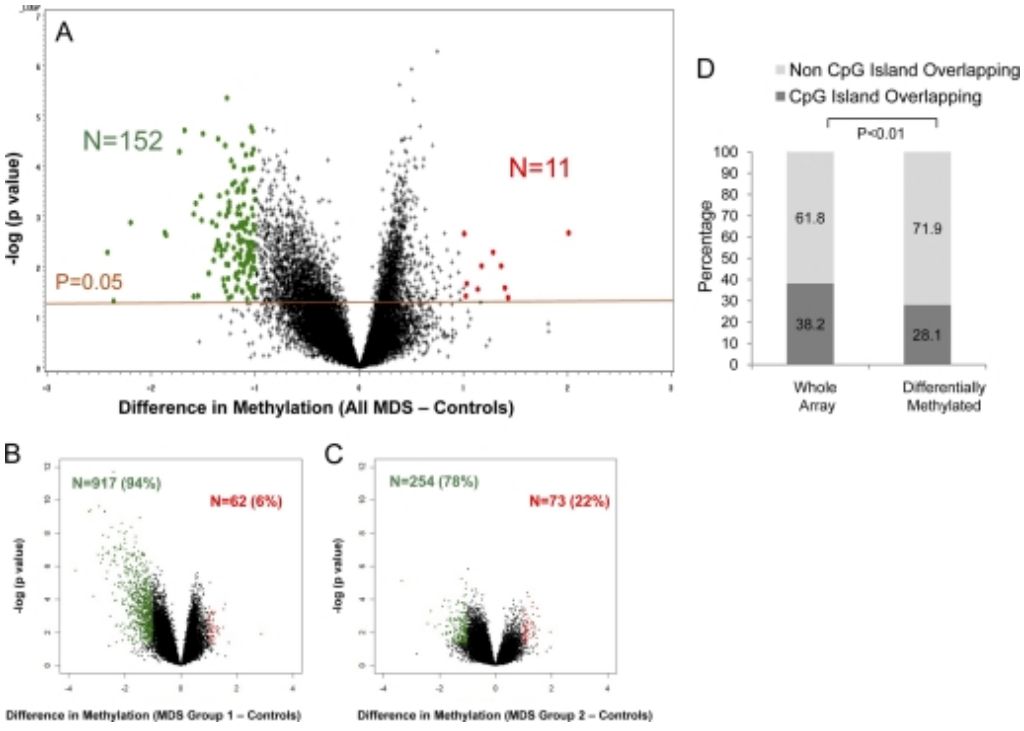

Majority of differentially methylated loci are hypermethylated in MDS leukocytes and reside outside of CpG islands. A volcano plot is shown demonstrating the difference in mean methylation between all MDS samples and controls on the *x* axis and the log of the *p* values between the means on the *y* axis. A two-tailed *t* test was used to calculate the *p* values. Significantly methylated loci with a log fold change in mean methylation are labeled in *green*, and significantly hypomethylated loci are labeled in *red* (*A*). Volcano plots for MDS subgroups 1 and 2 also reveal mostly hypermethylated loci with a variable number of hypomethylated loci. *B* and *C*, genomic position of every HpaII-amplifiable fragment on the HELP array was compared with the location of known CpG islands, and the fragments on the array were divided into two categories, those overlapping with these genomic elements and those not overlapping. To determine whether the differentially methylated genes between MDS and controls were enriched for either one of these types of elements, a proportions test was used to compare the relative proportion of the two types of HpaII fragments in the signature with the relative proportion on the array. *Stacking bars* are used to illustrate the finding of a significant enrichment for HpaII-amplifiable fragments not overlapping with CpG islands (*D*).

TABLE 2

Functional grouping of hypermethylated genes in MDS (Gene Ontology)

Biogroup	*p* value	Genes
GTPase regulator activity	6.90E-06	*DOCK4, DOCK2, ARHGEF4, CDC42SE1, FARP1, GIT2, IQGAP2, RALGPS1*
Calcium-dependent cell-cell adhesion	9.10E-05	*PCDH12, PCDHB11*
Spermatid development	9.10E-05	*H1FNT, NME5*
Small nuclear ribonucleoprotein complex	0.0001	*GEMIN4, PRPF8, SNRPF*
Nuclear organization and biogenesis	0.0003	*H1FNT, SYNE1*
Transcription	0.0008	*HOXB3, RUNX3, CCRN4L, KLF3, PLAGL2, MED12, PPARGC1A, HMGN3, ZFX, ENG, PRKAR1A*

TABLE 3

Transcription factor binding sites enriched in hypermethylated genes in MDS

Transcription factors	No. of genes	*p* value	Genes	Motif
SP1	12	3.10E-05	*DOCK4, PLAGL2, ZFX, C11ORF30, DDAH2, SYNE1, SV2A, ARRDC4, SEZ6, STRN, NXT2, SLC35D1*	GGGCGGR
AHR	5	4.19E-04	*PLAGL2, ZFX, RUNX3, ANGPTL2, VAMP3*	CCYCNRRSTNGCGTGASA
E12	14	3.78E-03	*PLAGL2, C11ORF30, DDAH2, SYNE1, SV2A, DUSP4, PPARGC1A, HOXB3, ADAMTS15, GIT2, ODC1, ITPK1, IQGAP2, LEPREL1*	CAGGTG
FOXO4	11	4.93E-	*MDS1, HSPG2, KLF3, C11ORF30, DOCK4, DUSP4,*	TTGTTT

		03	*PPARGC1A, HOXB3, HMGN3, ABCC1, DNAH11*	
NFY	4	5.80E-03	*ARRDC4, ADAMTS15, JMJD2A, IMP4*	GATTGGY
CHX10	2	8.60E-03	*SEZ6, MDS1*	TAATTA
AREB6	2	9.96E-03	*ADAMTS15, SEZ6*	CAGGTA
MAZ	14	1.22E-02	*ZFX, DDAH2, SYNE1, DOCK4, ARRDC4, RUNX3, DUSP4, ADAMTS15, MDS1, HSPG2, JMJD2A, JPH4, DAB2IP, GSPT1*	GGGAGGRR
GABP	2	1.32E-02	*GIT2, JPH4*	MGGAAGTG
LEF1	12	1.60E-02	*DOCK4, SEZ6, ANGPTL2, DUSP4, PPARGC1A, HOXB3, ODC1, KLF3, DAB2IP, NUP107, FARP1, ARHGEF4*	CTTTGT
NF1	2	1.81E-02	*DUSP4, HCN1*	TGCCAAR
SOX9	6	2.05E-02	*DOCK4, HSPG2, KLF3, MBP, PCDH12, ZNF502*	NNNNAACAATRGNN

FIGURE 3.

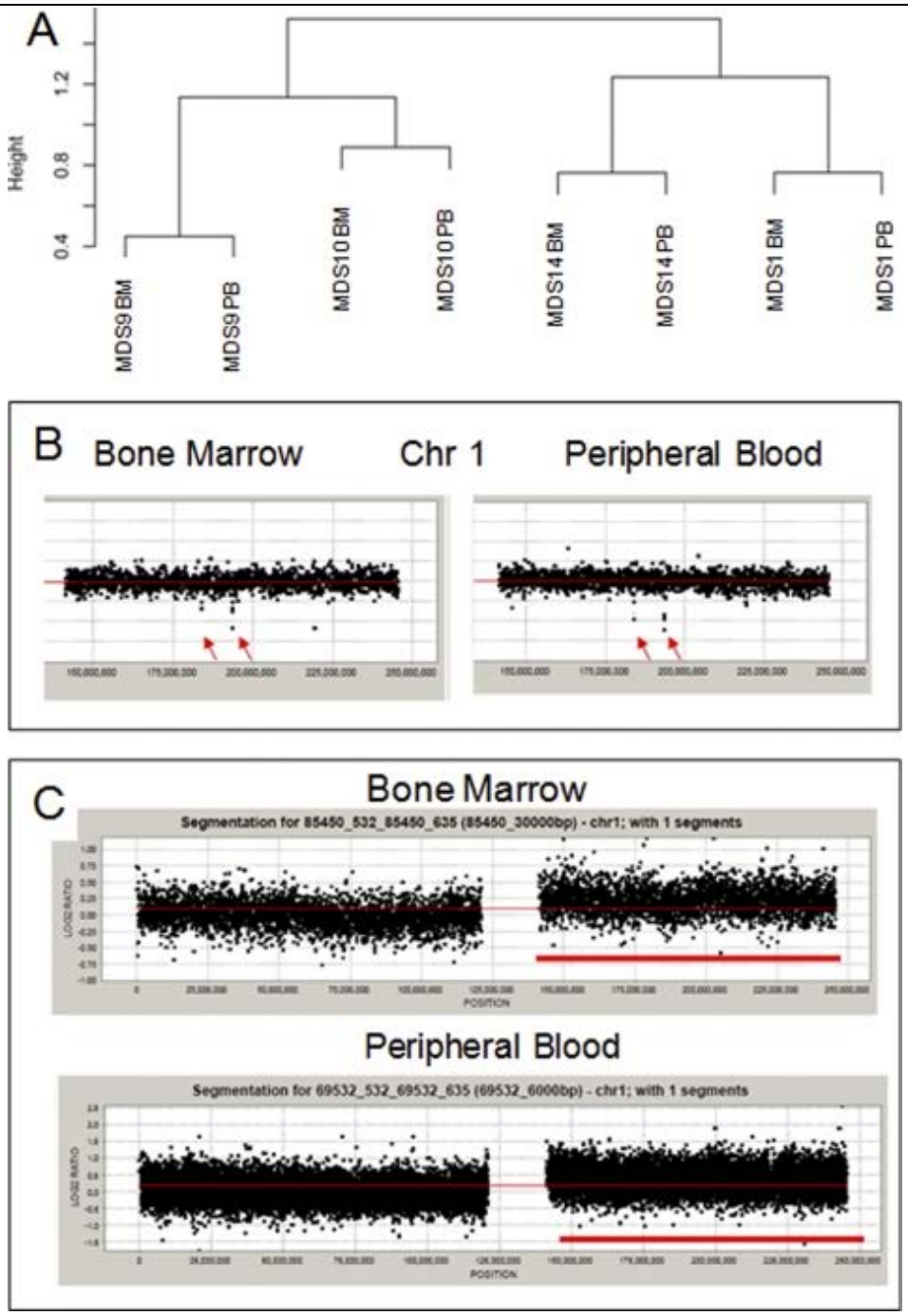

Array CGH can detect copy number variations in MDS leukocytes. Unsupervised clustering of copy number analysis reveals similarity between matched marrow (*BM*) and peripheral blood (*PB*) samples from the same patient (*A*). Array CGH plots of chromosome 1 reveal small deletions seen in both bone marrow and peripheral blood samples from one patient (*B*). In another patient with amplification of the short arm of chromosome 1 in bone marrow cells, the amplification is also seen in peripheral blood (*C*).

TABLE 4

CHROMOSOMAL LOCATION	GENE ID
chr1q32	CDS; CFHL1; complement factor H-related 1; Homo sapiens complement factor H-related 1, mRNA (cDNA clone MGC:13525 IMAGE:3934474), complete cds.
chr14q11	CDS; POTE14; protein expressed in prostate, ovary, testis, and placenta 14 isoform POTE-14B; Homo sapiens protein expressed in prostate, ovary, testis, and placenta 14 (POTE14), transcript variant POTE-14B, mRNA. CDS; N/A; N/A; human full-length cDNA 5-PRIME end of clone CS0DK007YB08 of HeLa cells of Homo sapiens (human). CDS; OR4Q3; olfactory receptor, family 4, subfamily Q, member 3; Homo sapiens olfactory receptor, family 4, subfamily Q, member 3 (OR4Q3), mRNA.
chr5q13	CDS; SMA5; N/A; H.sapiens SMA5 mRNA. CDS; N/A; basic transcription factor 2; Homo sapiens basic transcription factor 2 mRNA, complete cds. CDS; OCLN; occludin; Homo sapiens occludin (OCLN), mRNA. CDS; SERF1B; small EDRK-rich factor 1B, centromeric; Homo sapiens small EDRK-rich factor 1B (centromeric) (SERF1B), mRNA. CDS; N/A; basic transcription factor 2; Homo sapiens basic transcription factor 2 mRNA, complete cds. CDS; BIRC1; baculoviral IAP repeat-containing 1; Homo sapiens baculoviral IAP repeat-containing 1 (BIRC1), mRNA. CDS; psiNAIP; psi neuronal apoptosis inhibitory protein; Homo sapiens psiNAIP mRNA for psi neuronal apoptosis inhibitory protein, partial cds. CDS; BTNL8; butyrophilin-like 8; Homo sapiens butyrophilin-like 8 (BTNL8), mRNA.
chr5q22	CDS; KCNN2, potassium intermediate/small conductance calcium-activated channel, subfamily N, member 2 CDS; PGGT1B, protein geranylgeranyltransferase type I, beta subunit
chr7q21	CDS; TNFAIP9, tumor necrosis factor, alpha-induced protein 9
chr7q22	CDS; PRES, prestin (motor protein)
chr7q31	CDS; DOCK4, dedicator of cytokinesis 4
chr7q35	CDS; CTAGE6; CTAGE6 protein; Homo sapiens CTAGE family, member 6, mRNA (cDNA clone MGC:41943 IMAGE:5296763), complete cds. CDS; N/A; PRO2751; Homo sapiens PRO2751 mRNA, complete cds.
chr8p23	CDS; N/A; skin-antimicrobial peptide 1 (SAP1); H.sapiens mRNA for skin-antimicrobial-peptide 1 (SAP1). CDS; DEFB104; defensin, beta 104; Homo sapiens defensin, beta 104 (DEFB104), mRNA. CDS; SPAG11; N/A; Homo sapiens sperm associated antigen 11 (SPAG11), transcript variant B, mRNA.

Chromosomal regions commonly deleted in MDS

TABLE 5

CHROMOSOMAL LOCATION	GENE ID
chr1 (q41-q42)	CDS; MPN2; marapsin 2; Homo sapiens marapsin 2 (MPN2), mRNA. CDS; WNT9A; wingless-type MMTV integration site family, member 9A; Homo sapiens wingless-type MMTV integration site family, member 9A (WNT9A), mRNA. CDS; ARF1; ADP-ribosylation factor 1; Homo sapiens ADP-ribosylation factor 1, mRNA (cDNA clone MGC:9347 IMAGE:3463523), complete cds. CDS; MRPL55; mitochondrial ribosomal protein L55 isoform b; CDS; GUK1; guanylate kinase 1; Homo sapiens guanylate kinase 1, mRNA (cDNA clone MGC:10618 IMAGE:3946293), complete cds. CDS; OBSCN; obscurin, cytoskeletal calmodulin and titin-interacting RhoGEF; Homo sapiens obscurin, cytoskeletal calmodulin and titin-interacting RhoGEF (OBSCN), mRNA. CDS; KIAA1639; KIAA1639 protein; Homo sapiens mRNA for KIAA1639 protein, partial cds.
chr15(q11)	CDS; POTE15; protein expressed in prostate, ovary, testis, and placenta 15; Homo sapiens protein expressed in prostate, ovary, testis, and placenta 15 (POTE15), mRNA.
chr17(q12-q21)	CDS; CCL3L1; chemokine (C-C motif) ligand 3-like 1 precursor; Homo sapiens chemokine (C-C motif) ligand 3-like 1 (CCL3L1), mRNA. CDS; LOC51326; ARF protein; Homo sapiens ARF protein (LOC51326), mRNA. CDS; NSF; N-ethylmaleimide-sensitive factor; Homo sapiens N-ethylmaleimide-sensitive factor (NSF), mRNA.
chr19(q13)	CDS; GPVI; platelet glycoprotein VI-3; Homo sapiens GPVI mRNA for platelet glycoprotein VI-3, complete cds. CDS; RDH13; retinol dehydrogenase 13 (all-trans and 9-cis); Homo sapiens retinol dehydrogenase 13 (all-trans and 9-cis) (RDH13), mRNA. CDS; EPS8L1; epidermal growth factor receptor pathway substrate 8-like protein 1 isoform c; Homo sapiens EPS8-like 1 (EPS8L1), transcript variant 3, mRNA. CDS; PPP1R12C; protein phosphatase 1, regulatory subunit 12C; Homo sapiens protein phosphatase 1, regulatory (inhibitor) subunit 12C (PPP1R12C), mRNA. CDS; TNNI3; troponin I, cardiac; Homo sapiens troponin I, cardiac (TNNI3), mRNA. CDS; SYT5; synaptotagmin V; Homo sapiens synaptotagmin V (SYT5), mRNA. CDS; PTPRH; protein tyrosine phosphatase, receptor type, H precursor; Homo sapiens protein tyrosine phosphatase, receptor type, H (PTPRH), mRNA. CDS; HSPBP1; hsp70-interacting protein; Homo sapiens hsp70-interacting protein (HSPBP1), mRNA. CDS; SUV420H2; suppressor of variegation 4-20 homolog 2; Homo sapiens suppressor of variegation 4-20 homolog 2 (Drosophila) (SUV420H2), mRNA. CDS; COX6B2; cytochrome c oxidase subunit VIb, testis-specific isoform; Homo sapiens cytochrome c oxidase subunit VIb polypeptide 2 (testis) (COX6B2), mRNA. CDS; IL11; interleukin 11 precursor; Homo sapiens interleukin 11 (IL11), mRNA. CDS; MDAC1; MDAC1; Homo sapiens MDAC1 (MDAC1), mRNA. CDS; RPL28; ribosomal protein L28; Homo sapiens ribosomal protein L28 (RPL28), mRNA. CDS; UBE2S; UBE2S protein; Homo sapiens ubiquitin-conjugating enzyme E2S, mRNA (cDNA clone MGC:801 IMAGE:2988449), complete cds. CDS; ZEC; ZEC protein; Homo sapiens zinc finger protein Zec, mRNA (cDNA clone IMAGE:4449741), partial cds. CDS; KLP1; K562 cell-derived leucine-zipper-like protein 1; Homo sapiens K562 cell-derived leucine-zipper-like protein 1 (KLP1), mRNA.
	CDS; GGT2; gamma-glutamyl transpeptidase small subunit; Human kidney gamma-

chr22(q11)	glutamyl transpeptidase type II mRNA, 3' end. CDS; USP41; ubiquitin-specific protease 41; Homo sapiens partial mRNA for ubiquitin-specific protease 41 (USP41 gene).
chr7(q22)	CDS; POLR2J2; DNA directed RNA polymerase II polypeptide J-related gene isoform 1; CDS; RASA4; RAS p21 protein activator 4; Homo sapiens RAS p21 protein activator 4 (RASA4), mRNA.
chr8(p11)	CDS; ADAM5; ADAM5 protein; Homo sapiens a disintegrin and metalloproteinase domain 5.
chr8(q24)	CDS; GPR20; G protein-coupled receptor 20; Homo sapiens G protein-coupled receptor 20 (GPR20), mRNA. CDS; PTP4A3; protein tyrosine phosphatase type IVA, member 3 isoform 1; Homo sapiens protein tyrosine phosphatase type IVA, member 3 (PTP4A3), transcript variant 1, mRNA. CDS; BAI1; brain-specific angiogenesis inhibitor 1 precursor; Homo sapiens brain-specific angiogenesis inhibitor 1 (BAI1), mRNA. CDS; ARC; activity-regulated cytoskeleton-associated protein; Homo sapiens activity-regulated cytoskeleton-associated protein (ARC), mRNA. CDS; PSCA; prostate stem cell antigen; Homo sapiens prostate stem cell antigen (PSCA), mRNA. CDS; LY6K; cDNA for differentially expressed CO16 gene; Homo sapiens cDNA for differentially expressed CO16 gene (LY6K), mRNA. CDS; LOC51337; mesenchymal stem cell protein DSCD75; Homo sapiens mesenchymal stem cell protein DSCD75, mRNA (cDNA clone MGC:5515 IMAGE:3453935), complete cds. CDS; ARS; ARS component B precursor; Homo sapiens ARS component B (ARS), mRNA. CDS; LYNX1; Ly-6 neurotoxin-like protein 1; Homo sapiens Ly-6 neurotoxin-like protein 1 (LYNX1), transcript variant 3, mRNA. CDS; LY6D; LY6D protein; Homo sapiens lymphocyte antigen 6 complex, locus D, mRNA (cDNA clone IMAGE:5429968), partial cds. CDS; GML; GPI anchored molecule like protein; Homo sapiens GPI anchored molecule like protein (GML), mRNA. CDS; CYP11B1; cytochrome P450, subfamily XIB (steroid 11-beta-hydroxylase), polypeptide 1 precursor; CDS; LY6E; LY6E protein; Homo sapiens lymphocyte antigen 6 complex, locus E, mRNA (cDNA clone IMAGE:3447182), complete cds. CDS; HHCM; Mahlavu hepatocellular carcinoma protein; Homo sapiens Mahlavu hepatocellular carcinoma (HHCM), mRNA. CDS; LY6H; lymphocyte antigen 6 complex, locus H; Homo sapiens lymphocyte antigen 6 complex, locus H, mRNA (cDNA clone MGC:24913 IMAGE:4939118), complete cds. CDS; LOC338328; high density lipoprotein-binding protein; Homo sapiens high density lipoprotein-binding protein (LOC338328), mRNA. CDS; GLI4; GLI-Kruppel family member GLI4; Homo sapiens GLI-Kruppel family member GLI4 (GLI4), mRNA. CDS; TOP1MT; mitochondrial topoisomerase I; Homo sapiens topoisomerase (DNA) I, mitochondrial (TOP1MT), nuclear gene encoding mitochondrial protein, mRNA. CDS; RHPN1; RHPN1 protein; Homo sapiens rhophilin, Rho GTPase binding protein 1, mRNA (cDNA clone MGC:34714 IMAGE:5211354), complete cds. CDS; MAFA; v-maf musculoaponeurotic fibrosarcoma oncogene homolog A; Homo sapiens v-maf musculoaponeurotic fibrosarcoma oncogene homolog A (avian) (MAFA), mRNA. CDS; ZC3HDC3; zinc finger CCCH type domain containing 3; Homo sapiens zinc finger CCCH type domain containing 3 (ZC3HDC3), mRNA. CDS; GSDMDC1; gasdermin domain containing 1; Homo sapiens gasdermin domain containing 1 (GSDMDC1), mRNA. CDS; EEF1D; eukaryotic translation elongation factor 1 delta, isoform 2; CDS; TIGD5; tigger transposable element derived 5; Homo sapiens tigger transposable element derived 5 (TIGD5), mRNA. CDS; PYCRL; pyrroline-5-carboxylate reductase-like; Homo sapiens pyrroline-5-carboxylate reductase-like (PYCRL), mRNA. CDS; TSTA3; tissue specific transplantation antigen P35B; Homo sapiens tissue specific transplantation antigen P35B, mRNA (cDNA clone MGC:4302 IMAGE:2819332), complete cds.
chrX(q28)	CDS; OPN1MW; opsin 1 (cone pigments), medium-wave-sensitive (color blindness, deutan);

Chromosomal regions commonly amplified in MDS

FIGURE 4.

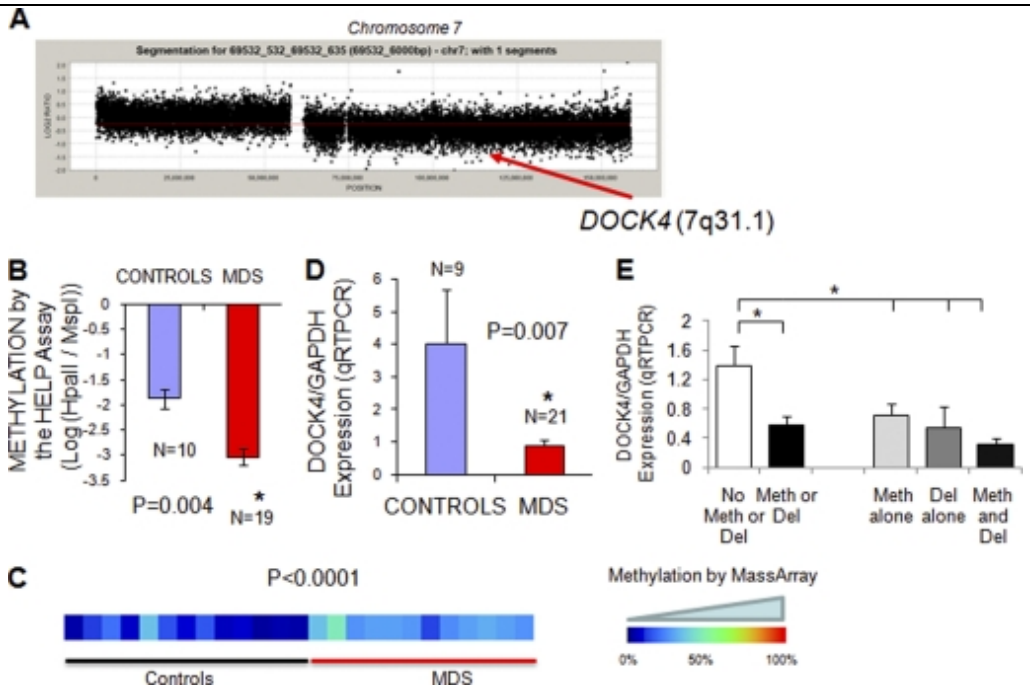

Integrative analysis reveals *DOCK4* to be silenced by both deletion and hypermethylation in MDS. The aCGH plot of chromosome 7 from an MDS patient with 7q deletion shows the location of the *DOCK4* gene (*A*). Mean methylation from the HELP assay (depicted by $\log_2$(HpaII/MspI)) is significantly higher in MDS samples as evident from a more negative value (two-tailed *t* test) (*B*). Methylation analysis of the DOCK4 promoter by MassArray analysis reveals greater methylation in MDS samples as depicted in the heat map (*C*). quantitative RT-PCR was performed on RNA from MDS leukocytes and control samples and showed a significantly reduced expression in MDS (*D*). Means ± S.E. with *p* value were calculated by two-tailed *t* test. Expression of DOCK4 was evaluated in MDS samples with or without deletions (*Del*) and promoter methylation (*Meth*) and shows significant reduction with either genetic or epigenetic silencing. Means ± S.E. with *p* value were calculated by two-tailed *t* test (*E*).

FIGURE 5.

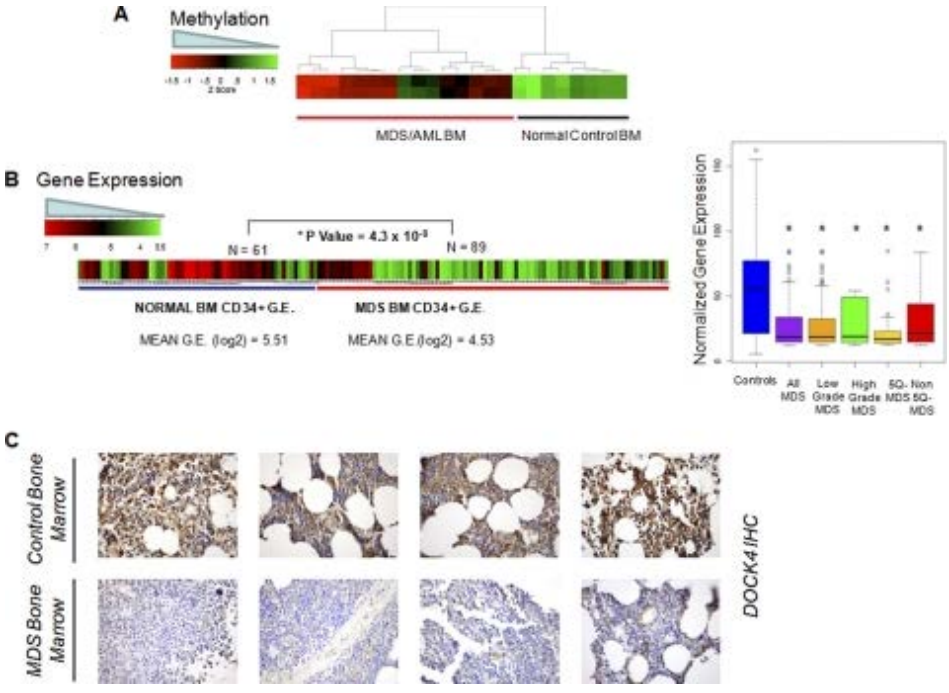

Validation in independent cohorts demonstrate reduction in DOCK4 in marrow samples from MDS/AML.

Methylation values obtained from the HELP assay performed on marrow (*BM*) samples in an independent cohort of patients (38) show hypermethylation of the promoter in MDS/AML samples (*A*). Gene expression values from various studies on MDS and normal bone marrow-derived $CD34^+$ cells were obtained and normalized. Mean expression of *DOCK4* was significantly reduced in 89 MDS cases when compared with 61 controls (two-tailed *t* test) (*B, left panel*); box plots of MDS subtypes show significantly reduced levels of DOCK4 in all subtypes of MDS (*B, right panel*). Bone marrow biopsy samples were stained with DOCK4 antibody and show decreased expression in four representative cases of MDS when compared with controls (*C*).

FIGURE 6.

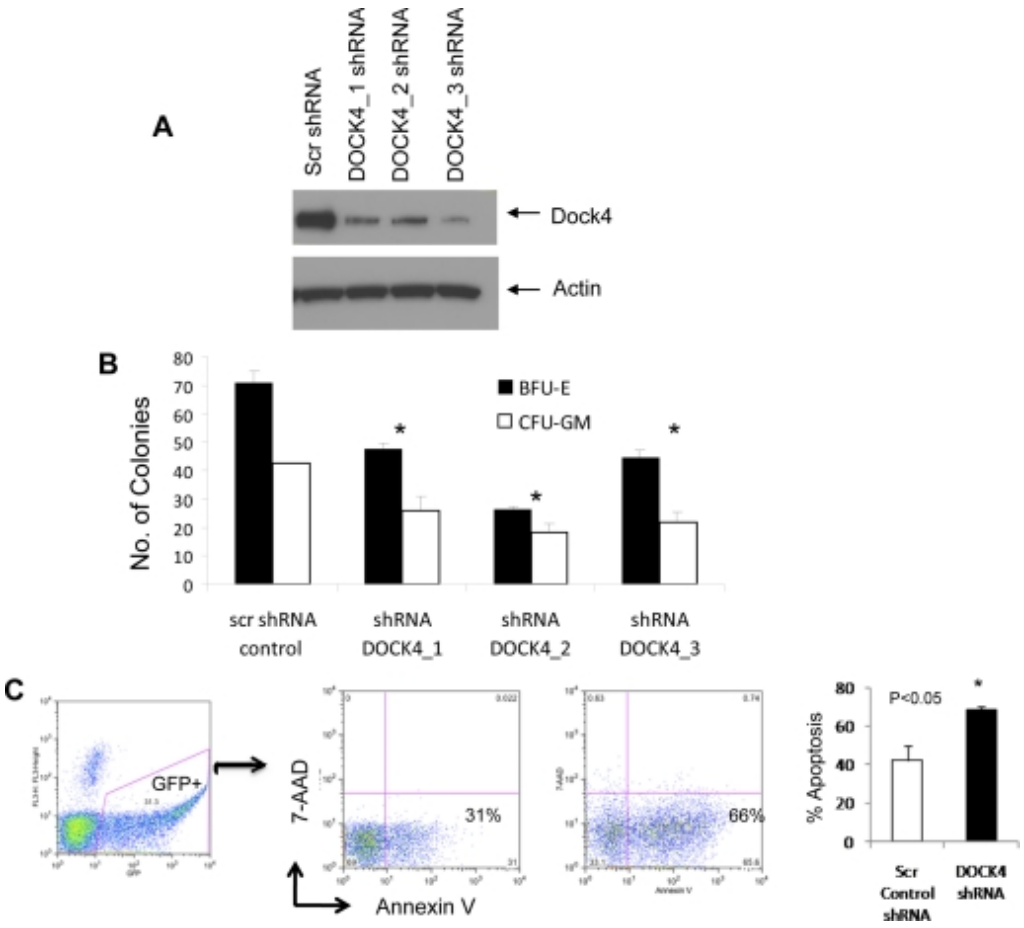

DOCK4 knockdown leads to ineffective hematopoiesis *in vitro*. DOCK4 protein expression was reduced by three lentiviral mediated shRNA constructs (*A*). Primary bone marrow $CD34^+$ stem cells with DOCK4 shRNAs produced fewer erythroid (erythroid burst-forming units (*BFU-E*)) and myeloid (*CFU-GM*) colonies (means ± S.E.; *t* test, *p* value< 0.05) (*B*). DOCK4 shRNA was able to increase apoptosis significantly in GFP^+-sorted $CD34^+$ cells (*t* test, *p* value< 0.05). Three independent experiments shown as means ± S.E. (*C*).

Published in final edited form as:
Cancer Res. 2011 February 1; 71(3): 955–963. doi:10.1158/0008-5472.CAN-10-2933.

Reduced SMAD7 leads to overactivation of TGF-beta signaling in MDS that can be reversed by a specific inhibitor of TGF-beta receptor I kinase

L Zhou[1], **C McMahon**[1], **T Bhagat**[1], **C Alencar**[1], **Y Yu**[1], **M Fazzari**[1], **D Sohal**[1], **C Heuck**[1], **K Gundabolu**[1], **C Ng**[1], **Y Mo**[1], **W Shen**[1], **A Wickrema**[2], **G Kong**[1], **E Friedman**[1], **L Sokol**[3], **G Mantzaris**[1], **A Pellagatti**[4], **J Boultwood**[4], **LC. Platanias**[5], **U Steidl**[1], **L Yan**[6], **JM Yingling**[6], **MM Lahn**[6], **A List**[3], **M Bitzer**[7], and **A Verma**[1]

[1]Albert Einstein College of Medicine, Bronx, NY

[2]University of Chicago, Chicago, IL

[3]Moffitt Cancer Center, Tampa, FL

[4]John Radcliffe Hospital, Oxford, UK

[5]Northwestern University Robert H Lurie Cancer Center, Chicago, IL

[6]Eli Lilly

[7]University of Michigan

Abstract

Even though myelodysplastic syndromes are characterized by ineffective hematopoiesis, the molecular alterations that lead to marrow failure have not been well elucidated. We have previously shown that the myelosuppressive TGF-β pathway is constitutively activated in MDS progenitors. Since there is conflicting data about upregulation of extracellular TGF-b levels in MDS, we wanted to determine the molecular basis of TGF-β pathway overactivation and consequent hematopoietic suppression in this disease. We observed that SMAD7, a negative regulator of TGF-β receptor I (TBRI) kinase is markedly decreased in a large meta-analysis of gene expression studies from MDS marrow derived CD34+ cells. SMAD7 protein was also found to be significantly decreased in MDS marrow progenitors when examined immunohistochemically in a bone marrow tissue microarray. Reduced expression of SMAD7 in hematopoietic cells led to increased TGF-β mediated gene transcription and enhanced sensitivity to TGF-β mediated suppressive effects. The increased TGF-β signaling due to SMAD7 reduction could be effectively inhibited by a novel clinically relevant TBRI (ALK5 kinase) inhibitor, LY-2157299. LY-2157299 could inhibit TGF-β mediated SMAD2 activation and hematopoietic suppression in primary hematopoietic stem cells. Furthermore, in vivo administration of LY-2157299 ameliorated anemia in a TGF-β overexpressing transgenic mouse model of bone marrow failure. Most importantly, treatment with LY-2157199 stimulated hematopoiesis from primary MDS bone marrow specimens. These studies demonstrate that reduction in SMAD7 is a novel molecular alteration in MDS that leads to ineffective hematopoiesis by activating of TGF-β signaling in hematopoietic cells. These studies also illustrate the therapeutic potential of TBRI inhibitors in MDS.

Correspondence to: Amit Verma, MD, Chanin 302B, Albert Einstein Cancer Center, 1300 Morris Park Avenue, Bronx, NY 10461, averma@aecom.yu.edu.

Keywords

Myelodysplasia; TGF; SMAD7; LY-2157299

INTRODUCTION

The myelodysplastic syndromes (MDS) are clonal stem cell disorders characterized by cytologic dysplasia and ineffective hematopoiesis(1-3). Although approximately a third of patients may progress to acute leukemia, refractory cytopenias are the principal cause of morbidity and mortality in patients with MDS(4). In fact, approximately two-thirds of patients present with lower risk disease characterized by a hypercellular marrows with increased rates of apoptosis in the progenitor and differentiated cell compartments in the marrow (5-8). Ineffective hematopoiesis arising from abortive maturation leads to peripheral cytopenias. Higher grade or more advanced disease categories are associated with a significant risk of leukemia transformation with a corresponding lower apoptotic index and higher percentage of marrow blasts.

Cytokines play important roles in the regulation of normal hematopoiesis and a balance between the actions of hematopoietic growth factors and myelosuppressive factors is required for optimal production of different hematopoietic cell lineages. Excess production of inhibitory cytokines amplifies ineffective hematopoiesis inherent to the MDS clone. TGF-β is a myelosuppressive cytokine that has been implicated in the hematopoietic suppression in MDS. The plasma levels of TGF-β have been reported to be elevated in some(9-13) but not all studies (14-17) and are supported by greater TGF-β immunohistochemical staining in selected studies. In addition to direct myelosuppressive effects, TGF-β has also been implicated in the autocrine production of other myelosuppressive cytokines (TNF, IL-6, and IFN γ) in MDS (18). Conflicting data may arise from technical limitations of bone marrow immunohistochemical analyses of a secreted protein as well as the biological heterogeneity of the disease itself. Thus we investigated the role of TGF-β in MDS by direct examination of receptor signal activation to conclusively determine its role in the pathogenesis of ineffective hematopoiesis in MDS. We determined that the SMAD2 is upregulated and overactivated in MDS bone marrow progenitors, thereby demonstrating sustained TGF-β signal activation in this disease. We also determined that inhibition of SMAD2 activation can stimulate hematopoiesis from primary MDS progenitors, demonstrating its activation by TGF beta receptor as an important event in ineffective hematopoiesis. Since there is conflicting data about upregulation of extracellular TGF-β levels in MDS, we next sought to determine the molecular basis of TGF-β receptor-I (TBRI) overactivation and subsequent SMAD2 phosphorylation / activation in this disease in the present study. We observed that SMAD7, a negative regulator of TBRI kinase, is markedly decreased in MDS and that this leads overactivation of TGF-β signal transduction even in the absence of increased levels of extracellular TGF-β. Our studies also show that this can be reversed by a clinically relevant novel inhibitor of TGF--β receptor I kinase, LY-2157299, and points to the therapeutic potency of this approach in MDS.

MATERIALS AND METHODS

Cells Lines and Reagents

Human CD34+ cells were isolated from bone marrows of normal or MDS patients, after obtaining informed consent approved by the institutional review board of Albert Einstein College of Medicine. Bone marrow CD34+ cells from various normal donors were also obtained from AllCells (Emeryville, CA). K562 and HS-5 cell lines were purchased from ATCC. Erythropoietin and Transforming growth factor-β1 (TGF-β1) were bought from

R&D Systems (Minneapolis, MN). The phos-SMAD2 (S465/467) and actin antibodies were from Cell Signaling Technology (Beverly, MA), and SMAD2 antibody from Invitrogen. TBRI inhibitor LY-2157299 was provided by Eli Lilly. LY-2157299 was diluted in DMSO (20 mM stock solution) and kept at -20°C until use.

Cell Lysis and immunoblotting

Cells were lysed in phosphorylation lysis buffer as previously described (19). In the experiments in which the effects of LY-2157299 were studied, DMSO (diluent)-treated cells were used as control. Immunoblotting was performed as previously described (19).

ShRNA knockdown experiments: (only use nucleofection, not virus)

The Human Lentiviral shRNAmir (pGIPZ) containing the hairpin sequence (TGCTGTTGACAGTGAGCGAGCTGTGTTGCTGTGAATCTTATAGTGAAGCCACAG ATGTATAA GATTCACAGCAACACAGCCTGCCTACTGCCTCGGA) targeting SMAD7 and the non-silencing negative control were obtained from OpenBiosystems (OpenBiosystems, AL). Nucleofection of CD34+ cells or MDS BM MNCs was performed according to the manufacturer's instructions, by using the Nucleofector machine (Amaxa, Germany). The $CD34^+$ cells were thawed and cultured for 2 hours, 2×10^6 cells were resuspended in 100 μl human $CD34^+$ nucleofection solution (Amaxa, Germany). Samples were transferred into cuvettes and transfected by using program U08. $CD34^+$ cells were collected, dispensed in the wells of a 24-well plate containing 1 ml prewarmed StemSpan (StemCell Tech), supplemented with 100 ng/ml human FLt-3, SCF and TPO. The lentiviral transfected $CD34^+$ cells were sorted 24 hours later according to the GFP intensity using Moflow (Becton Dickinson, CA). Quantitative RT-PCR for SMAD7 expression was done on total RNA from HS-5 and K562 cells obtained by RNAeasy mini kit (Qiagen, CA). cDNA was synthesized with SuperScript Reverse Transcriptase III (Invitrogen). Real-time PCR was performed with SYBR green PCR Master Mix (Applied Biosystems, Foster City, CA) and SMAD7 and GAPDH (control) were simultaneously amplified with specific primers.

Primers for GADPH: Forward: 5'-CGACCACTTTGTCAAGCTCA-3' Reverse: 5'-CCCTGTTGCTGTAGCCAAAAT-3'

Primers for SMAD7: Forward:5'-GACAGCTCAATTCGGACAAC-3', Reverse: 5'-TCTCGTAGTCGAAAGCCTTG-3'

Meta-analysis

NCBI's GEO database was searched for gene expression studies on MDS and normal CD34 cells. A total of 3 MDS datasets with 89 unique MDS CD34+ studies(20,21) (ref BJH) and 61 normal CD34+ datasets from 6 studies (20-24) were identified and downloaded. The data was integrated using unigene IDs. Studies were done using Affymetrix U133A/B and Plus 2.0 platforms. After interarray quantile normalization, SMAD7 expression was assessed and visually represented as a heat map using R statistical software. All genes belonging to TGF-b signaling pathway were examined in the database. To strengthen the criteria for selecting genes that were differentially expressed in MDS, we only selected genes that were significantly different in the combined dataset as well as in the 2 major MDS cohorts (20,25) when studied independently.

Murine Experiments

Transgenic mice expressing a fusion gene (Alb/TGF) consisting of modified porcine TGF-β1 cDNA under the control of the regulatory elements of the mouse albumin gene (26) were used under animal institute approved protocol. Mice were given LY-2157299 at a dose of

100mg/kg/day in NaCMC/SLS/PVP/antifoam solution by gastric lavage using a curved 14 G needle. Blood counts were analyzed by Advia machine. Mice femurs were flushed and bone marrows cells were used for clonogenic assays.

TGF-β gene reporter assay—HS-5 cells were plated in six-well plates 24 hours before transfection. Cells were transfected in triplicate with SuperFect (Qiagen, CA) according to the manufacturer's instruction using the reporter plasmid (pGL2-3TP-Lux)(27). pSV-B-Gal was used to normalize the transfection efficiency. After an overnight incubation, the medium was replaced with serum-free medium with or without LY-215as necessary for the experiment. After 48 hours, cells were treated with 10 ng/ml TGFβ1. Cells were harvested 24 hours later in reporter lysis buffer (Promega, WI), and luciferase and β-galactosidase activities were determined using Dual Luciferase System (Promega, WI).

Hematopoietic progenitor cell assays—Hematopoietic progenitor colony formation was determined by clonogenic assays in methylcellulose, as in our previous studies (19,28). All participants in the study signed informed consent, approved by the institutional review board of Albert Einstein College of Medicine. Granulocyte/macrophage colony-forming (CFU-GM) units and erythroid burst forming units (BFU-E) from bone marrow samples were scored on day 14 of culture.

Immunohistochemistry on Bone Marrow Tissue Microarray

Tissue microarrays (TMAs) were constructed from formalin-fixed, paraffin-embedded bone marrow core biopsies from patients with MDS and control patients with anemia whose bone marrow showed no evidence of neoplasia. The tissue blocks were procured from Jacobi Hospital after approval by the Internal Review Board. For each patient, three 0.5 mm cores were placed in a tissue array using a manual arrayer (Chemicon International, Tenecula, CA). Sections of the TMAs were cut to 5 μm thickness, placed on positively charged slides, and heated to 60°C for one hour. They were then deparaffinized in xylene and rehydrated with graded alcohols. Endogenous peroxidase activity was quenched with 3% hydrogen peroxide. Antigen retrieval was accomplished by microwaving the slides in Dako Target Retrieval Solution, pH 6.0 (Dako Cytomation, Dako, Carpinteria, CA, USA), and subseqently steaming them in a vegetable steamer for 30 minutes. The slides were stained using a rabbit polyclonal anti-SMAD7 antibody, provided at 1:200 dilution, followed by Dako EnVision labeled polymer-HRP anti-rabbit antibody. Antibody binding was detected using DAB chromogen (Cell Marque, Rocklin, CA, USA). The slides were lightly counterstained with hematoxylin, dehydrated with graded alcohols, cleared with xylene, and coverslipped using Cytoseal 60 (Thermo Scientific, Waltham, MA, USA). The tissue cores were then scored for weak versus strong staining for SMAD7 by a hematopathologist who was blinded to the patient identities. Tissue cores that did not contain at least 10% evaluable marrow were excluded from the analysis.

RESULTS

SMAD7 is reduced in bone marrow progenitors in low grade MDS

To determine the molecular events that lead to overactivation of TGF-β signaling in MDS, we examined the expression of genes that are involved in and regulate the TGF-β signaling cascade in a large number of MDS patient samples. We used a meta-analysis of publicly available microarray studies in MDS, comprising a total of 89 unique MDS patient CD34+ gene expression profiles and 61 normal CD34+ controls. These data were obtained from published studies (20-25,29), were integrated using Unigene protein IDs, subjected to interarray normalization and then used for analysis. This strategy was shown to be biologically valid strategy for analysis previously by us (30). Our analysis of this integrated

dataset demonstrated that the SMAD7, a negative regulator of the TGF-β receptor kinase, was the most significantly differentially expressed gene in MDS and was markedly reduced in most cases (Fig 1, mean log2 expression 8.31 in controls vs 6.32 in mds cases, $p < 0.0001$, Bejmanin Hochberg correction, multiple testing). Subgroup analysis revealed that SMAD7 was significantly reduced (> 2 mean log fold reduction) in both low and high grade MDS samples, though most of the cases examined belonged to low risk MDS (83/89 cases). Subgroup analysis within low grade MDS revealed lower expression in cases with and without deletion of chromosome 5q, demonstrating that decrease in SMAD7 is an widespread and significant change in MDS bone marrow stem cells.

To confirm these results, bone marrows of patients with MDS were assessed for the SMAD7 expression by immunohistochemistry. A tissue microarray containing bone marrow samples from MDS and control bone marrow biopsies was prepared to minimize staining variability between individual slides. MDS bone marrow samples were compared to 24 age matched controls with non-MDS causes of cytopenias [iron deficiency anemia, chemotherapy related anemia, hyperplenism, drug induced marrow suppression, autoimmune anemia, Myelofibrosis and unexplained cytopenias in the absence of any dysplasia]. Significant reduction in SMAD7 was seen in bone marrow cells of patients with low risk MDS (75% of samples had reduced expression vs 9%of controls, $P<0.05$, proportions test), (Fig 2). Since SMAD7 is ubiquitously expressed, we also investigated the phenotypes of bone marrow cells that had reduced levels of this protein. Histological examination revealed that SMAD7 was reduced in hematopoietic progenitors of all lineages in MDS, including erythroid and myeloid progenitors.

Reduction in SMAD7 can lead to increased sensitivity to suppressive effects of TGF-β on hematopoiesis

We wanted to study the effect of SMAD7 reduction on TGF-β signaling in the hematopoietic system. A lentiviral vector based shRNA vector targeting SMAD7 was developed (Fig 3A) and was successfully able to inhibit SMAD7 expression when compared to scrambled control in various hematopoietic cells. (Fig 3B). Primary bone marrow derived CD34+ stem cells were infected with lentiviruses containing anti-SMAD7 and control shRNA constructs and then GFP selected and grown in methylcellulose in the presence and absence of varying amounts of TGF-β. Downregulation of SMAD7 led to significantly increased sensitivity to TGF-β and very low amounts of TGF-β was able to significantly inhibit erythroid colony formation when compared to controls, .

Next, we wanted to study the effect of SMAD7 downregulation on TGF-β signaling at the transcriptional level. Luciferase reporter assays that were dependant on SMAD2 binding demonstrated that shRNA mediated downregulation of SMAD7 led to increase in TGF-β mediated gene transcription in bone marrow stromal cells stably transfected with lentiviral shRNAs, Since previous studies have shown that SMAD7 can inhibit TGF-β receptor I kinase (TBRI) in other model systems, we hypothesized that reduction in SMAD7 levels leads to overactivation of TBRI and subsequent downstream signaling in hematopoietic cells in MDS. To test this we used a specific inhibitor of TBRI kinase (LY-2157299) and observed that inhibition of this kinase abrogates the stimulation of TGF-β gene transcription that is induced by SMAD7 downregulation.

LY-2157299 is an effective and functionally active inhibitor of TGF-β signaling in hematopoietic cells

Having demonstrated an important role of SMAD7 reduction and subsequent TGF-β receptor I kinase activation in hematopoiesis, we next wanted to test the efficacy of LY-2157299, a novel clinically relevant small molecule inhibitor of TBRI (31-35). We first

demonstrated that LY-2157299 was able to potently inhibit TBRI mediated SMAD2 activation in hematopoietic cells (Fig 4A,B). Next, we tested whether LY-215 was able to reverse the inhibitory effects of TGF-β in primary hematopoietic stem cells. Primary CD34+cells were grown in methylcellulose in the presence and absence of TGF-β and LY-2157299. As predicted, TGF-β led to quantitative and qualitative inhibition of hematopoietic colonies (Fig 4C,D). LY-215 was also able to abrogate the suppressive effects of TGF-β on erythroid and myeloid colonies in a dose dependant manner (Fig 4C,D) thus demonstrating the its functional ability in hematopoiesis.

LY-2157299 can improve anemia in a model of bone marrow failure

To further examine the efficacy of LY-2157299 *in vivo*, tested it in a transgenic mouse expressing a fusion gene (Alb/TGF) consisting of modified porcine TGF-β cDNA under the control of the regulatory elements of the mouse albumin gene. (26). We have shown that these mice constitutively secrete TGF-β, become anemic and have histologic marrow findings that mimic human MDS, thus serving as an in vivo model of bone marrow failure. (36) These mice were randomized into treatment or placebo groups on the basis of pretreatment hemocrits. Blood counts were measured after 14 days of oral administration of LY-2157299 or vehicle. TBRI inhibitor treatment led to inhibition of constitutive SMAD2 activation in murine bone marrows (Fig 5) and significant increases in hematocrit in these mice demonstrating the specificity of LY-2157299 in inhibiting TGF-β signaling and abrogating the hematopoietic defects induced by it. (Fig 5)

LY-2157299 can stimulate MDS hematopoiesis

Finally, we tested the ability of LY-2157299 *in vitro* in 10 primary MDS bone marrow samples. These patients had low grade MDS and did not have increased blast counts (Table 1). Mononuclear cells from the bone marrow were grown in methylcellulose with cytokines in the presence and absence of varying doses of LY-2157299. MDS bone marrow cells exhibit poor hematopoietic colony formation in concordance with the hematopoietic failure seen in these patients (Table 1). Treatment with the TBRI inhibitor, LY-2157299, resulted in a significant increase in Erythroid (BFU-E) and Myeloid (CFU-Granulocytic Monocytic) colony numbers in all patients (Results depicted as means Fig 6), These results point to a high therapeutic potential of TBRI inhibition by LY-2157299 in low grade MDS.

DISCUSSION

The discovery of effective treatments for MDS has been challenged by the limited insight into molecular pathogenesis of the ineffective hematopoiesis seen in these disorders. Even though TGF-β levels have been shown to be elevated in subset of MDS cases, our previous work has shown that intracellular signaling is activated in large proportion of cases. Thus, based on our findings, SMAD7 downregulation may be the key mechanism driving the suppression of hematopoiesis in MDS via overactivation of the TGF-SMAD2 pathway. This would also explain increased TGF-β signal transduction even in the absence of large amounts of circulating TGF-β that has been observed in various studies in MDS patients (14-17).

SMAD7 is an important regulatory protein that has been implicated in TGF mediated effects in many disease and cancer models (37). In fact genome wide association studies have shown SMAD7 snps to be most significant alterations (38) in colorectal cancer demonstrating its importance in maintaining cellular homoeostasis. Another recent study showed that decreased SMAD7 is also seen in idiopathic pulmonary fibrosis and contributes to TGF-β mediated fibrosis seen in this disease (39). Our studies demonstrate the role of SMAD7 in hematologic malignancies for the first time and implicate its reduction as an

important molecular alteration in preleukemic bone marrow failure disorders such as MDS. The bone marrow at earlier stages of MDS is hypercellular and is characterized by ineffective hematopoiesis affecting both stem and progenitor cells. Since TGF-β is a well known critical regulator of hematopoiesis and affects both stem and progenitor growth and maturation (40), increased TGF-β signaling may potentially explain the dysplastic appearance of progenitors as well as ineffective hematopoiesis of stem cells seen in these patients

There could be many possible reasons for SMAD7 reduction in MDS. Nearly 40% of MDS cases are characterized by deletions affecting chromosomes 5, 7, 18, 20, Y and others. In fact, the deletion of chromosome 18/18q, where the SMAD7 gene is located, was noticed to be the 4th commonest deletion in the largest cohort of MDS patients described recently (41). Additionally, it has been shown that reduction in levels of genes that are deleted in MDS can have functional consequences on disease pathobiology as illustrated recently by the deletion of ribosome gene, RPS14, in subset of MDS with chr5q deletion (42). Thus, SMAD7 reduction could be a result of 18q deletions seen in patients. Recent studies using high resolution array based technologies have shown that small deletions can also be seen commonly in MDS and thus can also affect the SMAD7 locus in patients that do not have large 18q deletions as seen on conventional karyotyping studies (43). In addition to genomic deletions, gene silencing in MDS also occurs via aberrant promoter methylation. (44,45). In fact, DNA methyltransferase inhibitors, 5-azacytidine and decitabine, have been approved for the treatment of this disease. Furthermore, newer data from genome wide methylation studies suggests that epigenetic silencing may be a dominant pathological alteration in the disease pathophysiology of MDS (46). Thus, it is quite possible SMAD7 is also silenced epigenetically in MDS and this may result in increased TGF beta signaling and resulting hematopoietic suppression.

Most importantly, our results demonstrate that the activation of TGF-β pathway by SMAD7 reduction can be reversed in TBRI inhibition, especially with a clinically relevant inhibitor that is effective in vitro and in vivo. Ineffective hematopoiesis is the cause of most of morbidity in patients with low risk MDS. Two thirds of all MDS cases are at the low risk stage, have a lower chance of progressing to leukemia and mainly suffer problems associated with low blood counts. Thus strategies aimed at raising blood counts are needed to treat these patients. Our data provides a rationale for using inhibitors of TGF-β signaling and especially inhibitors of TBRI in this stage of MDS. The type I TGF-β receptor selectively participates in TGF-β signaling while other activin like and TGF-beta receptors can also participate in BMP and activin ligand signaling (47,48). Therefore, LY-2157299 selectively inhibits TGF-β signaling, as it has demonstrated specificity for the TGF-β type I receptor. LY-2157299 is a selective dihydropyrrolopyrazole, small molecule inhibitor that competitively binds to the ATP binding site of the TBRI kinase domain. (31-34) This compound is clinically relevant and is presently being tested in Phase I trials in advanced malignancies. Additionally other small molecule and large molecule TBRI inhibitors are also in development (33,49) for various other indications. Our findings provide a preclinical rationale for bringing LY-2157299 and other similar agents into clinical trials for MDS.

Acknowledgments

Supported by NIH 1R01HL082946. Partnership for cures grant, ACS RSG-09-037 and Leukemia and Lymphoma society Translational research award to AV, NIH RO1 AG029138 to LCP and Immunology and Immunooncology Training Program T32 CA009173 to LZ

References

1. Heaney ML, Golde DW. Myelodysplasia. N Engl J Med 1999;340:1649–60. [PubMed: 10341278]

2. Sanz GF, Sanz MA, Greenberg PL. Prognostic factors and scoring systems in myelodysplastic syndromes. Haematologica 1998;83:358–68. [PubMed: 9592987]
3. Greenberg PL. Biologic nature of the myelodysplastic syndromes. Acta Haematol 1987;78(Suppl 1): 94–9. [PubMed: 2829490]
4. Greenberg P, Cox C, LeBeau MM, et al. International scoring system for evaluating prognosis in myelodysplastic syndromes. Blood 1997;89:2079–88. [PubMed: 9058730]
5. Raza A, Gezer S, Mundle S, et al. Apoptosis in bone marrow biopsy samples involving stromal and hematopoietic cells in 50 patients with myelodysplastic syndromes. Blood 1995;86:268–76. [PubMed: 7795232]
6. Greenberg PL. Apoptosis and its role in the myelodysplastic syndromes: implications for disease natural history and treatment. Leuk Res 1998;22:1123–36. [PubMed: 9922076]
7. Westwood NB, Mufti GJ. Apoptosis in the myelodysplastic syndromes. Curr Hematol Rep 2003;2:186–92. [PubMed: 12901339]
8. Ohshima K, Karube K, Shimazaki K, et al. Imbalance between apoptosis and telomerase activity in myelodysplastic syndromes: possible role in ineffective hemopoiesis. Leuk Lymphoma 2003;44:1339–46. [PubMed: 12952227]
9. Zorat F, Shetty V, Dutt D, et al. The clinical and biological effects of thalidomide in patients with myelodysplastic syndromes. Br J Haematol 2001;115:881–94. [PubMed: 11843822]
10. Allampallam K, Shetty V, Mundle S, et al. Biological significance of proliferation, apoptosis, cytokines, and monocyte/macrophage cells in bone marrow biopsies of 145 patients with myelodysplastic syndrome. Int J Hematol 2002;75:289–97. [PubMed: 11999358]
11. Allampallam K, Shetty V, Hussaini S, et al. Measurement of mRNA expression for a variety of cytokines and its receptors in bone marrows of patients with myelodysplastic syndromes. Anticancer Res 1999;19:5323–8. [PubMed: 10697556]
12. Powers MP, Nishino H, Luo Y, et al. Polymorphisms in TGFbeta and TNFalpha are associated with the myelodysplastic syndrome phenotype. Arch Pathol Lab Med 2007;131:1789–93. [PubMed: 18081437]
13. Akiyama T, Matsunaga T, Terui T, et al. Involvement of transforming growth factor-beta and thrombopoietin in the pathogenesis of myelodysplastic syndrome with myelofibrosis. Leukemia 2005;19:1558–66. [PubMed: 16034467]
14. Taketazu F, Miyagawa K, Ichijo H, et al. Decreased level of transforming growth factor-beta in blood lymphocytes of patients with aplastic anemia. Growth Factors 1992;6:85–90. [PubMed: 1591018]
15. Gyulai Z, Balog A, Borbenyi Z, Mandi Y. Genetic polymorphisms in patients with myelodysplastic syndrome. Acta Microbiol Immunol Hung 2005;52:463–75. [PubMed: 16400883]
16. Aguayo A, Kantarjian H, Manshouri T, et al. Angiogenesis in acute and chronic leukemias and myelodysplastic syndromes. Blood 2000;96:2240–5. [PubMed: 10979972]
17. Yoon SY, Li CY, Lloyd RV, Tefferi A. Bone marrow histochemical studies of fibrogenic cytokines and their receptors in myelodysplastic syndrome with myelofibrosis and related disorders. Int J Hematol 2000;72:337–42. [PubMed: 11185990]
18. Verma A, List AF. Cytokine targets in the treatment of myelodysplastic syndromes. Curr Hematol Rep 2005;4:429–35. [PubMed: 16232378]
19. Verma A, Deb DK, Sassano A, et al. Cutting edge: activation of the p38 mitogen-activated protein kinase signaling pathway mediates cytokine-induced hemopoietic suppression in aplastic anemia. J Immunol 2002;168:5984–8. [PubMed: 12055203]
20. Pellagatti A, Cazzola M, Giagounidis AA, et al. Gene expression profiles of CD34+ cells in myelodysplastic syndromes: involvement of interferon-stimulated genes and correlation to FAB subtype and karyotype. Blood 2006;108:337–45. [PubMed: 16527891]
21. Sternberg A, Killick S, Littlewood T, et al. Evidence for reduced B-cell progenitors in early (low-risk) myelodysplastic syndrome. Blood 2005;106:2982–91. [PubMed: 16076868]
22. Su AI, Wiltshire T, Batalov S, et al. A gene atlas of the mouse and human protein-encoding transcriptomes. Proc Natl Acad Sci U S A 2004;101:6062–7. [PubMed: 15075390]
23. Oswald J, Steudel C, Salchert K, et al. Gene-expression profiling of CD34+ hematopoietic cells expanded in a collagen I matrix. Stem Cells 2006;24:494–500. [PubMed: 16166251]

24. Eckfeldt CE, Mendenhall EM, Flynn CM, et al. Functional analysis of human hematopoietic stem cell gene expression using zebrafish. PLoS Biol 2005;3:e254. [PubMed: 16089502]
25. Boultwood J, Pellagatti A, Cattan H, et al. Gene expression profiling of CD34+ cells in patients with the 5q- syndrome. Br J Haematol 2007;139:578–89. [PubMed: 17916100]
26. Sanderson N, Factor V, Nagy P, et al. Hepatic expression of mature transforming growth factor beta 1 in transgenic mice results in multiple tissue lesions. Proc Natl Acad Sci U S A 1995;92:2572–6. [PubMed: 7708687]
27. Yu L, Hebert MC, Zhang YE. TGF-beta receptor-activated p38 MAP kinase mediates Smad-independent TGF-beta responses. Embo J 2002;21:3749–59. [PubMed: 12110587]
28. Verma A, Deb DK, Sassano A, et al. Activation of the p38 mitogen-activated protein kinase mediates the suppressive effects of type I interferons and transforming growth factor-beta on normal hematopoiesis. J Biol Chem 2002;277:7726–35. [PubMed: 11773065]
29. Bhatia M. Molecular Signatures Orchestrating fate of Human Hematopoietic Stem Cells Originating From Different Stages of Ontogeny. Accession No. GSE3823.
30. Sohal D, Yeatts A, Ye K, et al. Meta-analysis of microarray studies reveals a novel hematopoietic progenitor cell signature and demonstrates feasibility of inter-platform data integration. PLoS ONE 2008;3:e2965. [PubMed: 18698424]
31. Liu Z, Kobayashi K, van Dinther M, et al. VEGF and inhibitors of TGFbeta type-I receptor kinase synergistically promote blood-vessel formation by inducing alpha5-integrin expression. J Cell Sci 2009;122:3294–302. [PubMed: 19706683]
32. Li HY, Wang Y, Heap CR, et al. Dihydropyrrolopyrazole transforming growth factor-beta type I receptor kinase domain inhibitors: a novel benzimidazole series with selectivity versus transforming growth factor-beta type II receptor kinase and mixed lineage kinase-7. J Med Chem 2006;49:2138–42. [PubMed: 16539403]
33. Yingling JM, Blanchard KL, Sawyer JS. Development of TGF-beta signalling inhibitors for cancer therapy. Nat Rev Drug Discov 2004;3:1011–22. [PubMed: 15573100]
34. Bueno L, de Alwis DP, Pitou C, et al. Semi-mechanistic modelling of the tumour growth inhibitory effects of LY2157299, a new type I receptor TGF-beta kinase antagonist, in mice. Eur J Cancer 2008;44:142–50. [PubMed: 18039567]
35. Calvo-Aller E, B J, Glatt S, Cleverly A, Lahn M, Arteaga L, Rothenberg ML, Carducci MA. First human dose escalation study in patients with metastatic malignancies to determine safety and pharmacokinetics of LY2157299, a small molecule inhibitor of the transforming growth factor-beta receptor I kinase. J Clin Oncol 2008;26 May 20 suppl; abstr 14554) 2008.
36. Zhou L, Nguyen AN, Sohal D, et al. Inhibition of the TGF-beta receptor I kinase promotes hematopoiesis in MDS. Blood 2008;112:3434–43. [PubMed: 18474728]
37. Akhurst RJ. TGF beta signaling in health and disease. Nat Genet 2004;36:790–2. [PubMed: 15284845]
38. Tenesa A, Farrington SM, Prendergast JG, et al. Genome-wide association scan identifies a colorectal cancer susceptibility locus on 11q23 and replicates risk loci at 8q24 and 18q21. Nat Genet 2008;40:631–7. [PubMed: 18372901]
39. Liu G, Friggeri A, Yang Y, et al. miR-21 mediates fibrogenic activation of pulmonary fibroblasts and lung fibrosis. J Exp Med 2010;207:1589–97. [PubMed: 20643828]
40. He W, Dorn DC, Erdjument-Bromage H, Tempst P, Moore MA, Massague J. Hematopoiesis controlled by distinct TIF1gamma and Smad4 branches of the TGFbeta pathway. Cell 2006;125:929–41. [PubMed: 16751102]
41. Haase D, Germing U, Schanz J, et al. New insights into the prognostic impact of the karyotype in MDS and correlation with subtypes: evidence from a core dataset of 2124 patients. Blood 2007;110:4385–95. [PubMed: 17726160]
42. Ebert BL, Pretz J, Bosco J, et al. Identification of RPS14 as a 5q- syndrome gene by RNA interference screen. Nature 2008;451:335–9. [PubMed: 18202658]
43. Gondek LP, Tiu R, O'Keefe CL, Sekeres MA, Theil KS, Maciejewski JP. Chromosomal lesions and uniparental disomy detected by SNP arrays in MDS, MDS/MPD, and MDS-derived AML. Blood 2008;111:1534–42. [PubMed: 17954704]

44. Kroeger H, Jelinek J, Estecio MR, et al. Aberrant CpG island methylation in acute myeloid leukemia is accentuated at relapse. Blood 2008;112:1366–73. [PubMed: 18523155]
45. Figueroa ME, Skrabanek L, Li Y, et al. MDS and secondary AML display unique patterns and abundance of aberrant DNA methylation. Blood. 2009
46. Jiang Y, Dunbar A, Gondek LP, et al. Aberrant DNA methylation is a dominant mechanism in MDS progression to AML. Blood 2009;113:1315–25. [PubMed: 18832655]
47. Massague J, Seoane J, Wotton D. Smad transcription factors. Genes & development 2005;19:2783–810. [PubMed: 16322555]
48. Shi Y, Massague J. Mechanisms of TGF-beta signaling from cell membrane to the nucleus. Cell 2003;113:685–700. [PubMed: 12809600]
49. Akhurst RJ. Large- and small-molecule inhibitors of transforming growth factor-beta signaling. Curr Opin Investig Drugs 2006;7:513–21.

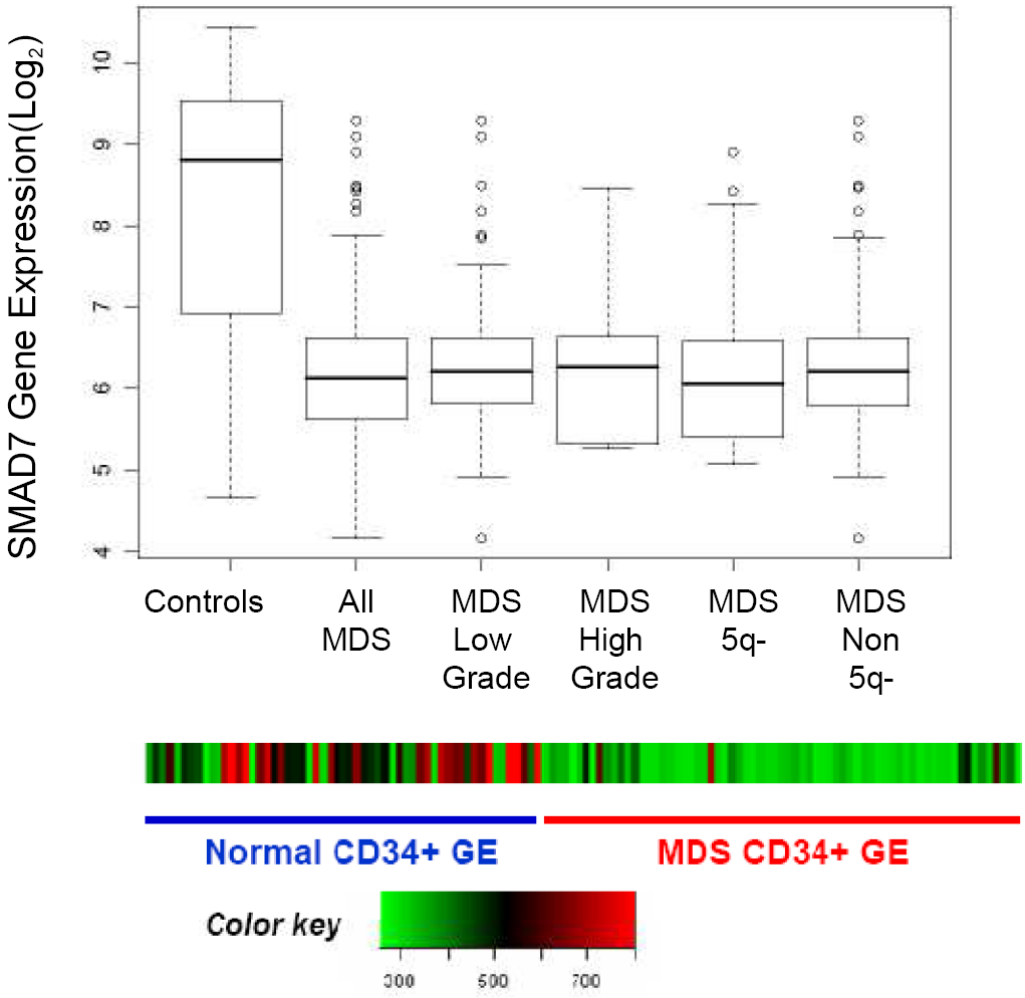

FIGURE 1. SMAD7 is significantly decreased in MDS

Differences in SMAD7 expression were also evaluated in normalized meta-analysis of MDS CD34+ (89 cases) and normal CD34+ (61 cases) cell derived gene expression microarray studies. Box plots show SMAD7 gene expression was significantly downregulated in MDS bone marrow CD34+ cells after multiple testing with Benjamin Hochberg correction with p value < 0.01. The reduction is seen in both low (n=83) and high grade (n=6) cases and also in cases with (n=29) and without (n=60) 5q deletion. Heat map shows individual values of all samples.

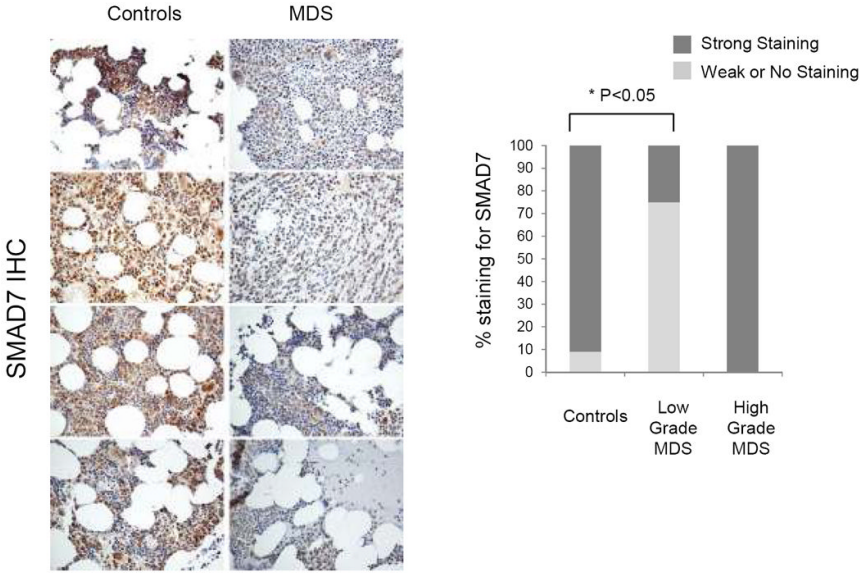

Figure 2. SMAD7 protein is decreased in MDS marrow progenitors

Tissue microarray was prepared from bone marrow (BM) biopsies from patients with MDS and controls with non-MDS Bone marrow biopsy samples were stained with SMAD7 antibody and show decreased expression in 4 representative cases of MDS when compared to controls. Low grade MDS samples revealed significantly less SMAD7 staining when compared to controls (Propotions test,$p<0.05$)

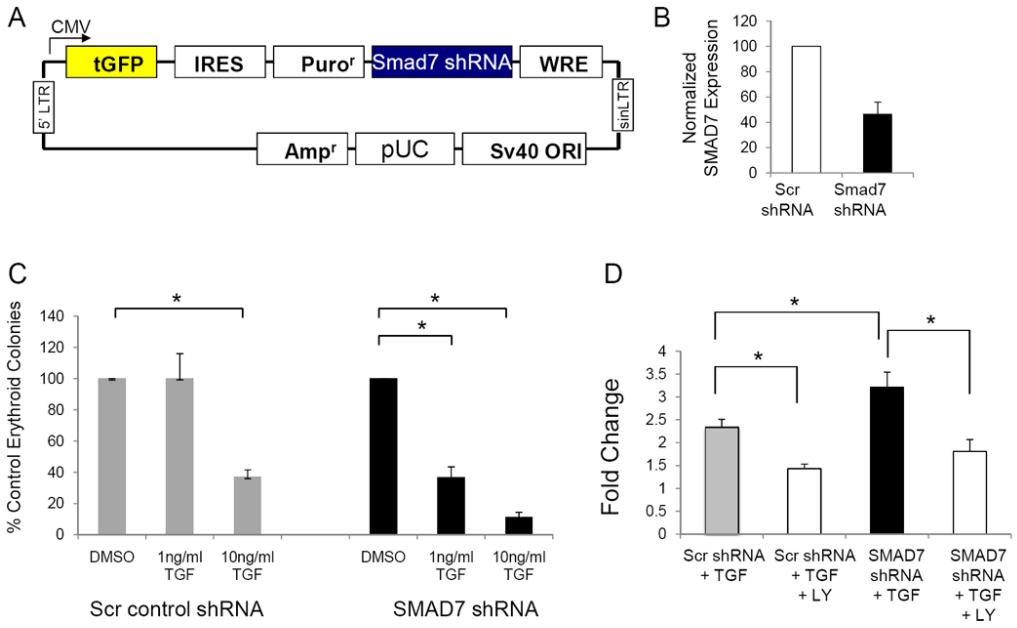

Figure 3. Reduction in SMAD7 can lead to increased sensitivity to suppressive effects of TGF-β on hematopoiesis

GFP expressing Lentiviral based shRNA against SMAD7 (**A**) was used to knockdown SMAD7 in hematopoeitic cells. qPCR shows decrease in SMAD7 mRNA expression after lentiviral shRNA-TBRI infection in bone marrow stromal (HS-5) cells when compared to scrambled control (**B**). Primary CD34+ progenitors were electroporated with GFP coexpressing anti-SMAD7 shRNA construct and sorted after 48 hours. GFP positive cells were grown in methylcellulose with cytokines and erythroid colonies were counted after 14 days. SMAD7 shRNA transfected progenitors were significantly inhibited at lower concentrations of TGF-b when compared to cells transfected with scrambled control shRNA. Expressed as Means +/- s.e.m of 3 independent experiments. ($p<0.05$, Two Tailed T test) (C). Bone marrow stroma derived cells (HS-5) with stable expression of anti-SMAD7 and control shRNAs were generated. These cells were transfected with plasmids expressing smad binding 3TP-Luciferase and beta-galactisidose (transfection control) and stimulated with TGF-β1 in the presence and absence of LY-215 (dose .5uM). Tgf-β1 induced control normalized Luciferase activity was significantly increased after SMAD7 knockdown. This increase was potently inhibited by LY-2157299.(**D**).

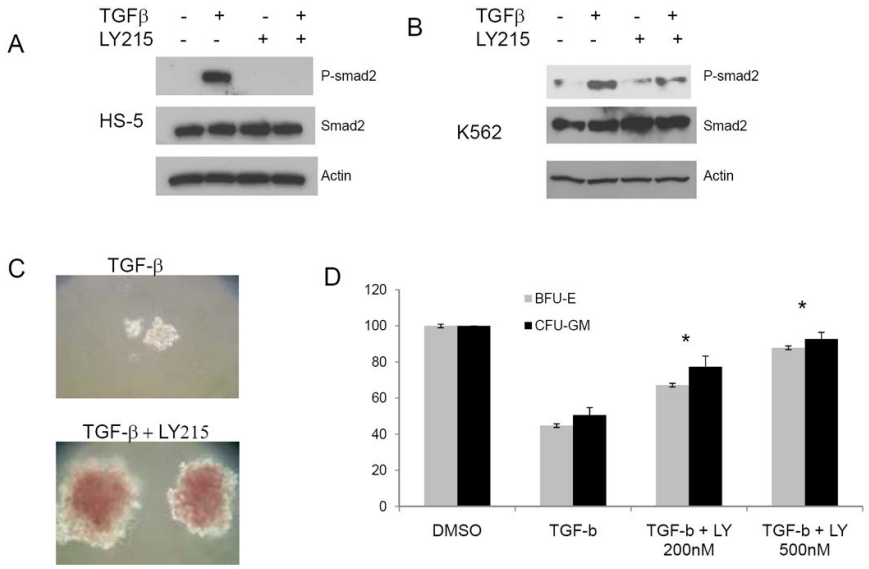

Figure 4. LY-2157299 is an effective and functionally active inhibitor of TGF-β signaling in hematopoietic cells

Leukemic cells (K562) and marrow stromal cells (HS-5) were treated with TGF-β1 (20ng/ml) in the presence and absence of LY-2157299 (.5uM) and assessed for SMAD2 phosphorylation by immunoblotting. LY-215 pretreament (1 hr) led to attenuation of activation/phosphorylation of SMAD2 (**A,B**). Healthy CD34+ progenitors were plated in methylcellulose and cytokines in the presence and absence of TGF-b and TBRI inhibitor LY-2157299 (200nM and 500nM). Colonies were scored at Day 14 and results were expressed as means + S.E.M of 3 independent experiments. TGF-b exposure led to smaller (C) and lesser numbers (D) of colonies. These effects were reversed in the presence of LY215 treatment.

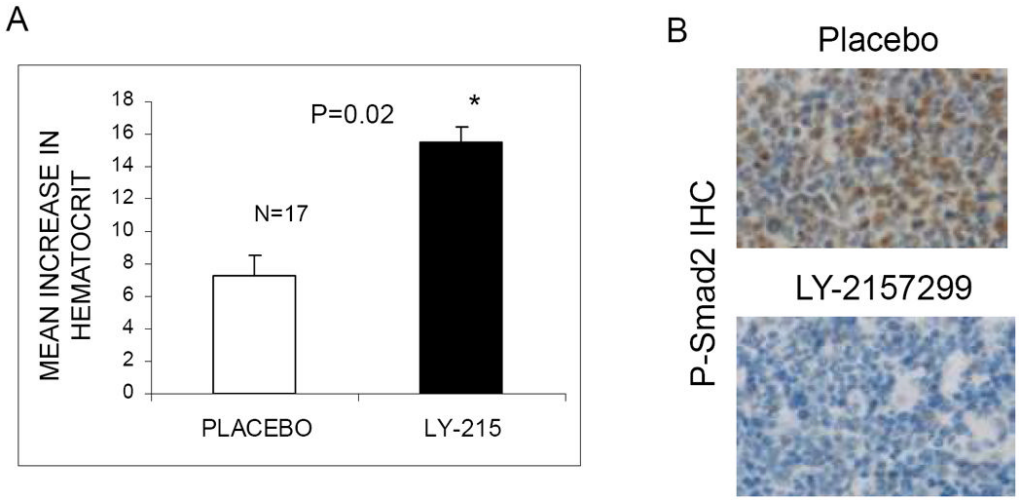

Figure 5. LY-2157299 can improve anemia in a murine model of TGF-β1 driven bone marrow failure

Mice transgenic for alb/TGF-β were treated with either LY-2157299 (100 mg/kg/d) or vehicle (Placebo) daily by gastric lavage for 14 days. Blood counts were done on the 14th day and revealed a significant rise in hematocrit after LY-2157299 treatment. (**A**) The mice were sacrificed and bone marrow biopsies were immunostained with antibody against phosphor-SMAD2. Representative sample shows inhibition of SMAD2 activation after LY-2157299 treatment. (B)

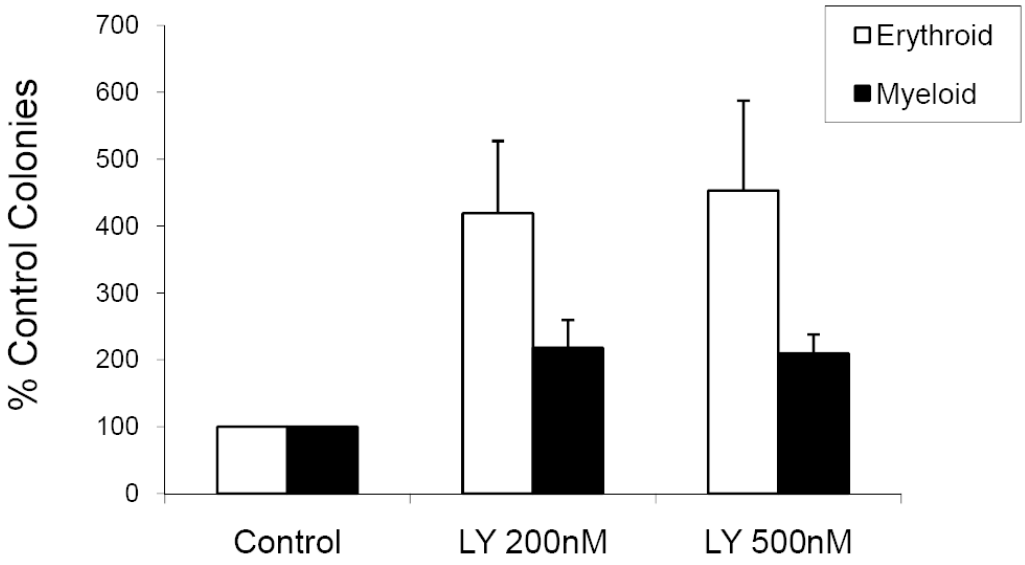

FIGURE 6. TBRI inhibition stimulates hematopoiesis in MDS

MDS Bone marrow derived MNCs from 10 patients were plated in methylcellulose and cytokines in the presence and absence of TBRI inhibitor LY-2157299 (200nM and 500nM). Colonies were scored at Day 14 and results were expressed as means + S.E.M of 10 independent experiments.

Table 1

MDS patient characteristics and hematopoietic colony data after LY-215 treatment

N	Age/Sex	WBC (10^3/cc)	Hgb (gm/dls)	Plt (10^3/cc)	Subtype	Cytogenetics	Colonies Pretreatment		Colonies Post LY Treatment	
							BFU-E	CFU-GM	BFU-E	CFU-GM
1	68/M	4.5	9	118	RCMD	+8	17	11	49	32
2	79/f	4.4	8	71	RCMD	Nml	3	9	8	15
3	54/F	2.7	8.4	20	RCMD	Nml	7	3	16	6
4	59/M	7.8	7.7	13	RCMD	20q-	2	5	30	5
5	69/F	31	8.8	411	RA	Nml	8	5	38	9
6	70/F	2.8	8	533	RA	5q-	4	3	14	11
7	85/M	2.6	9.6	4	RCMD	20q-	6	9	53	8
8	78/M	4.6	8.5	325	RA	Nml	15	8	24	15
9	84/M	3.5	11	110	RA	20q-, +8	12	7	23	22
10	49/M	3.4	11.5	75	RCMD	Nml	10	8	19	16

Regular Article

MYELOID NEOPLASIA

IL8-CXCR2 pathway inhibition as a therapeutic strategy against MDS and AML stem cells

Carolina Schinke,[1] Orsolya Giricz,[1] Weijuan Li,[1] Aditi Shastri,[1] Shanisha Gordon,[1] Laura Barreryo,[1] Tushar Bhagat,[1] Sanchari Bhattacharyya,[1] Nandini Ramachandra,[1] Matthias Bartenstein,[1] Andrea Pellagatti,[2] Jacqueline Boultwood,[2] Amittha Wickrema,[3] Yiting Yu,[1] Britta Will,[1] Sheng Wei,[4] Ulrich Steidl,[1] and Amit Verma[1]

[1]Division of Hemato-Oncology, Albert Einstein College of Medicine, Montefiore Medical Center, Bronx, NY; [2]Leukemia and Lymphoma Research Molecular Haematology Unit, Nuffield Division of Clinical Laboratory Sciences, John Radcliffe Hospital, and National Institute for Health Research Biomedical Research Centre, Oxford, United Kingdom; [3]Department of Medicine, Hematology-Oncology, Cancer Research Center, University of Chicago, Chicago, IL; and [4]Department of Immunology, Clinical Immunology, Moffitt Cancer Center, Tampa, FL

Key Points

- IL8-CXCR2 is overexpressed in purified stem cells from AML and MDS, and CXCR2 expression is associated with worse prognosis.
- Inhibition of CXCR2 by genetic and pharmacologic means leads to decreased viability in AML/MDS stem cells and in vitro and in vivo models.

Acute myeloid leukemia (AML) and myelodysplastic syndromes (MDS) are associated with disease-initiating stem cells that are not eliminated by conventional therapies. Novel therapeutic targets against preleukemic stem cells need to be identified for potentially curative strategies. We conducted parallel transcriptional analysis of highly fractionated stem and progenitor populations in MDS, AML, and control samples and found interleukin 8 (IL8) to be consistently overexpressed in patient samples. The receptor for IL8, CXCR2, was also significantly increased in MDS CD34$^+$ cells from a large clinical cohort and was predictive of increased transfusion dependence. High CXCR2 expression was also an adverse prognostic factor in The Cancer Genome Atlas AML cohort, further pointing to the critical role of the IL8-CXCR2 axis in AML/MDS. Functionally, CXCR2 inhibition by knockdown and pharmacologic approaches led to a significant reduction in proliferation in several leukemic cell lines and primary MDS/AML samples via induction of G0/G1 cell cycle arrest. Importantly, inhibition of CXCR2 selectively inhibited immature hematopoietic stem cells from MDS/AML samples without an effect on healthy controls. CXCR2 knockdown also impaired leukemic growth in vivo. Together, these studies demonstrate that the IL8 receptor CXCR2 is an adverse prognostic factor in MDS/AML and is a potential therapeutic target against immature leukemic stem cell–enriched cell fractions in MDS and AML. (*Blood*. 2015;125(20):3144-3152)

Introduction

Acute myeloid leukemia (AML) and myelodysplastic syndromes (MDSs) are heterogeneous malignancies that are thought to arise from a small pool of cancer-initiating cells residing within hematopoietic stem (HSC) and progenitor (HSPC) compartments.[1-9] Despite the use of poly-chemotherapy and the development of newer agents, clinical outcome remains poor. The disease course is frequently characterized by relapse or failure to achieve durable remission, indicating that current treatment regimens do not target the cancer-initiating cells. Recently, there have been increasing efforts to identify molecular aberrations that could serve as pharmacologic targets within AML and MDS stem cell compartments.[10-16] Resulting therapies have shown promising effects in preclinical studies,[17,18] but further work will be necessary to identify therapeutic targets against preleukemic stem cells that would lead to long-term remission and prevention of relapse in AML and MDS.[19,20] Previously, we identified quantitative and qualitative alterations in AML and MDS HSCs and progenitors and showed that genetically aberrant HSCs survive during morphologic remissions and expand before clinical relapse.[2] In an effort to identify aberrant targets in MDS/AML HSPCs, we conducted transcriptomic profiling of stem cells (long-term HSCs [LT-HSCs], short-term HSCs [ST-HSCs]) and progenitors (granulocyte-monocyte progenitors [GMPs]) and compared them to healthy aged-matched control counterparts. Interleukin 8 (IL8) was one of the most significantly upregulated genes in both HSCs and GMPs, suggesting that it might play a crucial role in the carcinogenesis of AML and MDS. IL8 is a known potent proinflammatory cytokine that exerts its effects through binding to its G protein-coupled receptors CXCR1 and CXCR2. Extensive work in solid tumors has shown that IL8 is critical in survival, invasion, and proliferation of cancer cells[21-24] and might be an important regulator of cancer stem cell activity.[25-27] Activation of multiple pathways by IL8, including phosphatidylinositol 3-kinase/protein kinase B (AKT), phospholipase C/protein kinase C, and mitogen-activated protein kinase (MAPK) signaling, leads to increased expression of various

Submitted January 16, 2015; accepted March 15, 2015. Prepublished online as *Blood* First Edition paper, March 25, 2015; DOI 10.1182/blood-2015-01-621631.

The online version of this article contains a data supplement.

There is an Inside *Blood* Commentary on this article in this issue.

The publication costs of this article were defrayed in part by page charge payment. Therefore, and solely to indicate this fact, this article is hereby marked "advertisement" in accordance with 18 USC section 1734.

transcription factors such as hypoxia inducible factor 1, nuclear factor-κB, activator protein-1, signal transducer and activator of transcription 3, and β-catenin, which promote tumor growth and survival.[21] Blocking the IL8-CXCR1/CXCR2 axis has shown to be of therapeutic potential in a variety of solid tumors[27-30]; however, there is little known of its role in hematologic malignancies. Our study reveals that IL8 is significantly overexpressed in AML and MDS LT-HSCs, ST-HSCs, and GMPs compared with healthy controls. The IL8 receptor CXCR2 was highly expressed in a variety of leukemic cell lines, as well as in AML and MDS patient cohorts, and higher expression levels correlated with worse clinical outcomes. Functional studies showed that inhibiting and/or down-regulating CXCR2 leads to decreased viability and clonogenic capacity of primary AML/MDS patients' cells, but had no effect on healthy controls. Interestingly, CXCR2 inhibition decreased viability in the $CD34^+/CD38^-$ HSC fraction from AML/MDS patients but had no impact on healthy control HSCs. Our studies suggest that the IL8-CXCR2 pathway is frequently dysregulated in AML and MDS stem cells and can serve as a novel therapeutic target in these diseases.

Methods

Patient samples, cell lines, and reagents

Specimens were obtained from patients diagnosed with MDS and AML after institutional review board approval by the Albert Einstein College of Medicine (supplemental Table 1, available on the *Blood* Web site), in accordance with the Declaration of Helsinki. The AML cell lines KG1, HL-60, Molm 13, U937, and THP-1 were grown in RPMI supplemented with 10% fetal bovine serum and 1% penicillin/streptomycin. CXCR2 inhibitor SB-332235 was obtained from GlaxoSmithKline, dissolved in dimethylsulfoxide, and stored at −20°C at a concentration of 100 mM.

Cell viability assay

Cell lines and primary samples were incubated at varying concentrations of the CXCR2 inhibitor SB-332235. Viability was assessed by addition of Cell Titer Blue (Promega) and measured via Fluostar Omega Microplate reader (BMG Labtech).

Cell lysis and immunoblotting

Cells were lysed in phosphorylation lysis buffer as previously described.[31] Immunoblotting was performed as previously described.[31]

Multiparameter high-speed fluorescence-activated cell sorter of stem and progenitor cells

Processing and sorting of hematopoietic stem and progenitor cells was performed as previously described.[10] Briefly, mononuclear cells were isolated from bone marrow aspirates and peripheral blood samples by density gradient centrifugation and then subjected to immunomagnetic enrichment of $CD34^+$ cells (Miltenyi-Biotec). $CD34^+$ cells were stained with PE-Cy5 (Tricolor)-conjugated monoclonal antibodies against lineage antigens (CD2 [RPA-2.10], CD3 [UCHT1], CD4 [S3.5], CD7 [6B7], CD8 [3B5], CD10 [CB-CALLA], CD11b [VIM12], CD14 [TueK4], CD19 [HIB19], CD20 [2H7], CD56 [MEM-188], Glycophorin A [CLB-ery-1(AME-1)]), as well as fluorochrome-conjugated antibodies against CD34 [581/CD34 (class III epitope)], CD38 (HIT2), CD90 (5E10), CD45RA (MEM-56), and CD123 (6H6). Cells were sorted with a 5-laser FACSAria II Special Order System flow cytometer (Becton Dickinson). Based on established surface marker characterization, we distinguished and sorted LT-HSCs (Lin^-, $CD34^+$, $CD38^-$, $CD90^+$), ST-HSCs (Lin^-, $CD34^+$, $CD38^-$, $CD90^-$), and GMPs (Lin^-, $CD34^+$, $CD38^+$, $CD123^+$, $CD45RA^+$).[32] Flow cytometry data were analyzed with BD FACSDiva (Becton Dickinson) and FlowJo (TreeStar) software. After sorting, RNA was extracted with the RNeasy Micro kit (Qiagen).

RNA amplification and real-time polymerase chain reaction

RNA was extracted with the RNeasy Micro kit (Qiagen), and quantity and quality were assessed with a Nanodrop 3000 instrument (Thermo Scientific). RNA extracted from sorted primary LT-HSCs, ST-HSCs, and GMP cells was amplified with the Ovation One Direct System (Nugen) and converted to single-strand cDNA. RNA extracted from cell lines and primary $CD34^+$ cells was reverse-transcribed with Superscript III reverse transcriptase (Invitrogen). IL8 expression was measured by quantitative reverse transcriptase-polymerase chain reaction (qRT-PCR) with SYBR green on a CFX 96 Real Time System (BioRad).

Lentiviral short hairpin RNA vectors and transduction

For knockdown studies, 2 short hairpin RNAs (shRNAs) against CXCR2 were used (GIPZ system, catalog nos. RHS4430-99883569 and RHS4430-99891604; Open Biosystems). For production of lentiviral particles, lentiviral shRNA expression constructs were transfected together with packaging vectors into 293T producer cells using Lipofectamine LTX transfection reagent (Invitrogen), and supernatants were harvested after 48 and 72 hours and concentrated by ultracentrifugation. AML cell lines were transduced with the shRNA-containing lentiviruses (multiplicity of infection = 6-10). After culture in fresh medium, green fluorescent protein (GFP)-positive and 4,6 diamidino-2-phenylindole (DAPI)-negative cells were sorted 48 to 72 hours after infection using a FACSAria II sorter (BD Biosciences) and used for experiments. CXCR2 knockdown efficiency was measured by real-time PCR and flow cytometry.

Clonogenic assays

For clonogenic assays, primary patient samples and healthy controls were plated in methylcellulose (Stem Cell Technologies H4435) in 35-mm dishes and incubated with the CXCR2 inhibitor at 10 μM. Colonies were counted after 14 to 17 days in culture. Clonogenic assays with shRNA-mediated CXCR2 knockdown were performed 48 to 72 hours after lentiviral transduction of the respective cell line (U937, THP-1, and MOLM13). DAPI-negative and GFP-positive cells were sorted and plated in methylcellulose (StemCell Technologies H4435) in 35-mm dishes. Colonies were counted after 7 to 10 days in culture.

Cell cycle analysis

Cell cycle analysis was performed as previously described.[33] In brief, 1×10^6 AML cells were incubated at varying doses of the CXCR2 inhibitor. After 24 hours, the cells were rinsed with ice-cold phosphate-buffered saline (PBS) and incubated for 45 minutes at 37°C in the dark with 0.5 mL Hoechst buffer (20 μg/mL Hoechst 33342 in Hanks balanced salt solution containing 10% fetal bovine serum, 20 mM *N*-2-hydroxyethylpiperazine-*N*′-2-ethanesulfonic acid, pH 7.2, 1 g/L glucose, and 50 μg/mL verapamil; Sigma-Aldrich). Pyronin Y (Sigma-Aldrich) was added at 1 μg/mL, and cells were incubated for 15 minutes at 37°C in the dark, washed with PBS, and analyzed by flow cytometry using a FACSAria II Special Order System (BD Biosciences).

Evaluation of viability in primary $CD34^+CD38^-$ HSCs

Primary AML, MDS, and healthy control samples were incubated with 1 and 10 μM of the CXCR2 inhibitor SB-332235 in Iscove's modified Dulbecco's medium with 10% fetal bovine serum at 37°C. After 24 hours, cells were rinsed with PBS and stained with antibodies against CD34 (8G12) and CD38 (HIT2). After washing with PBS, cells were mixed with prediluted fluorescein isothiocyanate-conjugated annexin V (Invitrogen), incubated at room temperature for 15 minutes, and resuspended in 0.5 mL of annexin binding buffer (Invitrogen). Just before flow cytometric analysis, DAPI (Acros Organics) was added to the cells at a final concentration of 1 μg/mL. Viability, apoptosis, and necrosis of $CD34^+/CD38^-$ and $CD34^+/CD38^+$ cells were analyzed by flow cytometry using a FACSAria II Special Order System (BD Biosciences) as performed previously.[34-36]

Patient database and survival data

Gene expression data from 183 MDS $CD34^+$ samples and 17 controls were obtained from Gene Expression Omnibus (GEO) (GSE19429).[37] Data on 200

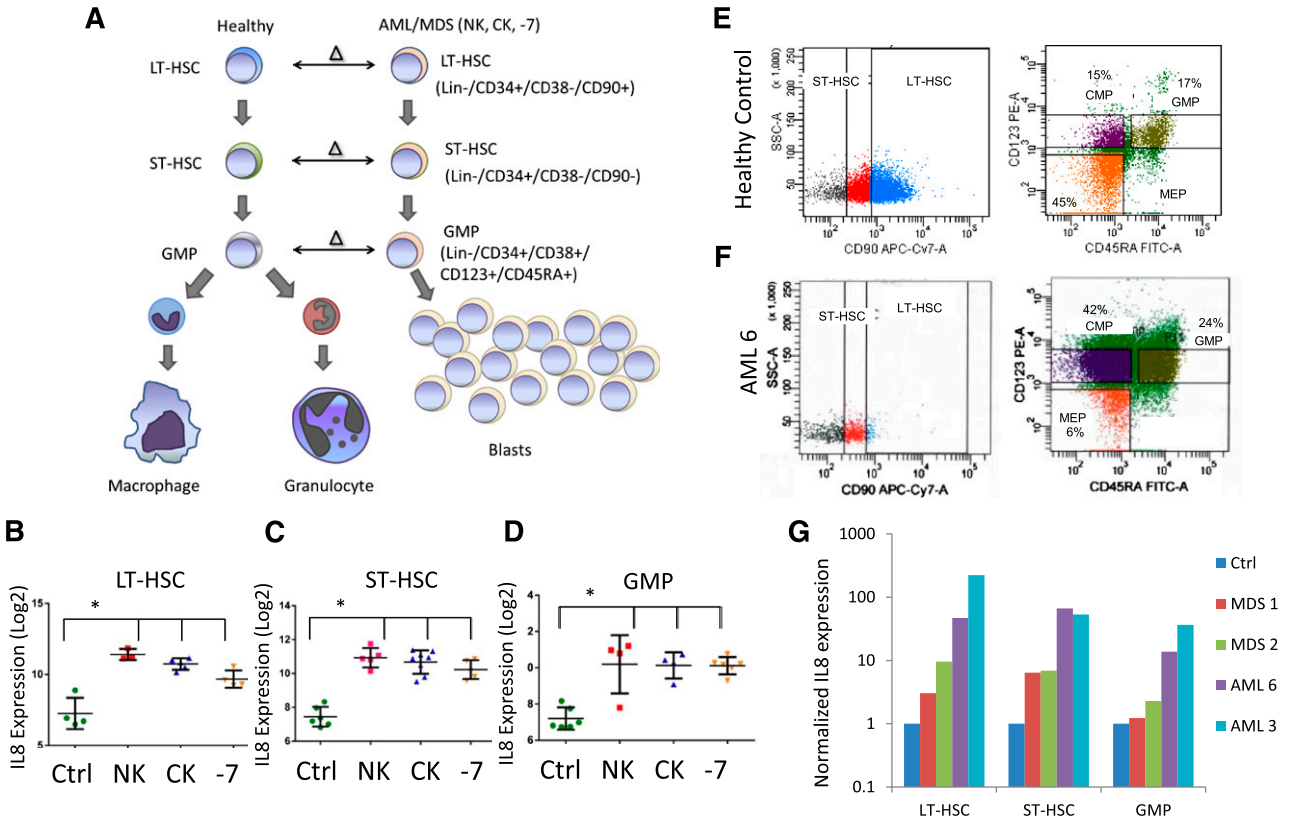

Figure 1. IL8 is overexpressed in stem and progenitor cells in MDS and AML. (A) Gene expression data from sorted AML/MDS bone marrow samples were compared with healthy controls and (B-D) revealed significantly increased IL8 expression in LT-HSCs (Lin-ve, $CD34^+$, $CD38^-$, $CD90^+$, N = 12 AML/MDS, HC = 4), ST-HSCs (Lin-ve, $CD34^+$, $CD38^-$, $CD90^-$), and GMP (Lin-ve, $CD34^+$, $CD38^+$, $CD123^+$, $CD45RA^+$) ($P < .001$, FDR < 5%). Cytogenetic abnormalities are depicted as follows: NK, normal karyotype; CK, complex karyotype; −7 = deletion of chr7. Representative flow plots show sorting strategy for (E) healthy control and (F) AML sample. (G) qRT-PCR on sorted cells reveals increased expression of IL8 in all AML/MDS HSCs (LT/ST) and GMP.

AML samples were obtained from The Cancer Genome Atlas (TCGA).[38] Gene expression data on sorted LT-HSCs, ST-HSCs, and GMPs from AML/MDS patients and healthy controls are deposited in the GEO database (accession nos. GSE35008 and GSE35010). Gene Set Enrichment Analysis was performed by comparing the CXCR2 high signature to 2 published preleukemic HSC signatures (GSE35008[10] and GSE30377[4]).

Leukemia xenografts

NOD/SCID IL2Rγ knockout mice were injected with 10^5 U937 cells that had been transduced with nonsilencing shRNA and CXCR2 knockdown shRNAs. Overall survival was measured and analyzed by Kaplan-Meier plotting and the log-rank test.

Results

IL8 is overexpressed in MDS and AML HSCs and progenitors

Leukemia- and MDS-initiating cells including preleukemic stem cells reside in the lineage-negative phenotypic stem and progenitor compartments and need to be targeted for curative strategies. To determine aberrantly expressed genes in MDS and AML stem and progenitor cells, we previously conducted a parallel transcriptional study comparing LT-HSCs, ST-HSCs, and GMPs from AML samples with deletion of chromosome 7 (−7) to healthy control counterparts[10] (Figure 1A). A small set of 7 genes was found to be consistently overexpressed in all compartments (LT-HSCs, ST-HSCs, and GMPs) and included IL8. We expanded our initial study to include sorted samples from normal karyotype and complex karyotype AML/MDS samples (Figure 1A). Our sorting strategy uses rigorous lineage depletion to avoid analysis of the leukemic bulk (blast) population and to focus on the earliest known stem cell and committed myeloid progenitor populations in humans. Sorting of 12 AML/MDS samples and 4 controls followed by gene expression analysis revealed that the IL8 gene was significantly overexpressed by several log-fold in all samples in both HSCs and GMP populations, across normal karyotype, complex karyotype, and −7 cases (Figure 1B). These results were validated in an independent cohort of samples by qRT-PCR. Two AML, 2 MDS, and 2 control samples were sorted (Figure 1E-F shows representative samples), analyzed, and confirmed significant upregulation of IL8 in the MDS/AML samples (Figure 1G).

CXCR2 is expressed in primary AML and MDS samples and is associated with worse clinical outcomes

IL8 and other CXCL ligands bind to the CXCR1 and CXCR2 receptors to trigger many different biological processes. We evaluated the expression of these ligands and receptors in a large cohort of AML samples analyzed by RNA-seq (TCGA, n = 200).[38] We observed that among the CXCR1 and 2 ligands, IL8 was most significantly expressed in AML (mean reads per kilobase per million = 36 [IL8] vs 12 [CXCL2], 3 [CXCL3], 2 [CXCL1], and 0.2 [CXCL5]; $P < .001$), and CXCR2 expression was significantly higher than CXCR1 expression (mean reads per kilobase per million = 4 [CXCR2] vs 2 [CXCR1]; $P < .001$) in leukemic cells (Figure 2A-B). We evaluated CXCR2 overexpression for prognostic impact in this cohort and observed that samples with higher expression of the receptor had

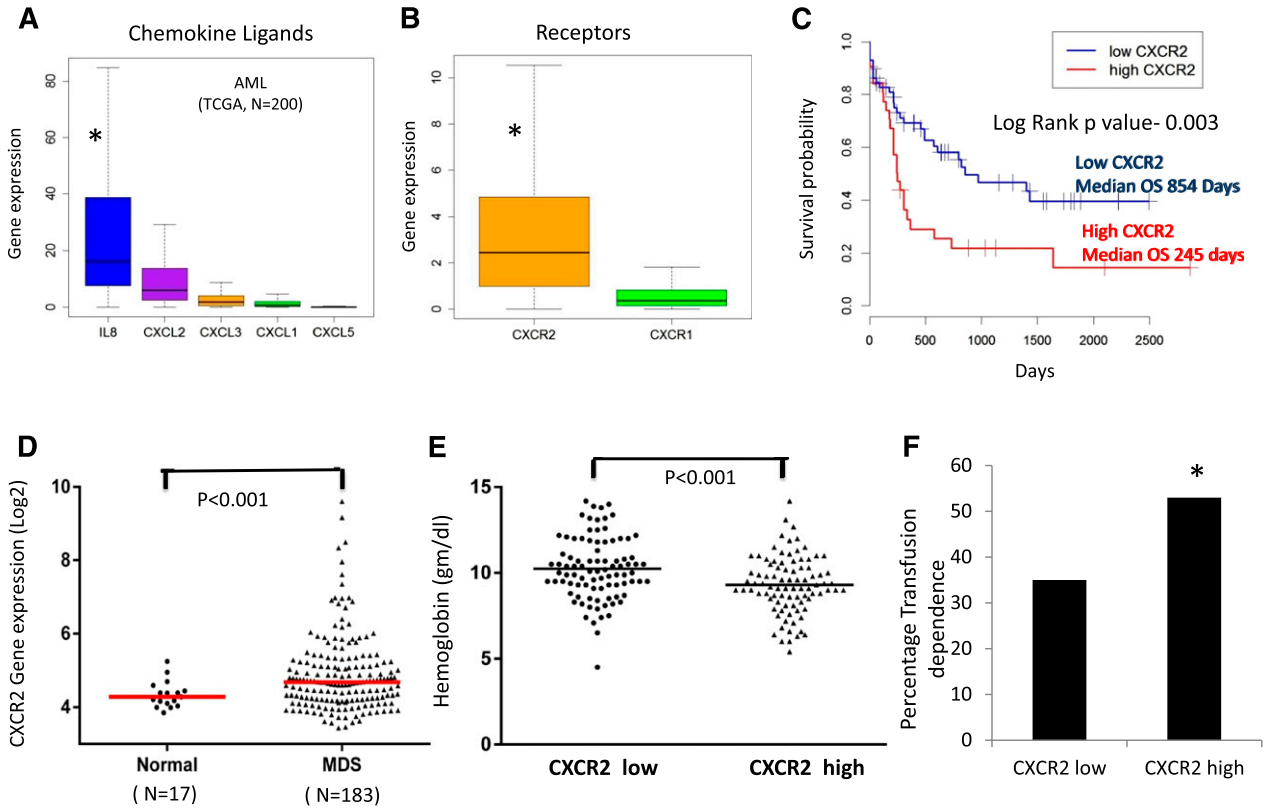

Figure 2. CXCR2 is expressed in primary AML and MDS samples and is associated with worse clinical outcomes. Expression of (A) chemokine ligands and (B) receptors was evaluated in the TCGA RNA-seq dataset from 200 AML samples (data shown as boxplots). (C) Median overall survival of AML patients with high CXCR2 was significantly worse than in patients with lower expression (log rank, $P = .003$). (D) Gene expression data of CD34$^+$ cells from 183 MDS patients and 17 healthy controls shows significantly higher expression of CXCR2 in MDS CD34$^+$ cells (t test, $P < .001$, FDR < 5%). MDS patients with (E) high CXCR2 expression (>median) have lower hemoglobin levels (t test, $P < .001$) and (F) higher RBC transfusion dependence (test of proportions, $P < .05$).

a significantly worse prognosis compared with CXCR2 lower-expressing patients (median overall survival of 245 days in high CXCR2 cases vs 854 in low CXCR2 cases; log rank, $P = .003$; Figure 2C). Next, we evaluated the expression of CXCR2 in MDS HSPCs in another large cohort of 183 samples.[37] CXCR2 expression was found to be higher in MDS samples compared with healthy controls ($P = .001$, false discovery rate [FDR] < 10%; Figure 2D). Cases with high CXCR2 were found to present with worse disease phenotype manifesting with lower hemoglobin levels and a higher percentage of transfusion dependence (53% for CXCR high vs 35% for CXCR2 low; $P < .001$; Figure 2E-F). Correlation with mutations obtained from targeted sequencing of a subset of MDS cases[39] revealed significant enrichment of TET2 mutations in CXCR2 low expressers, with no other significant correlations with other mutations (supplemental Table 2). Taken together, these data demonstrate that high CXCR2 expression in HSPCs is an adverse prognostic factor in both AML and MDS.

Gene expression signature of MDS HSPCs with high CXCR2 is similar to known preleukemic stem cell profiles and includes many important functional pathways

To determine the genetic pathways that were differentially expressed in MDS HSPCs with high expression of CXCR2, we identified differentially expressed transcripts between the CXCR2 high and low patient subsets (using median CXCR2 expression as cutoff in a cohort of 183 MDS CD34$^+$ samples; FDR < 0.1; Figure 3A). Ingenuity pathway analysis revealed significant dysregulation of pathways involved in chemokine signaling, cytokine-cytokine receptor interaction, innate immunity signaling, hematopoietic cell lineage regulation, and others in CXCR2 high patients and also included many genes that play important roles in molecular leukemogenesis (Figure 3B; supplemental Table 3). Next, we tested whether the high CXCR2 expression signature had any overlap with known preleukemic stem cell gene expression profiles. Gene set enrichment analysis with 2 recently published preleukemic stem cell signatures (GSE35008[10] and GSE30377[4]), including 1 from our own group, revealed highly significant enrichment, demonstrating that HSPCs from CXCR2 high MDS patients have a similar transcriptomic profile than known preleukemic and leukemia-initiating cell populations (Figure 3C).

Inhibition of CXCR2 leads to decreased proliferation and cell cycle arrest in leukemic cells

To determine the functional role of the IL8-CXCR2 pathway in leukemia biology, we first evaluated the expression of the receptor in AML cell lines. We determined that AML cell lines significantly overexpressed CXCR2, ranging from 3-fold (KG1) to 300-fold overexpression (THP1) compared with healthy CD34$^+$ cells (Figure 4A).To determine the functional role of CXCR2 in these cells, we used a specific inhibitor of CXCR2, SB332235, that is a clinically available compound that has 100-fold selectivity for CXCR2 over CXCR1.[40] CXCR2 inhibition led to a dose-dependent decrease in proliferation in all cell lines (Figure 4B). CXCR2 inhibition also led to a significant inhibition of proliferation in primary samples from AML and high-risk MDS cases (Figure 4C). Next, we designed shRNAs against CXCR2 (Figure 4D; supplemental Figure 1) and found that decreased expression of this receptor also led to significantly reduced

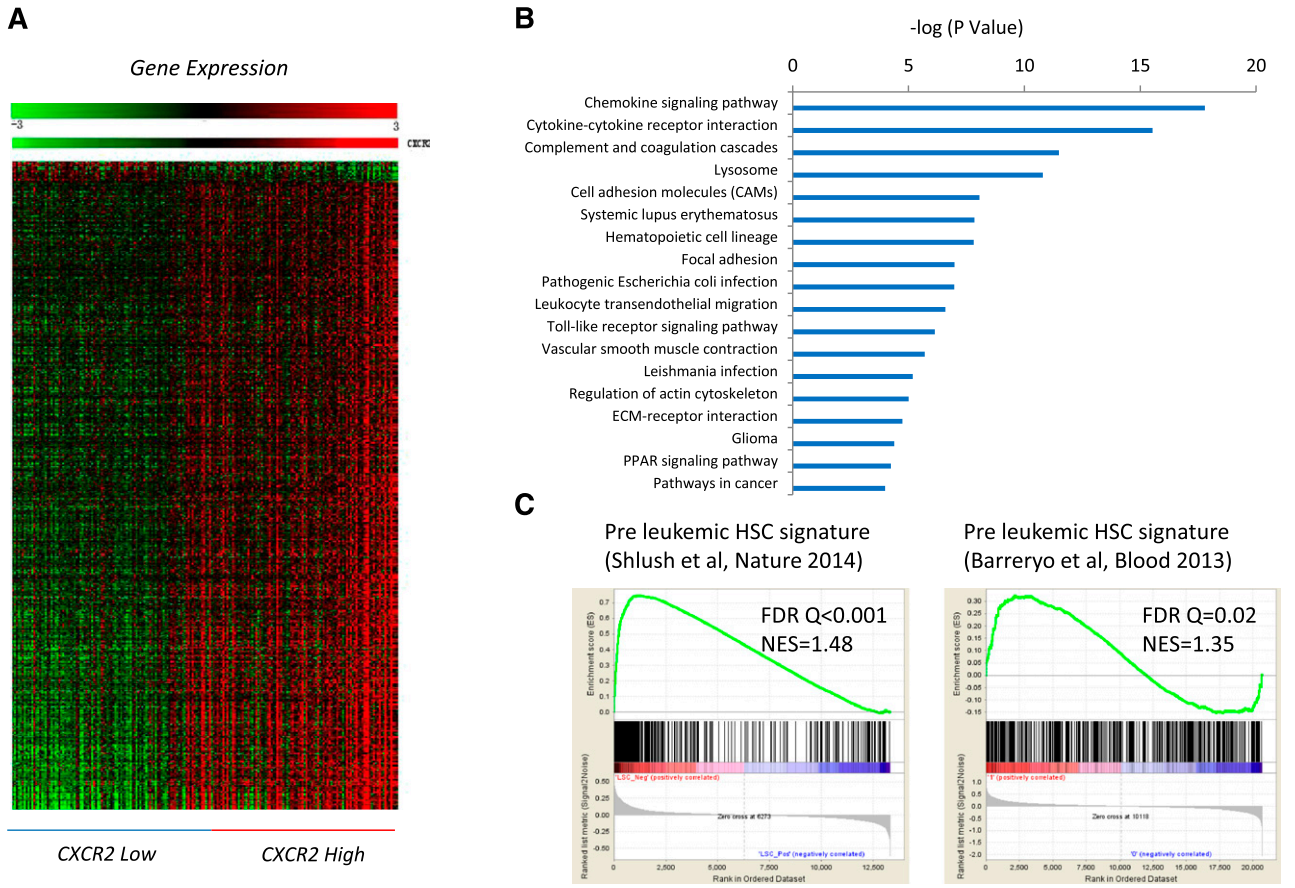

Figure 3. Important functional pathways are dysregulated in MDS cases with high expression of cxcr2. (A) Gene expression profiles from samples with low and high CXCR2 were compared, and differentially expressed transcripts were identified (FDR < 0.1). (B) Significantly dysregulated pathways are shown. The gene signature of high CXCR2 MDS cases is similar to previously published preleukemic stem cell signatures. (C) Gene Set Enrichment Analysis plots show significant enrichment of 2 recent preleukemic gene expression signatures.

leukemic colony formation capacity of AML cell lines ($P < .001$; Figure 4E). The reduction in colony numbers was also accompanied by decreased size of individual leukemic colonies (Figure 4F).

To determine the mechanism of growth arrest, we performed cell cycle analysis and observed a significant arrest of AML cells in the G0 stage ($P < .05$) after CXCR2 inhibition (Figure 5A-B). This was seen consistently in both cell lines examined (*t* test, $P < .05$; Figure 5B-C). At the molecular level, immunoblotting demonstrated that IL8 stimulation led to activation of proliferative extracellular signal-regulated kinase (ERK) MAPK and AKT pathways in leukemia cells, whereas no stimulation of the apoptotic p38 MAPK pathway was observed (Figure 5D-F). Pharmacologic inhibition of CXCR2 led to abrogation of IL8-stimulated signaling in these cells.

CXCR2 inhibition leads to selective targeting of AML/MDS HSCs

Next, we determined the functional role of the IL8-CXCR2 pathway in primary HSCs from patients, and treated 5 AML, 1 MDS, and 3 healthy control bone marrow samples with the CXCR2 inhibitor. Fluorescence-activated cell sorter analysis revealed that CXCR2 inhibition led to significantly decreased viability of $CD34^+/CD38^-$ HSCs from AML/MDS patients (Figure 6A-B). In contrast, no significant decrease in cell viability was seen in healthy control HSCs (Figure 6C-D). No significant decrease in viability of the $CD34^+/CD38^+$ population in AML/MDS samples was observed (supplemental Figure 2), demonstrating that CXCR2 inhibition preferentially targets leukemic HSCs.

CXCR2 inhibition leads to inhibition in primary AML/MDS samples and increased survival in vivo

Next, we determined the efficacy of CXCR2 inhibition in inhibiting leukemic colony formation from primary MDS and AML samples. CXCR2 inhibitor treatment led to a significant decrease in leukemic colony size and numbers (Figure 7A-B). This effect was seen in both the AML and high-risk MDS cases, whereas no decrease in erythroid/myeloid colonies was seen in healthy $CD34^+$ cells (Figure 7A). Finally, we examined the efficacy of CXCR2 knockdown in vivo using xenografts with U937 cells. U937 cells were infected with lentiviruses containing shRNA directed against CXCR2 or scrambled control shRNAs and a fluorescent reporter gene (GFP); cells were sorted for GFP and xenografted into NSG mice. CXCR2 knockdown led to significant improvement in overall survival (Figure 7C; $P = .02$, log rank), demonstrating CXCR2 as a therapeutic target in vivo.

Discussion

AML and MDS are diseases that are characterized by a high rate of relapse when treated with chemotherapy or non-chemotherapeutic approaches such as azacytidine and lenalidomide. Leukemia-initiating stem cells including preleukemic stem cells have been shown to persist even during morphologic remissions after these treatments

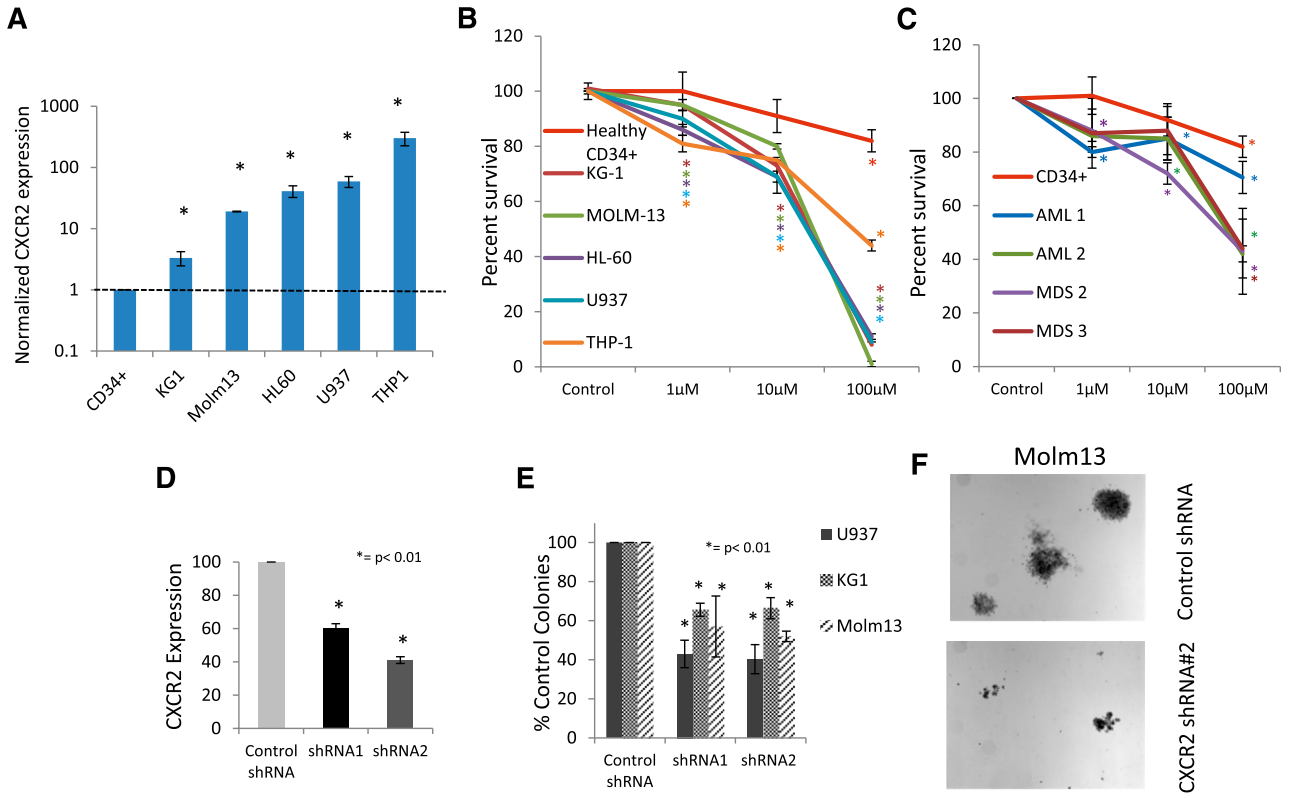

Figure 4. CXCR2 is highly expressed in human leukemic cell lines and regulates viability in cell lines and primary samples. (A) qRT-PCR for CXCR2 demonstrates significantly increased expression in AML cell lines (*t* test, $P < .05$). (B) Viability of AML cell lines is inhibited by the CXCR2 inhibitor SB332235 compared with healthy $CD34^+$ cells at 48 hours (*t* test, $^*P < .05$, $^{**}P < .01$). (C) Viability of primary MNCs from 2 AML and 2 high-risk MDS samples inhibited by the CXCR2 inhibitor. (D) shRNA against CXCR2 leads to significant knockdown by qRT-PCR in U937 cells (*t* test, $P < .05$). Colony growth shows significantly (E) decreased number and (F) size of leukemic colonies AML cells on CXCR2 knockdown compared with scrambled controls (*t* test, $P < .01$).

and have to be targeted for future curative approaches.[1,2,8,9,20,41] It has been shown that leukemia-initiating cells can reside in different phenotypic stem and progenitor compartments at relatively low frequencies and are associated with transcription factor alterations that result in pathogenic transcriptional changes.[2-7,11-13,32,42-44] Thus, to uncover newer stem cell-directed targets, we conducted a transcriptomic analysis on rigorously defined stem and progenitor populations in AML and MDS in comparison with their respective healthy counterparts. With this approach, we were able to identify IL8 as one of the few genes most significantly overexpressed across different stem and progenitor subsets in AML and MDS patients, indicating it might play a crucial role in the pathogenesis of AML and MDS. We were also able to show that the IL8 receptor CXCR2 is overexpressed in AML and MDS patient samples and in several myeloid leukemia cell lines. We also found that high CXCR2 expression correlates with worse clinical outcome. These data implicate the IL8-CXCR2 pathway as a novel therapeutic target in in AML and MDS.

The IL8-CXCR2 pathway has been shown to be important in the pathogenesis of solid tumors, and preclinical studies have demonstrated a role for this pathway in the breast cancer microenvironment.[22,27,28,30,45] Various small molecule CXCR2 inhibitors are being developed clinically, and one is being tested in a clinical trial in breast cancer. Our results demonstrate that this pathway is also functionally important for the viability of leukemic stem cell compartments in AML and MDS. Although healthy HSPCs also show a basal production of IL8, significant overexpression of IL8 within the malignant stem and progenitor compartment was detected in every case examined, with notably up to 100-fold upregulation seen in some cases compared with healthy controls. We also demonstrated that inhibition of the IL8 receptor, CXCR2, leads to a significant decrease in viability and colony formation in multiple leukemic cell lines, as well as patient samples. Most importantly, viability of the $CD34^+/CD38^-$ stem cell-enriched fraction was significantly decreased in AML/MDS patient cells after CXCR2 inhibition, whereas the inhibitor had no impact on healthy control stem cells, indicating that inhibition of the IL8-CXCR2 axis might selectively target the malignant stem cell clones. The role of IL8 in healthy HSCs is not well understood. Although murine models with IL8 receptor-deficient mice show relatively normal hematopoiesis arguing against a crucial role for IL8 in the regulation of healthy HSCs,[46] some reports suggest that IL8 might play a positive and protective role in mobilization of healthy HSCs and promotion of monocyte/macrophage growth and differentiation.[47,48] Further studies report increased IL8 to exert an inhibitory effect on healthy hematopoiesis and myeloid proliferation,[49-53] which could potentially explain the inhibition of growth and differentiation of healthy HSCs in an IL8-rich environment in AML and MDS. The IL8-CXCR2 signaling pathway has been shown to stimulate proliferative pathways such as the phosphatidylinositol 3-kinase/AKT, phospholipase C/protein kinase C, and ERK/MAPK pathways in various models. It has also been shown to activate oncogenic pathways such as hypoxia inducible factor 1, nuclear factor-κB, signal transducer and activator of transcription 3, and β-catenin, which help to promote tumor growth and survival.[21] We and others have shown that these transcription factors are important for survival of cancer stem cells.[2,34-36]

IL8 is also an important regulator of innate immunity. Recent data have shown that innate immune signaling mediators such as IL receptor 1 receptor accessory protein (IL1RAP), Toll-like receptors,

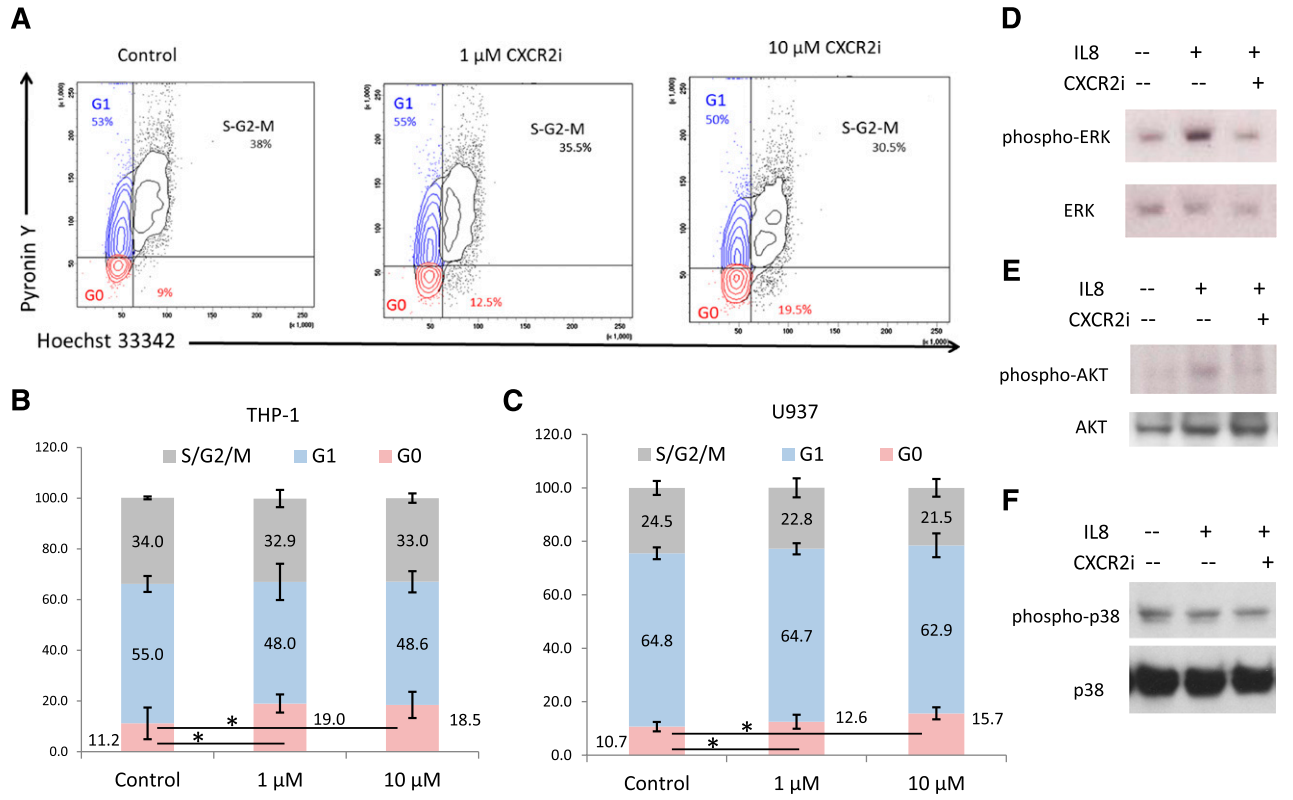

Figure 5. CXCR2 inhibition leads to cell cycle arrest in AML cells and inhibits IL8-stimulated signaling cascades. (A) Representative flow plots of THP-1 cells treated with the CXCR2 inhibitor demonstrate a significantly increased percentage of cells in G0 stage. (B-C) Data from 3 independent experiments demonstrate significantly increased G0 cell cycle arrest in THP-1 and U937 cell lines after CXCR2 inhibition (*t* test, $P < .05$). (D-F) THP-1 cells were stimulated with IL8 in the presence and absence of CXCR2 inhibitor (10 μm) and immunoblotted for phospho/activated ERK MAP kinase, p38 MAPK, and AKT with appropriate loading controls.

and myeloid-derived suppressor cells are activated in MDS.[10,54-56] The signaling protein, IL-1 receptor-associated kinase (IRAK4), has also been shown to be a therapeutic target in MDS.[57] Our findings further support the role of activated innate immune signaling pathways in MDS/AML and suggest that interaction of IL8-CXCR2 with these other pathways needs to be studied in future

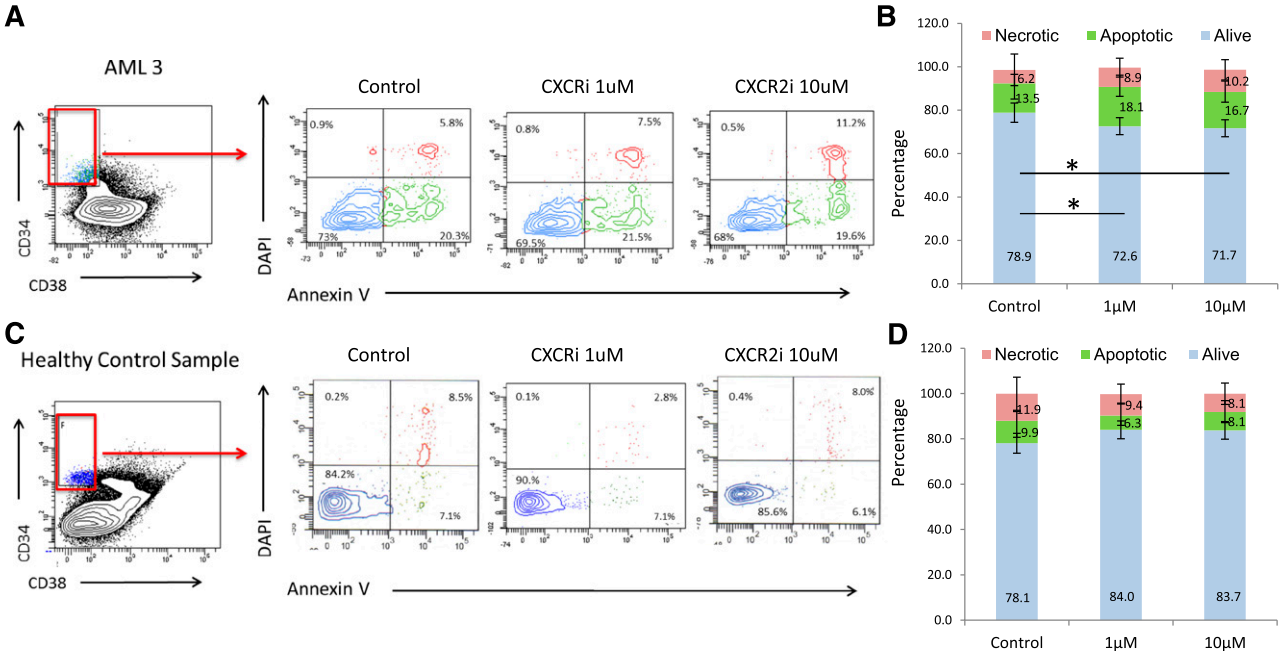

Figure 6. CXCR2 inhibition reduces viability in leukemic CD34$^+$/CD38$^-$ HSCs. Four AML and 1 MDS samples were treated with CXCR2 inhibitor, and viability was assessed in the CD34$^+$/CD38$^-$ HSC compartment. Viability in AML/MDS HSCs was significantly decreased after CXCR2 inhibition (*t* test, $P < .05$) with no change in the healthy controls (N = 3).

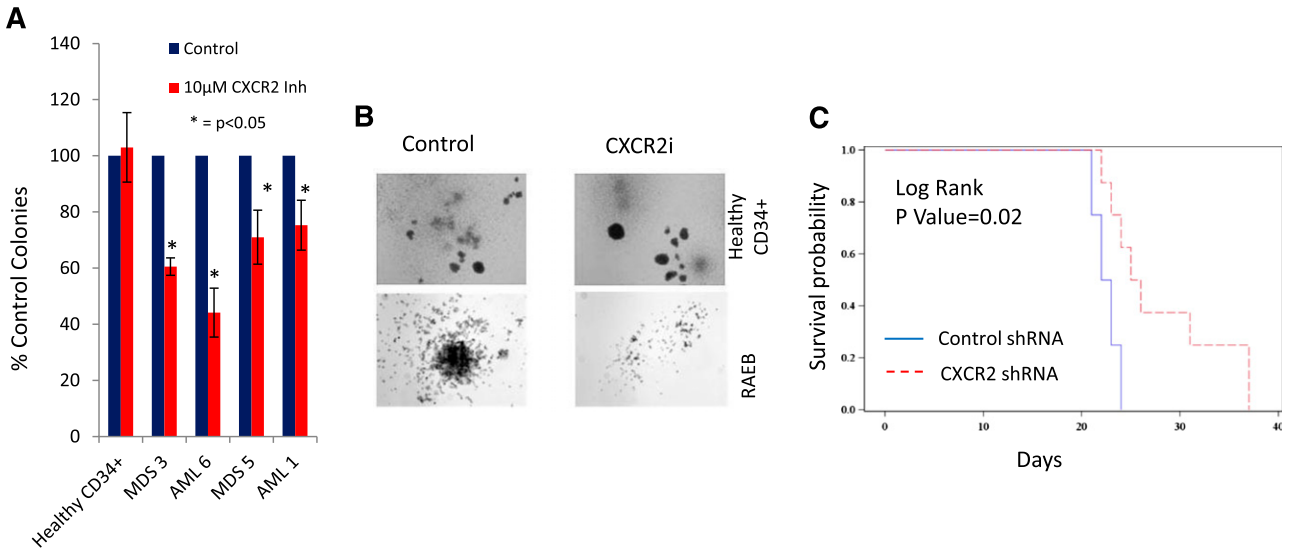

Figure 7. CXCR2 inhibition leads to inhibition in primary AML/MDS samples and increased survival in vivo. (A) Four primary MDS/AML samples were grown in the presence and absence of the CXCR2 inhibitor and demonstrated inhibition of leukemic colony growth after treatment. (B) The size of leukemic colonies was also reduced. NSG mice were xenografted with U937 cells containing control or CXCR2 shRNAs. (C) Mice with CXCR2 shRNA xenografts demonstrated significantly improved overall survival (log rank, $P = .02$).

studies. Taken together, our results provide a rationale for further evaluating the targeting of the IL8-CXCR2 axis and its specificity for aberrant AML/MDS stem and progenitor cells in vitro, as well as in preclinical in vivo studies.

Acknowledgments

This work was supported by the Leukemia Lymphoma Society, Department of Defense, and National Institutes of Health, National Institute of Diabetes and Digestive and Kidney Diseases grant R01DK1039615 and National Heart, Lung, and Blood Institute grant R01HL116336.

Authorship

Contribution: C.S. designed research; C.S., O.G., W.L., A.S., S.G., L.B., T.B., S.B., N.R., and M.B. performed research; A.P. and J.B. contributed data; A.W. contributed reagents; Y.Y., B.W., and S.W. analyzed data; and U.S. and A.V. wrote the paper and analyzed the data.

Conflict-of-interest disclosure: The authors declare no competing financial interests.

Correspondence: Amit Verma, Albert Einstein College of Medicine, 1300 Morris Park Ave, Chanin Building, Room 302B, Bronx, NY 10461; e-mail: amit.verma@einstein.yu.edu; or Ulrich Steidl, Albert Einstein College of Medicine, 1300 Morris Park Ave, Chanin Building, Room 606A, Bronx, NY 10461; e-mail: ulrich.steidl@einstein.yu.edu.

References

1. Elias HK, Schinke C, Bhattacharyya S, Will B, Verma A, Steidl U. Stem cell origin of myelodysplastic syndromes. *Oncogene.* 2014; 33(44):5139-5150.
2. Will B, Zhou L, Vogler TO, et al. Stem and progenitor cells in myelodysplastic syndromes show aberrant stage-specific expansion and harbor genetic and epigenetic alterations. *Blood.* 2012;120(10):2076-2086.
3. Jan M, Snyder TM, Corces-Zimmerman MR, et al. Clonal evolution of preleukemic hematopoietic stem cells precedes human acute myeloid leukemia. *Sci Transl Med.* 2012;4(149):149ra118.
4. Shlush LI, Zandi S, Mitchell A, et al; HALT Pan-Leukemia Gene Panel Consortium. Identification of pre-leukaemic haematopoietic stem cells in acute leukaemia. *Nature.* 2014;506(7488): 328-333.
5. Pang WW, Pluvinage JV, Price EA, et al. Hematopoietic stem cell and progenitor cell mechanisms in myelodysplastic syndromes. *Proc Natl Acad Sci USA.* 2013;110(8):3011-3016.
6. Woll PS, Kjällquist U, Chowdhury O, et al. Myelodysplastic syndromes are propagated by rare and distinct human cancer stem cells in vivo. *Cancer Cell.* 2014;25(6):794-808.
7. Jamieson CH, Ailles LE, Dylla SJ, et al. Granulocyte-macrophage progenitors as candidate leukemic stem cells in blast-crisis CML. *N Engl J Med.* 2004;351(7):657-667.
8. Konopleva MY, Jordan CT. Leukemia stem cells and microenvironment: biology and therapeutic targeting. *J Clin Oncol.* 2011;29(5):591-599.
9. Jordan CT. Searching for leukemia stem cells—not yet the end of the road? *Cancer Cell.* 2006;10(4):253-254.
10. Barreyro L, Will B, Bartholdy B, et al. Overexpression of IL-1 receptor accessory protein in stem and progenitor cells and outcome correlation in AML and MDS. *Blood.* 2012;120(6): 1290-1298.
11. Sarry JE, Murphy K, Perry R, et al. Human acute myelogenous leukemia stem cells are rare and heterogeneous when assayed in NOD/SCID/IL2Rγc-deficient mice. *J Clin Invest.* 2011;121(1): 384-395.
12. Majeti R, Becker MW, Tian Q, et al. Dysregulated gene expression networks in human acute myelogenous leukemia stem cells. *Proc Natl Acad Sci USA.* 2009;106(9):3396-3401.
13. Eppert K, Takenaka K, Lechman ER, et al. Stem cell gene expression programs influence clinical outcome in human leukemia. *Nat Med.* 2011; 17(9):1086-1093.
14. Jordan CT, Upchurch D, Szilvassy SJ, et al. The interleukin-3 receptor alpha chain is a unique marker for human acute myelogenous leukemia stem cells. *Leukemia.* 2000;14(10):1777-1784.
15. Jin L, Hope KJ, Zhai Q, Smadja-Joffe F, Dick JE. Targeting of CD44 eradicates human acute myeloid leukemic stem cells. *Nat Med.* 2006; 12(10):1167-1174.
16. van Rhenen A, van Dongen GA, Kelder A, et al. The novel AML stem cell associated antigen CLL-1 aids in discrimination between normal and leukemic stem cells. *Blood.* 2007;110(7): 2659-2666.
17. Busfield SJ, Biondo M, Wong M, et al. Targeting of acute myeloid leukemia in vitro and in vivo with an anti-CD123 mAb engineered for optimal ADCC. *Leukemia.* 2014;28(11):2213-2221.
18. Askmyr M, Ågerstam H, Hansen N, et al. Selective killing of candidate AML stem cells by antibody targeting of IL1RAP. *Blood.* 2013; 121(18):3709-3713.
19. Pandolfi A, Barreyro L, Steidl U. Concise review: preleukemic stem cells: molecular biology and clinical implications of the precursors to leukemia

stem cells. *Stem Cells Transl Med.* 2013;2(2):143-150.

20. Corces-Zimmerman MR, Majeti R. Pre-leukemic evolution of hematopoietic stem cells: the importance of early mutations in leukemogenesis. *Leukemia.* 2014;28(12):2276-2282.
21. Waugh DJ, Wilson C. The interleukin-8 pathway in cancer. *Clin Cancer Res.* 2008;14(21):6735-6741.
22. Sharma B, Nawandar DM, Nannuru KC, Varney ML, Singh RK. Targeting CXCR2 enhances chemotherapeutic response, inhibits mammary tumor growth, angiogenesis, and lung metastasis. *Mol Cancer Ther.* 2013;12(5):799-808.
23. Lee YS, Choi I, Ning Y, et al. Interleukin-8 and its receptor CXCR2 in the tumour microenvironment promote colon cancer growth, progression and metastasis. *Br J Cancer.* 2012;106(11):1833-1841.
24. Saintigny P, Massarelli E, Lin S, et al. CXCR2 expression in tumor cells is a poor prognostic factor and promotes invasion and metastasis in lung adenocarcinoma. *Cancer Res.* 2013;73(2):571-582.
25. Infanger DW, Cho Y, Lopez BS, et al. Glioblastoma stem cells are regulated by interleukin-8 signaling in a tumoral perivascular niche. *Cancer Res.* 2013;73(23):7079-7089.
26. Singh JK, Farnie G, Bundred NJ, et al. Targeting CXCR1/2 significantly reduces breast cancer stem cell activity and increases the efficacy of inhibiting HER2 via HER2-dependent and -independent mechanisms. *Clin Cancer Res.* 2013;19(3):643-656.
27. Singh JK, Simões BM, Howell SJ, Farnie G, Clarke RB. Recent advances reveal IL-8 signaling as a potential key to targeting breast cancer stem cells. *Breast Cancer Res.* 2013;15(4):210.
28. Wang S, Wu Y, Hou Y, et al. CXCR2 macromolecular complex in pancreatic cancer: a potential therapeutic target in tumor growth. *Transl Oncol.* 2013;6(2):216-225.
29. Ning Y, Labonte MJ, Zhang W, et al. The CXCR2 antagonist, SCH-527123, shows antitumor activity and sensitizes cells to oxaliplatin in preclinical colon cancer models. *Mol Cancer Ther.* 2012;11(6):1353-1364.
30. Jamieson T, Clarke M, Steele CW, et al. Inhibition of CXCR2 profoundly suppresses inflammation-driven and spontaneous tumorigenesis. *J Clin Invest.* 2012;122(9):3127-3144.
31. Verma A, Deb DK, Sassano A, et al. Activation of the p38 mitogen-activated protein kinase mediates the suppressive effects of type I interferons and transforming growth factor-beta on normal hematopoiesis. *J Biol Chem.* 2002;277(10):7726-7735.
32. Steidl U, Rosenbauer F, Verhaak RG, et al. Essential role of Jun family transcription factors in PU.1 knockdown-induced leukemic stem cells. *Nat Genet.* 2006;38(11):1269-1277.
33. Will B, Kawahara M, Luciano JP, et al. Effect of the nonpeptide thrombopoietin receptor agonist Eltrombopag on bone marrow cells from patients with acute myeloid leukemia and myelodysplastic syndrome. *Blood.* 2009;114(18):3899-3908.
34. Hassane DC, Guzman ML, Corbett C, et al. Discovery of agents that eradicate leukemia stem cells using an in silico screen of public gene expression data. *Blood.* 2008;111(12):5654-5662.
35. Guzman ML, Li X, Corbett CA, et al. Rapid and selective death of leukemia stem and progenitor cells induced by the compound 4-benzyl, 2-methyl, 1,2,4-thiadiazolidine, 3,5 dione (TDZD-8). *Blood.* 2007;110(13):4436-4444.
36. Guzman ML, Rossi RM, Neelakantan S, et al. An orally bioavailable parthenolide analog selectively eradicates acute myelogenous leukemia stem and progenitor cells. *Blood.* 2007;110(13):4427-4435.
37. Pellagatti A, Cazzola M, Giagounidis A, et al. Deregulated gene expression pathways in myelodysplastic syndrome hematopoietic stem cells. *Leukemia.* 2010;24(4):756-764.
38. Cancer Genome Atlas Research Network. Genomic and epigenomic landscapes of adult de novo acute myeloid leukemia. *N Engl J Med.* 2013;368(22):2059-2074.
39. Gerstung M, Pellagatti A, Malcovati L, et al. Combining gene mutation with gene expression data improves outcome prediction in myelodysplastic syndromes. *Nat Commun.* 2015;6:5901.
40. Braber S, Koelink PJ, Henricks PA, et al. Cigarette smoke-induced lung emphysema in mice is associated with prolyl endopeptidase, an enzyme involved in collagen breakdown. *Am J Physiol Lung Cell Mol Physiol.* 2011;300(2):L255-L265.
41. Craddock C, Quek L, Goardon N, et al. Azacitidine fails to eradicate leukemic stem/progenitor cell populations in patients with acute myeloid leukemia and myelodysplasia. *Leukemia.* 2013;27(5):1028-1036.
42. Steidl U, Steidl C, Ebralidze A, et al. A distal single nucleotide polymorphism alters long-range regulation of the PU.1 gene in acute myeloid leukemia. *J Clin Invest.* 2007;117(9):2611-2620.
43. Bullinger L, Döhner K, Bair E, et al. Use of gene-expression profiling to identify prognostic subclasses in adult acute myeloid leukemia. *N Engl J Med.* 2004;350(16):1605-1616.
44. Valk PJ, Verhaak RG, Beijen MA, et al. Prognostically useful gene-expression profiles in acute myeloid leukemia. *N Engl J Med.* 2004;350(16):1617-1628.
45. Du M, Qiu Q, Gruslin A, et al. SB225002 promotes mitotic catastrophe in chemo-sensitive and -resistant ovarian cancer cells independent of p53 status in vitro. *PLoS ONE.* 2013;8(1):e54572.
46. Cacalano G, Lee J, Kikly K, et al. Neutrophil and B cell expansion in mice that lack the murine IL-8 receptor homolog. *Science.* 1994;265(5172):682-684.
47. Corre I, Pineau D, Hermouet S. Interleukin-8: an autocrine/paracrine growth factor for human hematopoietic progenitors acting in synergy with colony stimulating factor-1 to promote monocyte-macrophage growth and differentiation. *Exp Hematol.* 1999;27(1):28-36.
48. Laterveer L, Lindley IJ, Hamilton MS, Willemze R, Fibbe WE. Interleukin-8 induces rapid mobilization of hematopoietic stem cells with radioprotective capacity and long-term myelolymphoid repopulating ability. *Blood.* 1995;85(8):2269-2275.
49. Broxmeyer HE, Cooper S, Cacalano G, Hague NL, Bailish E, Moore MW. Involvement of Interleukin (IL) 8 receptor in negative regulation of myeloid progenitor cells in vivo: evidence from mice lacking the murine IL-8 receptor homologue. *J Exp Med.* 1996;184(5):1825-1832.
50. Broxmeyer HE, Sherry B, Cooper S, et al. Comparative analysis of the human macrophage inflammatory protein family of cytokines (chemokines) on proliferation of human myeloid progenitor cells. Interacting effects involving suppression, synergistic suppression, and blocking of suppression. *J Immunol.* 1993;150(8 Pt 1):3448-3458.
51. Emadi S, Clay D, Desterke C, et al; French INSERM Research Network on MMM. IL-8 and its CXCR1 and CXCR2 receptors participate in the control of megakaryocytic proliferation, differentiation, and ploidy in myeloid metaplasia with myelofibrosis. *Blood.* 2005;105(2):464-473.
52. Daly TJ, LaRosa GJ, Dolich S, Maione TE, Cooper S, Broxmeyer HE. High activity suppression of myeloid progenitor proliferation by chimeric mutants of interleukin 8 and platelet factor 4. *J Biol Chem.* 1995;270(40):23282-23292.
53. Gewirtz AM, Zhang J, Ratajczak J, et al. Chemokine regulation of human megakaryocytopoiesis. *Blood.* 1995;86(7):2559-2567.
54. Dimicoli S, Wei Y, Bueso-Ramos C, et al. Overexpression of the toll-like receptor (TLR) signaling adaptor MYD88, but lack of genetic mutation, in myelodysplastic syndromes. *PLoS ONE.* 2013;8(8):e71120.
55. Wei Y, Dimicoli S, Bueso-Ramos C, et al. Toll-like receptor alterations in myelodysplastic syndrome. *Leukemia.* 2013;27(9):1832-1840.
56. Chen X, Eksioglu EA, Zhou J, et al. Induction of myelodysplasia by myeloid-derived suppressor cells. *J Clin Invest.* 2013;123(11):4595-4611.
57. Rhyasen GW, Bolanos L, Fang J, et al. Targeting IRAK1 as a therapeutic approach for myelodysplastic syndrome. *Cancer Cell.* 2013;24(1):90-104.

2015 125: 3144-3152
doi:10.1182/blood-2015-01-621631 originally published online March 25, 2015

IL8-CXCR2 pathway inhibition as a therapeutic strategy against MDS and AML stem cells

Carolina Schinke, Orsolya Giricz, Weijuan Li, Aditi Shastri, Shanisha Gordon, Laura Barreryo, Tushar Bhagat, Sanchari Bhattacharyya, Nandini Ramachandra, Matthias Bartenstein, Andrea Pellagatti, Jacqueline Boultwood, Amittha Wickrema, Yiting Yu, Britta Will, Sheng Wei, Ulrich Steidl and Amit Verma

Blood (print ISSN 0006-4971, online ISSN 1528-0020), is published weekly by the American Society of Hematology, 2021 L St, NW, Suite 900, Washington DC 20036.